Modelling the influence of biotic plant stress on atmospheric aerosol particle processes throughout a growing season

Ditte Taipale[1,2,3,4], Veli-Matti Kerminen[1], Mikael Ehn[1], Markku Kulmala[1], Ülo Niinemets[2]

[1]Institute for Atmospheric and Earth System Research / Physics, Faculty of Science, University of Helsinki, P.O. Box 64, 00014 Helsinki, Finland
[2]Institute of Agricultural and Environmental Sciences, Estonian University of Life Sciences, Kreutzwaldi 1, Tartu 51006, Estonia
[3]Institute for Atmospheric and Earth System Research / Forest Sciences, Faculty of Agriculture and Forestry, University of Helsinki, PO Box 27, 00014 Helsinki, Finland
[4]Hyytiälä Forestry Field Station, Hyytiäläntie 124, 35500 Korkeakoski, Finland

Correspondence to: Ditte Taipale (ditte.taipale@helsinki.fi)

Abstract. Most trees emit volatile organic compounds (VOCs) continuously throughout their life, but the rate of emission, and spectrum of emitted VOCs, become substantially altered when the trees experience stress. Still, models to predict the emissions of VOCs do not account for perturbations caused by biotic plant stress. Considering that such stresses have generally been forecast to increase in both frequency and severity in future climate, the neglect of plant stress-induced emissions in models might be one of the key obstacles for realistic climate change predictions, since changes in VOC concentrations are known to greatly influence atmospheric aerosol processes. Thus, we constructed a model to study the impact of biotic plant stresses on new particle formation and growth throughout a full growing season. We simulated the influence on aerosol processes caused by herbivory by European gypsy moth (*Lymantria dispar*) and autumnal moth (*Epirrita autumnata*) feeding on pedunculate oak (*Quercus robur*) and mountain birch (*Betula pubescens* var. *pumila*), respectively, and also fungal infections of pedunculate oak and balsam poplar (*Populus balsamifera* var. *suaveolens*) by oak powdery mildew (*Erysiphe alphitoides*) and poplar rust (*Melampsora larici-populina*), respectively. Our modelling results indicate that all the investigated plant stresses are capable of substantially perturbing both the number and size of aerosol particles in atmospherically relevant conditions, with increases in the amount of newly formed particles by up to about one order of magnitude and additional daily growth of up to almost 50 nm. We also showed that it can be more important to account for biotic plant stresses in models for local and regional predictions of new particle formation and growth during the time of infestation/infection than significant variations in e.g. leaf area index, and temperature and light conditions, which are currently the main parameters controlling predictions of VOC emissions. Our study, thus, demonstrates that biotic plant stress can be highly atmospherically relevant. To validate our findings, field measurements are urgently needed to quantify the role of stress emissions in atmospheric aerosol processes and for making integration of biotic plant stress emission responses into numerical models for prediction of atmospheric chemistry and physics, including climate change projection models, possible.

1 Introduction

Formation and subsequent growth of atmospheric aerosol particles is globally a major source of cloud condensation nuclei (CCN) (Spracklen et al., 2008; Merikanto et al., 2009; Dunne et al., 2016). CCN impact various cloud processes, such as cloud formation, albedo and lifetime (Twomey, 1977; Albrecht, 1989; Makkonen et al., 2009; Kerminen et al., 2005), and atmospheric aerosol particles are thereby able to influence our climate indirectly, in addition to interacting directly with incoming solar radiation. Though atmospheric aerosol particles provide the single largest cooling effect on our climate, they

are also connected with the greatest uncertainty in climate change projections (IPCC, 2013). Part of this uncertainty is caused by limited knowledge about the aerosol precursor molecules.

Oxidation products of certain volatile organic compounds (VOCs) participate in both the formation of new particles (Donahue et al., 2013; Schobesberger et al., 2013; Kulmala et al., 2014; Riccobono et al., 2014; Kirkby et al., 2016; Tröstl et al., 2016) and growth of existing particles via gas-to-particle condensation (Riipinen et al., 2012; Ehn et al., 2014; Bianchi et al., 2019). Globally, and especially in forested regions, the majority of these organic compounds originate from terrestrial vegetation (Kanakidou et al., 2005; Jimenez et al., 2009). Thus, increases in the emissions of certain biogenic VOCs can lead to enhanced formation of atmospheric aerosol particles and subsequently to a rise in CCN concentration (Kerminen et al., 2012; Paasonen et al., 2013).

Many plants emit VOCs constitutively, i.e. that they emit VOCs regardless of the experience of stress. Biotic plant stress (i.e. stress caused to a plant by living species such as e.g. herbivores and pathogens) is known to substantially alter both the rates of emission and spectrum of VOCs emitted constitutively (Holopainen and Gershenzon, 2010; Niinemets, 2010; Niinemets et al., 2013; Faiola and Taipale, 2020). For example, constitutively emitted isoprene, which is thought to suppress the formation of new atmospheric aerosol particles (Kiendler-Scharr et al., 2009, 2012; Lee et al., 2016; McFiggans et al., 2019; Heinritzi et al., 2020), is usually reduced in response to such stress (e.g. Brilli et al., 2009; Copolovici et al., 2014, 2017; Jiang et al., 2016), while the emissions of other VOCs are greatly increased. Emissions of VOCs which are increased, or started to be emitted, in response to plant stress, are referred to as induced plant volatile emissions. A large fraction of stress-induced compounds (e.g. monoterpenes, sesquiterpenes, 4,8-dimethyl-1,3,7-nonatriene (DMNT) and methyl salicylate) has a high potential to produce and grow atmospheric aerosol particles (e.g. Mentel et al., 2013; Joutsensaari et al., 2015; Yli-Pirilä et al., 2016; Ylisirniö et al., 2020), while other induced compounds (e.g. methanol and lipoxygenase oxidation products (LOX), which mostly include C_6 aldehydes, alcohols and esters) are anticipated to suppress aerosol processes (e.g. Mentel et al., 2013).

While much attention has been given to representing constitutive emissions of VOCs in numerical models, VOC emissions caused by stress, and in particular biotic stress, have been mostly excluded (Grote et al., 2013; Faiola and Taipale, 2020), despite the fact that biotic plant stress is largely ubiquitous. This is mainly due to a lack of measurements, combined with the fact that variations in emission responses are highly stressor-specific (e.g. Holopainen and Gershenzon, 2010; Niinemets, 2010; Faiola and Taipale, 2020). Thus, no consistent mechanism for the emissions of VOCs from plants under stress exists. Though the most extensively used biogenic emissions model, MEGAN (Guenther et al., 2012), considers a stress emission category, the treatment is not quantitative. The emission factor for stress VOCs is, for example, the same for all plant functional types and is supposed to represent a large range of different types of stresses. Recently, Grote et al. (2019) proposed a new modelling framework for estimating emissions of VOCs induced by both biotic and abiotic plant stresses, while Douma et al. (2019) developed a model to predict both the emissions and concentrations of stress-induced VOCs, which was parameterized to simulate a gypsy moth infested black poplar canopy. Both are promising tools, but in their current states, they exclude important storage emissions which are usually released upon wounding (e.g. Blande et al., 2009; Faiola et al., 2018; Kari et al., 2019), and they do not fully (Grote et al., 2019) - or at all (Douma et al., 2019) - consider how the constitutive emissions of isoprene are modulated. This is as such understandable considering that emissions of isoprene might be either reduced (e.g. Brilli et al., 2009; Copolovici et al., 2017) or increased (e.g. Schaub et al., 2010; Ye et al., 2019) in response to biotic plant stress, but nevertheless problematic since isoprene is globally the VOC that is emitted in largest quantities (Guenther et al., 2012) and it is thought to suppress the formation of aerosol particles (see above). Whilst Grote et al. (2019) assumed a linear response to the degree of damage, which has been shown not always to be true, especially at severe stress levels (e.g. Niinemets et al., 2013; Jiang et al., 2016; Yli-Pirilä et al. 2016; Copolovici et al., 2017; Faiola and Taipale, 2020), it is not obvious how the model results by Douma et al. (2019) depend on the degree of damage, as they operate with "number of larvae" rather than a stand level of defoliation. Additionally, Grote et al. (2019) did not account for an explicit dependency of the emissions on temperature, which is usually considered as one of the most important environmental parameters for

emissions of VOCs (e.g. Grote et al., 2013). Common for both studies is that they only simulate rather short time scales (i.e. a few days).

Since measurements have clearly illustrated that biotic plant stress is able to significantly influence the amount and size of formed atmospheric aerosol particles over short periods at least (Mentel et al., 2013; Joutsensaari et al., 2015; Yli-Pirilä et al., 2016; Faiola et al., 2019, 2018) via perturbations in VOC emissions, there is an urgent need to quantify the atmospheric importance of biotic plant stress. This need is amplified by the fact that insect outbreaks and fungal diseases generally are expected to increase in both frequency and severity in the future (Cannon, 1998; Bale et al., 2002; Harrington et al., 2007; Pautasso et al., 2012; Boyd et al., 2013). Unfortunately, such quantitative estimates are currently very scarce, connected with a large degree of uncertainty, and not necessarily reaching the same conclusions. For example, Berg et al. (2013) used bark beetle-induced monoterpene emission responses and several years of bark beetle-induced tree mortality data from western North America as input to a global model in order to investigate the impact of bark beetle attacks on regional secondary organic aerosol (SOA) formation. The authors found that the concentration of SOA might increase regionally by up to 40 % or 300 % in case of bark beetle attacks on lodgepole pine and spruce trees, respectively (Berg et al., 2013). At the same time, Berg et al. (2013) concluded that the enhancement in the concentrations of SOA is in most cases small in comparison to the impact of wildfires on total organic aerosol in western North America. Bergström et al. (2014), on the other hand, used a regional chemical transport model to simulate the impact of *de novo* emissions, induced by aphid infestation, on SOA formation, and estimated that these induced emissions currently account for 20-70 % of total biogenic SOA in northern and central European forests. Meanwhile, Joutsensaari et al. (2015) calculated a local increase of up to 480 % in aerosol mass and 45 % in CCN concentration, when it was assumed that 10 % of the boreal forest area experienced stress which increased constitutive monoterpenes emission rates by an order of magnitude. Using satellite observations, Joutsensaari et al. (2015) also found a 2-fold increase in aerosol optical depth over Canadian pine forests during a bark beetle outbreak. Thus, the degree of necessity of considering biotic plant stress emissions for predictions of new particle formation in the atmosphere is still uncertain, and therefore there is a great need for field observations of different scales to constrain and quantify the role of stress emissions in SOA formation, but also for innovative model approaches which improve the quantitative representation of the emissions. To our knowledge, no one has previously considered the dynamics of insect herbivory when simulating the emitted VOCs and produced and grown aerosols from stressed plants. Additionally, there has so far been no attempts to measure nor model the impact of pathogenic infections on atmospheric aerosol processes.

We constructed a conceptual model to investigate the atmospheric impacts of biotic plant stresses. We used this model to simulate formation and growth of atmospheric aerosol particles throughout a growing season in pure oak, poplar and birch forest stands in stress-free conditions and under herbivory or fungal stress. By considering the dynamics of insect herbivory and pathogenic infections in combination with seasonal changes in environmental parameters, our aim was to contribute to a discussion about whether biotic plant stress perturbs atmospheric aerosol processes sufficiently to warrant their inclusion in larger scale models.

2 Materials and methods

We constructed a 0D box model that includes modules for emissions of VOCs from stress-free and biotically stressed tree species (Sec. 2.4), boundary layer meteorology (Sec. 2.5), atmospheric chemistry (Sec. 2.6) and aerosol dynamics (Sec. 2.7). The calculated canopy VOC emissions from biotically stressed trees depend on the dynamics of the biotic stressors of interest (Sec. 2.1 and 2.2) and changes in the leaf area index (Sec. 2.3). The model is programmed in Fortran and the time step for each module is 60 s. The model was simulating one day at a time. The purpose of our study was to simulate the influence of low-volatility organic compounds on the evolution of aerosol number size distribution via new particle formation and subsequent particle growth. Thus, we were interested in changes in the nucleation mode dynamics, and not in aerosol mass concentration.

The individual processes included in the model (Sec. 2.1-2.7) are aimed to imitate our best mechanistic understanding of those processes. The descriptions of several of the individual processes have been evaluated separately in earlier studies by either us or by other researchers (following the references provided in the sections below). The model's ability to reproduce the influence of organic compounds on aerosol formation and growth in biotically stress-free conditions has furthermore been tested by constraining and validating the model with observations from the SMEAR II station (the Station for Measuring Ecosystem-Atmosphere Relations II) in Hyytiälä, Finland (Taipale, in prep).

2.1 Simulations of larval infestation dynamics

Whereas mountain birch (*Betula pubescens var. pumila*; former *spp. czerepanovii*, Fig. 1c) is the main host for autumnal moths (*Epirrita autumnata*, Fig. 1g, Klemola et al., 2004; Ammunét et al., 2011), European gypsy moth (*Lymantria dispar*, Fig. 1d) is one of the major defoliating insects feeding on pedunculate oak (*Quercus robur*, Fig. 1a, https://www.cabi.org/isc/datasheet/31807#tohostsOrSpeciesAffected, last accessed 11th of June, 2021). The larval eggs of both moths hatch in spring synchronously with bud burst (Kaitaniemi et al., 1997; Kaitaniemi and Ruohomäki, 1999; Spear, 2005; McManus et al., 1989). Both sexes have five larval stages (instar), though female gypsy moths have six. These stages are separated by periods of molting where the larvae do not feed. A complete defoliation of vast areas can occur within 4-6 weeks by autumnal moth (Kaitaniemi and Ruohomäki, 1999) and within 6-8 weeks by gypsy moth (McManus et al., 1989). Several thousands of square kilometres of birch forests have previously been reported to become defoliated due to just a single outbreak of autumnal moth in Fennoscandinavia (Tenow 1975; Nikula 1993), while gypsy moth, in North America alone, is estimated to have defoliated >95 million acres of forest during years 1920 to 2020 (Coleman et al., 2020). Adults do not feed on leaves (Tammaru et al., 1996; Waring and Townsend, 2009). For simulations of autumnal moth infested mountain birch, our model incorporates atmospheric and ecological conditions observed at the Station for Measuring Ecosystem-Atmosphere Relations (SMEAR I, Fig. 1h), Värriö, Eastern Finnish Lapland (e.g. Hari et al., 1994), due to the high data quality and availability, and since autumnal moth infested mountain birch is common at the site (Hunter et al., 2014). In our simulations, bud burst occurs on 6th of June, the subsequent full leaf state is attained on 10th of June (dates are based on long-term observations from the station), and senescence onsets on 20th of August (Gill et al., 2015). We assumed that the larvae feed for five weeks, starting on 6th of June and they pupate on 11th of July (Kaitaniemi and Ruohomäki, 1999). The larvae dynamics (i.e. relative leaf consumption and time spent in each larval stage) that is incorporated in our model is based on Lempa et al. (2004). For simulations of European gypsy moth infested pedunculate oak, our model incorporates mainly atmospheric conditions observed at the Meteorological Observatory Hohenpeißenberg (e.g. Birmili et al., 2003), rural southern Germany (Fig. 1h), since this station has been classified as a representative measurement location for central Europe (Naja et al., 2003), where oak is a very common species. In our simulations, bud burst occurs on 15th of May, the subsequent full leaf state is attained 20 days later on 4th of June, and senescence onsets on 20th of September (Gill et al., 2015). Durations of the various developmental states of the larvae are based on Zúbrik et al. (2007), which is also in agreement with Stoyenoff et al. (1994). Though the length of the larval state of female larvae feeding on pedunculate oak is typically a few days longer than the total duration of the male larval state (e.g. Zúbrik et al., 2007), we did not differentiate between the two genders, but utilised the length of the female larval state due to simplification and since the female is the main consumer (Miller et al., 1991). We assumed that the larvae feed for 41 days (Zúbrik et al., 2007), starting on 15th of May and they pupate on 25th of June. The relative leaf consumption within the different larval stages is based on Kula et al. (2013). The ratio in relative leaf consumption between 4th and 5th instar is also within the range that is reported by Stoyenoff et al. (1994) (where no other ratios were provided). We neglected periods of molting, as those are typically in the order of less than one day (Ayres and MacLean, 1987). We assumed that either 30 % or 80 % of the total leaf area in the forest stand was consumed by the end of the feeding period (Fig. 2a,b).
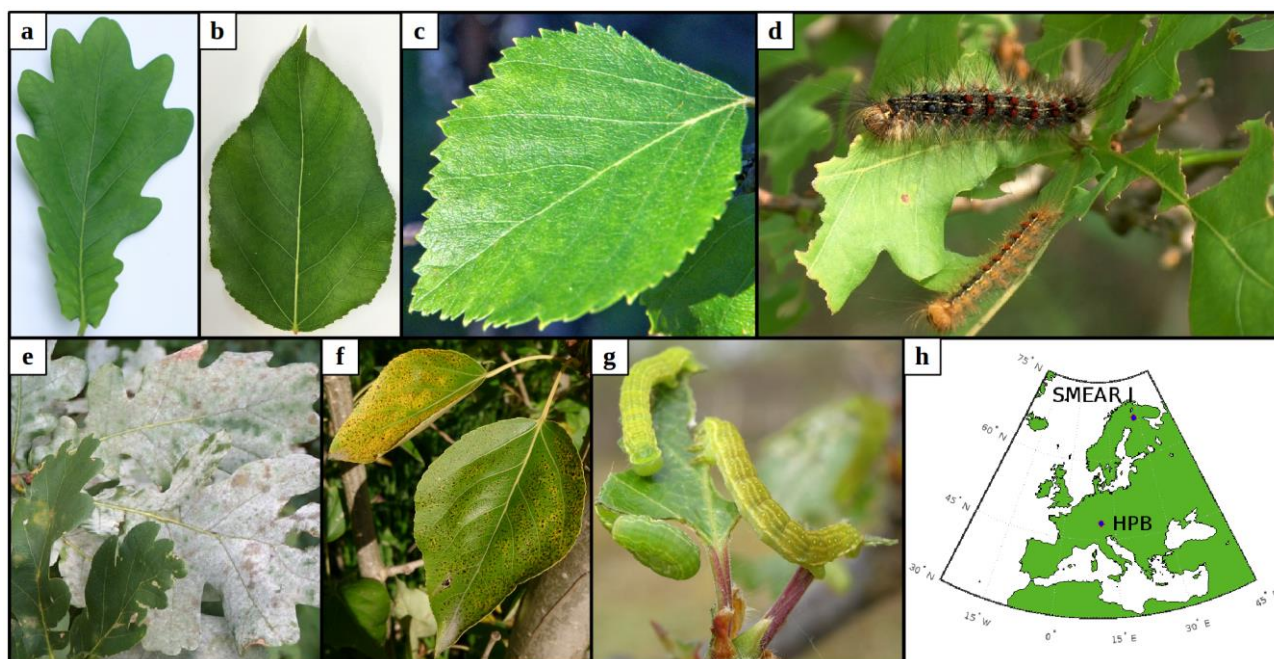
166

167
168 **Figure 1.** The plant species and biotic stresses we considered together with locations. Non-infected leaves; **(a)** pedunculate
169 oak (*Quercus robur*), **(b)** balsam poplar (*Populus balsamifera* var. *suaveolens*) and **(c)** mountain birch (*Betula pubescens* var.
170 *pumila*; former spp. *czerepanovii*). Fungal infected or moth infested leaves; pedunculate oak infested by **(d)** European gypsy
171 moth (*Lymantria dispar*) or infected by **(e)** oak powdery mildew (*Erysiphe alphitoides*), **(f)** poplar infected by rust fungus
172 (*Melampsora larici-populina*) and **(g)** mountain birch infested by autumnal moth (*Epirrita autumnata*). **(h)** location of the two
173 sites that serve as boundary conditions in our simulations. Photo courtesy: a+c: Juho Aalto, b: Yifan Jiang, d+e: Haruta Ovidiu,
174 University of Oradea, Bugwood.org, f: Ülo Niinemets, g: Tero Klemola.

175 **2.2 Simulations of fungal infection dynamics**

176 Oak powdery mildew (*Erysiphe alphitoides*) is one of the main foliar diseases of pedunculate oak (*Quercus robur*) in Europe
177 (Desprez-Loustau et al., 2011). Among the Melampsora species, *Melampsora larici-populina* is the most widespread poplar
178 rust (Vialle et al., 2011). *M. larici-populina* has five morphologically and functionally different spore stages during its life
179 cycle, where the two first stages are retrieved on larch and the last three on poplar (Vialle et al., 2011). The pathogenic fungal
180 infections do not decrease the leaf area of their victim, but as they cover the leaf, they absorb nutrients from the cells of the
181 leaf (Glawe, 2008) and change the physiology of the leaf (e.g. Major et al., 2010; Voegele and Mendgen, 2003; El-Ghany et
182 al., 2009). The severity and spread of fungal infections depend largely on weather and growth conditions (e.g. Åhman, 1998;
183 Johansson and Alström, 2000; Covarelli et al., 2013), where especially high rainfall in the beginning of the summer greatly
184 enhances both the severity, but also the onset of infection (Covarelli et al., 2013; Pinon et al., 2006). The onset of attack by
185 oak powdery mildew is limited by its morphological development, hence the infection usually starts to appear between the end
186 of June and August (in France; Marçais et al., 2009; Marçais and Desprez-Loustau, 2014; Bert et al., 2016). *M. larici-populina*
187 has been observed to attack young poplar trees as early as June (in Italy, Covarelli et al., 2013), though generally the disease
188 emerges between July and September (in France and Italy, Gérard et al., 2006; Covarelli et al., 2013). In our simulations, we
189 assumed that both fungi started to infect their host on 1st of August. In the case of *M. larici-populina* we only simulated the
190 attack on poplar as the host (and not larch). *Populus balsamifera* var. *suaveolens* was chosen as the poplar species due to the
191 availability of suitable published VOC emissions measurements. Based on Bert et al. (2016), we assumed that the severity of
192 infection increases linearly with time, starting on 1st of August and ending on 20th of September. We assumed that either 30 %
193 or 80 % of the total leaf area in the forest stands was covered by fungi by the end of the growing season (Fig. 2c,d). For these

5

194   simulations, our model incorporates the same atmospheric conditions as for simulations of gypsy moth infested oak. Poplar

195   bud burst occurs on 20th of April in our model (Tripathi et al., 2016) and we assumed the same timing of senescence as for

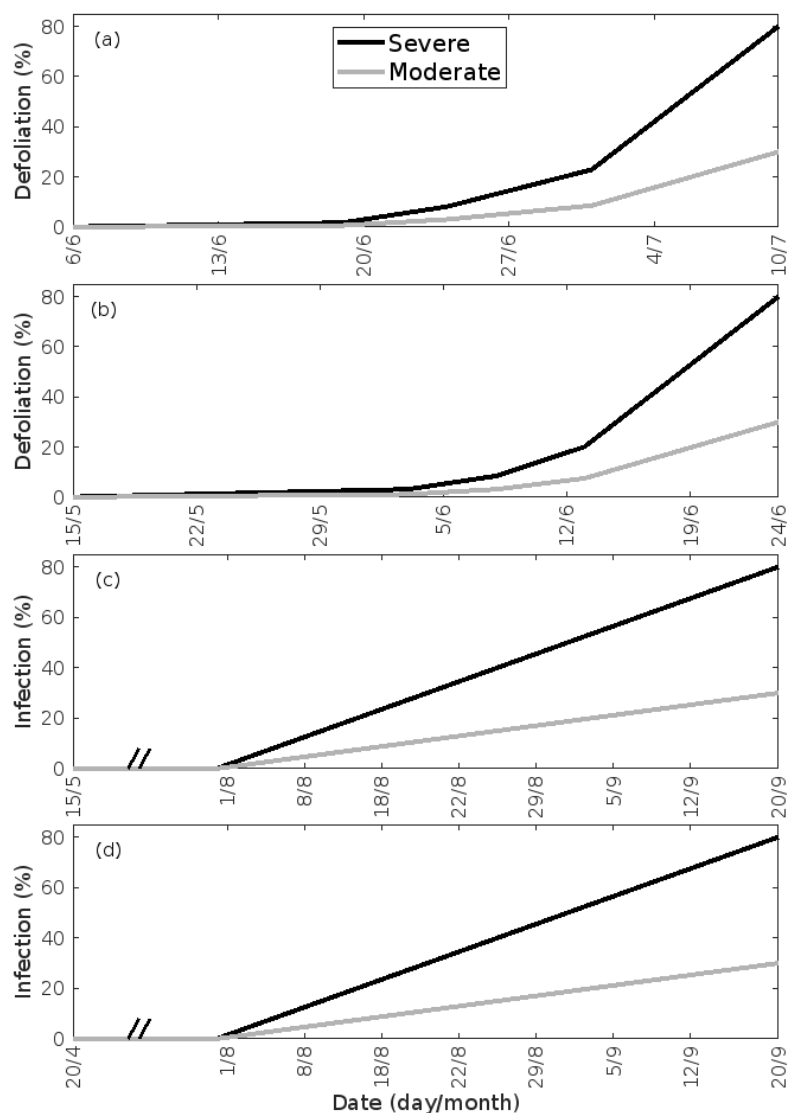196   simulations of oak (Gill et al., 2015; Tripathi et al., 2016).

197

198

199   **Figure 2.** Infection dynamics. **(a)** birch infested with autumnal moth larvae, **(b)** oak infested with European gypsy moth larvae,

200   **(c)** oak infected by oak powdery mildew and **(d)** poplar infected by rust fungus. The infection dynamics of oak powdery

201   mildew and rust fungus is assumed to be similar, but the duration of growth of the two tree species is different. The dynamics

202   are specific to the locations of Lapland **(a)** and central Europe **(b-d)**. 30 % (moderate infection scenario) or 80 % (severe

203   infection scenario) of the total leaf area in the forest stands is assumed to be consumed by the end of the feeding period or

204   infected by fungi by the onset of senescence. Note the different time axes.

205

206   **2.3 Treatment of the leaf area index**

207   Low soil temperatures usually prevent growth of a second leaf flush in birch trees (Aphalo et al., 2006). Thus, we assumed

208   that the leaf area index (LAI) of a non-infested mountain birch stand in Lapland increases linearly from $0 – 2.0$ m^2 m^{-2}

209   (Dahlberg et al., 2004) in the time period 6th-10th of June (bud burst to full leaf), and stays constant until the onset of senescence

210   (Fig. 3a). The LAI of an infested stand decreases proportionally with the level of defoliation (Fig. 3a). Refoliation only occurs

211   in totally, or near-totally, defoliated mountain birch trees (Kaitaniemi et al., 1997). Hence, we assumed that the LAI of a

212   heavily defoliated stand resumes to 70 % of the original LAI within three weeks of defoliation (personal communication with

adj. Prof. Dr. Pekka Kaitaniemi, University of Helsinki, Fig. 3a). Poplar trees produce leaves throughout the season, and we therefore assumed that the LAI of poplar stands increases quadratically from 20th of April (bud burst) until 15th of August (Fig. 3c, Tripathi et al., 2016). Oak, on the other hand, usually only produces one significant leaf flush, hence we assumed that the LAI of oak stands increases with a sigmoid shape from 15th of May (bud burst) until 4th of June (full leaf state attained) (Fig. 3b, Oláh et al., 2012). In our simulations, the maximum LAI of poplar and oak is 5.0 m^2 m^{-2}. The LAI of a gypsy moth infested oak stand decreases proportionally with the level of defoliation (Fig. 3b). The fungal infections do not decrease the leaf area of their host, nor do they prevent the tree from producing multiple flushes of leaves (Marçais and Desprez-Loustau, 2014). The LAI might, however, in reality be less in an infected stand than in a non-infected stand, though this depends highly on the specific genotypes and their individual fungal resistance (Verlinden et al., 2013; Shifflett et al., 2016), but naturally also on the timing of infection. Since most summer leaves already appear before the onset of infection, we did not assume a decrease in LAI. Severe powdery mildew infection (>50 %) has been shown to greatly reduce the infected leaf lifespan (Hajji et al., 2009). The median time before shedding of deformed oak leaves has been estimated to be 10-31 days (Hajji et al., 2009). In our scenario of a heavily infected stand (80 % of the stand leaf area is infected by the end of the season), an infection level of 50 % is reached on 1st of September. Since senescence is assumed to onset on 20th of September, we excluded an earlier shedding of leaves. Hence, in our simulations of fungal infections, we assumed that the LAI is the same as in a non-infected stand (Fig. 3b,c).
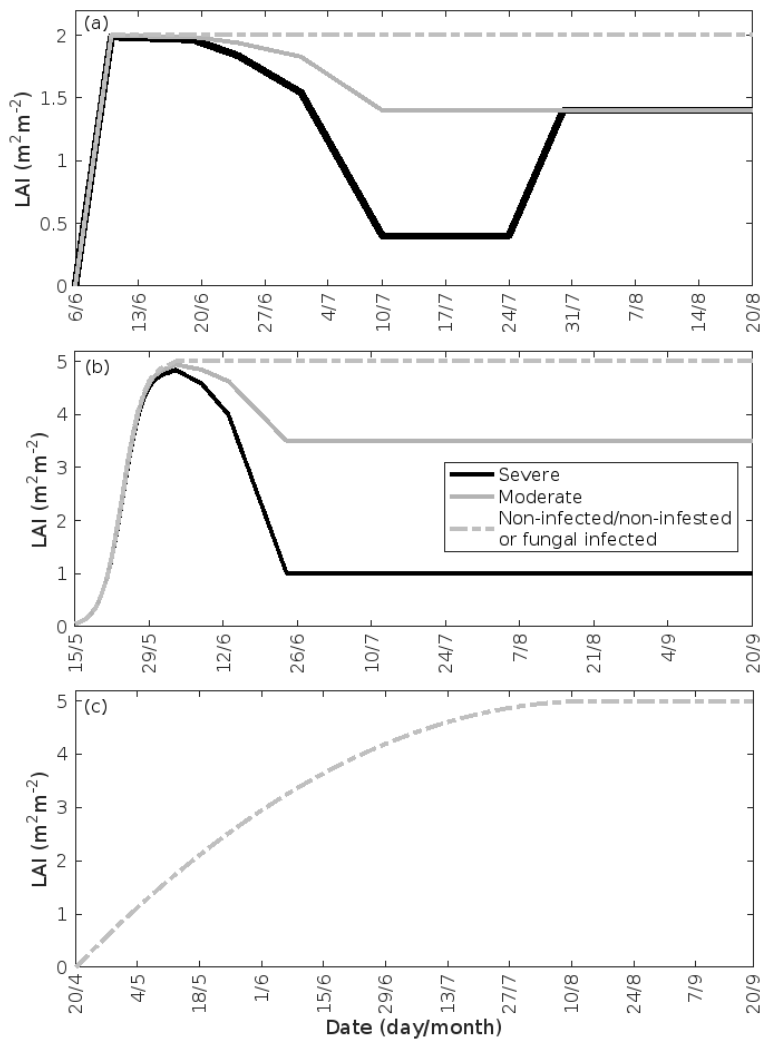

Figure 3. Leaf area index throughout the growing season in infected and non-infected forest stands. **(a)** mountain birch, **(b)** oak and **(c)** poplar. 30 % (moderate infection scenario) or 80 % (severe infection scenario) of the total leaf area in the forest

7

233 stands is assumed to be consumed by the end of the feeding period in simulations of herbivory, while fungal infections do not

234 decrease the leaf area. Note the different time axes.

235

2.4 Plant emissions of volatile organic compounds

237 The plant emissions (F_i) of individual VOCs (i) from various pure stands were computed as:

238 $$F_i = \varepsilon_i \times \text{LAI} \times \gamma_L \times \gamma_T \qquad\qquad (1)$$

239 where ε_i is the emission rate of i at standard conditions (25 ºC, 1000 µmol m^{-2} s^{-1}), LAI is the one-sided leaf area index and

240 treated as mentioned in Sec. 2.3, and γ_L and γ_T are the activity factors that account for changes in light and temperature from

241 standard conditions. This expression is adopted from Guenther et al. (2012), Eq. 1-2, when we assume that the soil moisture

242 and ambient CO_2 concentration in our stands are optimal. Generally, we excluded the effect of leaf age on the emissions of

243 VOCs, since we do not know the effect of leaf age on stress-induced emissions. However, we also tested whether the impact

244 of leaf maturity would be able to change the conclusions of our study when making certain assumptions about the leaf age

245 effect. The treatment of the leaf age effects and the results of these tests are presented in Appendix B and discussed in Sec.

246 3.2.

247 Similarly to e.g. Simpson et al. (1999; 2012) and Bergström et al. (2014), we utilised a simple non-canopy approach,

248 where ambient and leaf temperature are assumed to equal, and where the use of branch-level emission factors accounts for the

249 canopy shading effect (Guenther et al., 1994). We utilised emission rates, reported as a function of the degree of damage, from

250 Copolovici et al. (2017; 2014), Jiang et al. (2016), and Yli-Pirilä et al. (2016). The emission rates reported by Copolovici et al.

251 (2017; 2014) and Jiang et al. (2016) were all retrieved by leaf-level measurements, hence we decreased the reported emission

252 rates by a factor of 0.57, since branch-level emission factors for light sensitive emissions are typically a factor of 1.75 smaller

253 than the corresponding leaf-level values (Simpson et al., 1999; 2012). We did not decrease the emission rates reported by Yli-

254 Pirilä et al. (2016), since these were based on measurements of the whole plant. Instead, the emission rates from mountain

255 birch seedlings (Yli-Pirilä et al., 2016) were upscaled in order to represent the emissions from mature trees, assuming a leaf

256 mass area of 75 g m^{-2} for leaves growing on mature mountain birch trees (Riipi et al., 2005). Since emission response

257 measurements are usually stopped, at a maximum, a few days after the herbivore activity has ceased, we assumed that the

258 effect of stress on the emissions of VOC stops the day that the larvae pupate (e.g. Yli-Pirilä et al., 2016), in order to not

259 overestimate the impact of the stress. The light and temperature dependent emission activity factors are computed using Eq. 2

260 in Guenther (1997), since none of the considered broadleaved species poses storages and birch has specifically been shown to

261 only emit *de novo* (Ghirardo et al., 2010). Similarly to Guenther et al. (2012), we assumed that stress-induced emissions are

262 controlled by light and temperature in a similar way as constitutive emissions, thus the used emission rates from the literature

263 were standardised according to Eq. 1. Copolovici et al. (2014) and Jiang et al. (2016) have also shown that the emissions of

264 isoprene from oak powdery mildew and rust infected oaks and poplars have the same response to light as control plants.

265 Copolovici et al. (2014) additionally demonstrated that the emissions of monoterpenes from oak powdery mildew infected oak

266 depend strongly on light, even though the majority of emitted monoterpenes were not e.g. ocimene and linalool, which are

267 known to be light dependent (Niinemets et al., 2002; Arimura et al., 2008). LOX (lipoxygenase pathway volatile) compounds,

268 on the other hand, are released shortly after damage of leaf tissue, independent of the light conditions (Arimura et al., 2008).

269 LOX compounds do not contribute to the formation and growth processes of atmospheric aerosol particles, but they were

270 included in the model in order to illustrate the changes in the atmospheric concentrations of LOX as a function of stress severity

271 and stress type, and for evaluating the reliability of our modelling results, since LOX, in reality, affect the atmospheric

272 concentration of OH, which was constrained in the model. The equations, which we used in the model for linking the emission

273 factors to the severity of stress, are provided in Table 1 together with the parameters needed for the equations. The emission

factors at a few different degrees of stress are written out in Table A1 in Appendix A. It was assumed that the emitted VOCs were instantaneously evenly distributed within the mixing volume, which is defined by the boundary layer height.

Table 1. Equations to calculate the emission factors ($\varepsilon_{i,\text{Æ}}$, in unit nmol m^{-2} one-sided LAI s^{-1}), as a function of the degree of stress (Æ), together with the parameters needed for the equations. The equations are valid for infection levels ranging from 0 % to 80 % unless otherwise stated. The emission factors for oak and poplar are presented without the downscaling by a factor of 0.57 (see bulk text in Sec. 2.4). LMA$_f$ is the fraction of the leaf mass area of leaves growing on mature mountain birch / growing on mountain birch seedlings, which is included so that the emission factors for mountain birches are also representative of mature trees. ISO = isoprene, MT = monoterpenes, MeSa = methyl salicylate, LOX = lipoxygenase pathway volatile compounds, DMNT = 4,8-dimethyl-1,3,7-nonatriene, MeOH = methanol, SQT = sesquiterpenes, α-Eud = α-Eudesmol.

Infestation of pedunculate oak (*Quercus robur*) by European gypsy moth (*Lymantria dispar*) based on Copolovici et al. (2017).						
VOC	$\varepsilon_{i,\text{Æ}}$ (nmol m^{-2} s^{-1})	$\varepsilon_{i,0}$ (nmol m^{-2} s^{-1})	A (nmol m^{-2} s^{-1})	B	C (nmol m^{-2} s^{-1})	
ISO	$\varepsilon_{i,0} + \dfrac{\text{Æ} \times A}{B + \text{Æ}},\ \ 0 \le \text{Æ} \le 60$ $\varepsilon_{i,60} \times 0.5,\ \ \ 60 < \text{Æ} \le 80$	30.26	-47.40	34.48		
MT	$\varepsilon_{i,0} + \dfrac{\text{Æ} \times A}{B + \text{Æ}}$	$4.0 \cdot 10^{-2}$	9.22	33.42		
MeSa	$\text{Æ} \times A$		$3.5 \cdot 10^{-3}$			
LOX	$A \times \text{Æ}^2 + C \times \text{Æ}$		$1.1 \cdot 10^{-3}$		$4.7 \cdot 10^{-2}$	
DMNT	$A \times \text{Æ}^2 + C \times \text{Æ}$		$1.0 \cdot 10^{-5}$		$1.3 \cdot 10^{-3}$	
Infection of pedunculate oak (*Quercus robur*) by oak powdery mildew (*Erysiphe alphitoides*) based on Copolovici et al. (2014)						
VOC	$\varepsilon_{i,\text{Æ}}$ (nmol m^{-2} s^{-1})	$\varepsilon_{i,0}$ (nmol m^{-2} s^{-1})	A (nmol m^{-2} s^{-1})	B (nmol m^{-2} s^{-1})	C (nmol m^{-2} s^{-1})	
ISO	$\varepsilon_{i,0} + A \times \text{Æ} + B \times \text{Æ}^2 + C \times \text{Æ}^3$	10.6	-0.244	$3.69 \cdot 10^{-3}$	$-2.05 \cdot 10^{-5}$	
MT	$\varepsilon_{i,0} + A \times \text{Æ} + B \times \text{Æ}^2 + C \times \text{Æ}^3$	$4.0 \cdot 10^{-2}$	$8.7 \cdot 10^{-3}$	$-7.1 \cdot 10^{-5}$	$3.7 \cdot 10^{-7}$	
MeSa	$0,\ \ \text{Æ} = 0$ $A \times \dfrac{\varepsilon_{MT,\text{Æ}}}{\varepsilon_{MT,60}}, 0 < \text{Æ} \le 80$		0.437			
LOX	$A + B \times \text{Æ}$		$2.13 \cdot 10^{-3}$	$6.24 \cdot 10^{-3}$		
Infection of balsam poplar (*Populus balsamifera* var. *suaveolens*) by poplar rust (*Melampsora larici-populina*) based on Jiang et al. (2016)						
VOC	$\varepsilon_{i,\text{Æ}}$ (nmol m^{-2} s^{-1})	$\varepsilon_{i,0}$ (nmol m^{-2} s^{-1})	A (nmol m^{-2} s^{-1})	B (nmol m^{-2} s^{-1})	C	E (nmol m^{-2} s^{-1})

VOC	$\varepsilon_{i,Æ}$ (nmol m^{-2} s^{-1})	A	B	C	E (nmol m^{-2} s^{-1})	LMA$_f$
ISO	$A + \dfrac{B}{C + Æ}$		12.3	366.8	4.98	
MT	$0.0625,\ Æ = 0$; $A + B \times Æ + E \times Æ^2,\ 0 < Æ \leq 80$		0.112	$1.84 \cdot 10^{-3}$		$1.5 \cdot 10^{-4}$
MeSa	$A \times Æ + B \times Æ^2 + E \times Æ^3$		$6.32 \cdot 10^{-3}$	$-8.6 \cdot 10^{-5}$		$5.75 \cdot 10^{-7}$
LOX	$0.4814,\ Æ = 0$; $(A + B \times Æ + E \times Æ^2) \times C,\ 0 < Æ \leq 80$		2.51	$-2.51 \cdot 10^{-2}$	$0.76,\ 0 < Æ < 30$; $0.85,\ 30 \leq Æ < 60$; $0.93,\ 60 \leq Æ \leq 80$	$3.25 \cdot 10^{-3}$
DMNT	$\varepsilon_{DMNT,60} \times \dfrac{\varepsilon_{MeSa,Æ}}{\varepsilon_{MeSa,60}},\quad 0 \leq Æ < 60$; $\varepsilon_{MeSa,Æ} \times C,\quad 60 \leq Æ \leq 80$				0.36	
MeOH	$\varepsilon_{i,0} + A \times Æ + B \times Æ^2$	16.9	-0.338	$1.36 \cdot 10^{-2}$		
SQT	$\varepsilon_{SQT,60} \times \dfrac{\varepsilon_{MeSa,Æ}}{\varepsilon_{MeSa,60}},\quad 0 \leq Æ < 60$; $\varepsilon_{MeSa,Æ} \times C,\quad 60 \leq Æ \leq 80$				2.414	
α-Eud	$\varepsilon_{\alpha-Eud,60} \times \dfrac{\varepsilon_{MeSa,Æ}}{\varepsilon_{MeSa,60}},\quad 0 \leq Æ < 60$; $\varepsilon_{MeSa,Æ} \times C,\quad 60 \leq Æ \leq 80$				0.397	
Infestation of mountain birch (*Betula pubescens* var. *pumila*) by autumnal moth (*Epirrita autumnata*) based on Yli-Pirilä et al. (2016)						
VOC	$\varepsilon_{i,Æ}$ (nmol m^{-2} s^{-1})	A	B	C	E (nmol m^{-2} s^{-1})	LMA$_f$
MT	$\left(A + \dfrac{Æ \times B}{\sqrt{1 + \dfrac{B^2 \times Æ^2}{C^2}}}\right) \times E \times LMA_f$	$7.65 \cdot 10^{-2}$	$9.33 \cdot 10^{-3}$	0.2146	0.769	2.23
LOX	$(A \times Æ + B) \times E \times LMA_f$	$6.325 \cdot 10^{-3}$	$4.868 \cdot 10^{-2}$		0.8	2.23
DMNT	$\left(A + \dfrac{Æ \times B}{\sqrt{1 + \dfrac{B^2 \times Æ^2}{C^2}}}\right) \times E \times LMA_f$	$7.11 \cdot 10^{-4}$	$3.39 \cdot 10^{-4}$	$8.63 \cdot 10^{-3}$	0.769	2.23
SQT	$\dfrac{\varepsilon_{MT,Æ}}{3}$					

284

2.5 Meteorological conditions

The daily maximum radiation during the entire growing season was fixed to 1000 μmol m^{-2} s^{-1} (Table 2), which corresponds to the average maximum photosynthetic photon flux density (PPFD) observed at the SMEAR I station during the growing seasons of 2015-2017 (Aalto et al., 2019). The daily pattern of PPFD then follows the solar zenith angle. For simulations of

mountain birch, we utilised the maximum and minimum mean temperatures on every day in the growing season during 2015-2017 observed at 9 m at the SMEAR I station (Aalto et al., 2019). The daily maximum and minimum temperatures ranged from 9.8 to 19.6 ºC, and from 2.0 to 11.3 ºC, respectively, in the time period of interest (6th of June - 20th of August, Fig. 4a). For simulations of oak and poplar, we utilised the maximum and minimum temperatures for southern Germany averaged over the past three decades (data obtained via https://www.currentresults.com/Weather/Germany/average-annual-temperatures.php). This was done due to availability and restriction of data obtained at the Hohenpeißenberg Meteorological Observatory and since our aim was not as such to simulate the atmospheric impact at Hohenpeißenberg, but instead at any relevant location, i.e. where oaks and poplars, including the biotic stresses of interests, are common. The monthly averaged daily maximum and minimum temperatures ranged from 15 to 26 ºC, and from 6 to 16 ºC, respectively, in the time period of interest (April - September, Fig. 4b). For simplicity, the daily temperature pattern followed that of the solar zenith angle with a forward shift of 1 h. The default daytime mixing length was kept constant to a value of 700 m (simulations of mountain birch) and 2000 m (simulations of oak and poplar) above ground level (Seidel et al., 2012) (Table 2).

Table 2. Model inputs. Representative summer time conditions in rural central Europe (here indicated by HPB: the Hohenpeißenberg Meteorological Observatory) and Lapland (here indicated by the SMEAR I station), used as default model input. The conditions are chosen such that they are realistic and representative, but they do not inhibit the formation of new particles. The concentrations of OH and sulfuric acid are provided as daily maxima in the table, but their concentrations decrease as a function of the decrease in solar light in the simulations. The concentration of ozone and the condensation sink (CS) are both kept constant throughout the simulations. BLH is the planetary boundary layer height. The photosynthetic photon flux density (PPFD) is provided as the daily maximum in the table, but the daily pattern of PPFD follows the solar zenith angle in the model.

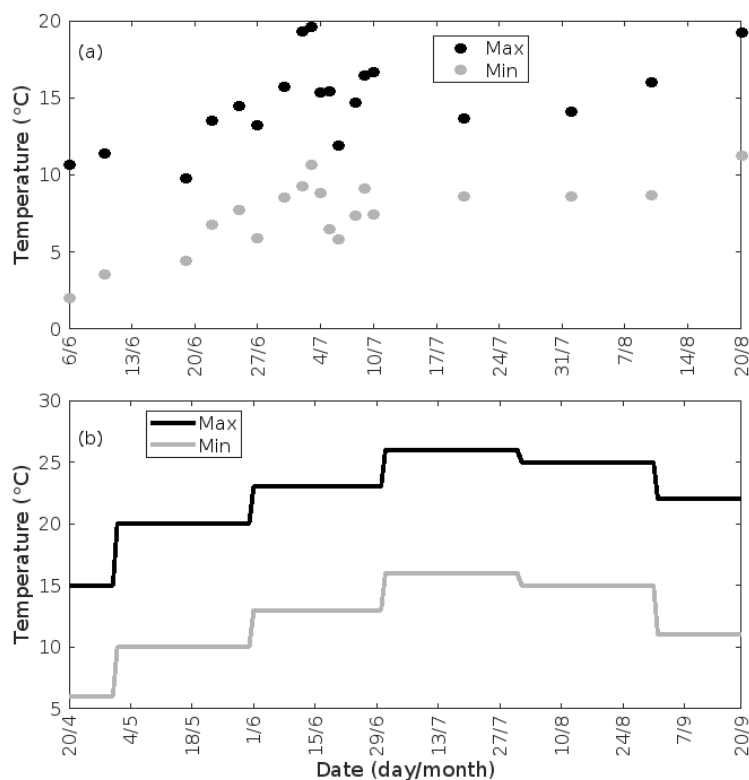|	HPB	SMEAR I
$[O_3]$ (ppb)	45	30
$[OH]_{max}$ (molec cm^{-3})	$6 \cdot 10^6$	$8 \cdot 10^5$
$[H_2SO_4]_{max}$ (molec cm^{-3})	$1 \cdot 10^7$	$2.5 \cdot 10^6$
CS (s^{-1})	$2.5 \cdot 10^{-3}$	$7 \cdot 10^{-4}$
BLH (m)	2000	700
PPFD$_{max}$ (μmol m^{-2} s^{-1})	1000	

Figure 4. Daily maximum and minimum temperatures throughout the growing season at **(a)** SMEAR I, Lapland, and **(b)** Southern Germany, used as default model input. Note the different time axes.

2.6 Atmospheric gas phase chemistry

We constrained the concentrations of atmospheric oxidants within the model, though in reality, the concentration of atmospheric oxidants can decrease or increase depending on changes in the concentrations of individual specific VOCs (Table 3). This was done, partly because it is difficult to accurately predict the concentration of oxidants (e.g. Di Carlo et al., 2004; Sinha et al., 2010; Mogensen et al., 2011, 2015; Nölscher et al., 2012, 2016; Zannoni et al., 2016; Praplan et al., 2019; Lelieveld et al., 2008; Taraborrelli et al., 2012), and partly because accounting for varying oxidant concentrations is not necessary for the objectives of our study (Sec. 3.2, Fig. 11a-b,f-g,k-l,p-q). Thus, in our simulations, the default daily maximum concentration of OH is therefore fixed to $6 \cdot 10^6$ molec cm^{-3} (Petäjä et al., 2009) and $8 \cdot 10^5$ molec cm^{-3} (calculated using observed summertime UVB radiation from the SMEAR I station and the proxy presented by Petäjä et al. (2009)) for simulations of Hohenpeißenberg and Lapland, respectively (Table 2). The daily pattern of the OH concentration then follows the solar zenith angle. The concentration of ozone is kept constant to a value of 45 ppb (Naja et al., 2003) and 30 ppb (Ruuskanen et al., 2003) for simulations of oak and poplar (Hohenpeißenberg conditions) and mountain birch (SMEAR I conditions), respectively (Table 2). NO$_3$ was not considered, since emission and atmospheric processes were only simulated during day time, when the concentration of NO$_3$ is insignificant.

The only source of sulfuric acid (H$_2$SO$_4$), in our model, is the reaction between OH and SO$_2$, while the only sink is the condensation sink. The concentration of SO$_2$ is chosen such that the default daytime maximum concentration of H$_2$SO$_4$ is $1 \cdot 10^7$ molec cm^{-3} in Hohenpeißenberg (Petäjä et al., 2009; Birmili et al., 2003) and $2.5 \cdot 10^6$ molec cm^{-3} in Lapland (Kyrö et al., 2014) (Table 2). The size distribution of the pre-existing particle population is kept fixed during the simulations, so the number concentration of pre-existing particles is defined by the condensation sink (CS), which is kept constant to a value of $2.5 \cdot 10^{-3}$ s^{-1} (in rural southern Germany) and $7 \cdot 10^{-4}$ s^{-1} (in Lapland; Dal Maso et al., 2007; Vana et al., 2016) (Table 2).

We included reactions for the atmospheric oxidation of SO$_2$ and the emitted VOCs (Appendix C). Certain VOCs, and especially VOCs with endocyclic double bonds, can form HOM (highly oxygenated organic molecules) upon oxidation by, in

particular O_3, but also OH and NO_3 (e.g. Ehn et al., 2012, 2014; Jokinen et al., 2015; Berndt et al., 2016; Bianchi et al., 2019; Zhao et al., 2020). HOM have been found to be a major component of secondary organic aerosol (e.g. Ehn et al., 2014; Mutzel et al., 2015). HOM yields are specific to individual molecules and isomers and most yields have not been investigated for the exact compounds, which are emitted from the tree species considered in this study. Thus, the yields applied for the production of HOM in the model (Appendix C) are connected with a large degree of uncertainty. The influence of changing HOM yields on our results was therefore also investigated (Sec. 3.2, Fig. 11e,j,o,t). Formation of oxygenated organics from oxidation of sesquiterpenes and methyl salicylate are also included (Appendix C). The sum of all organic compounds, which contribute to aerosol processes, is referred to as "OxOrg". The chemistry was solved by the ordinary differential equation solver DLSODE (Radhakrishnan and Hindmarsh, 1993), and it was assumed that the concentrations of all considered atmospheric molecules were homogeneously distributed within the mixing volume.

Table 3. Common changes in the atmospheric concentrations of volatile organic compounds (VOC) and OH during biotic plant stress. LOX are lipoxygenase pathway volatile compounds.

	Change in VOC concentration	Change in OH concentration	Reference
Stress↑	[LOX]↑ [methyl salicylate]↑ [methanol]↑ [monoterpenes]↑	[OH]↓	Mentel et al. (2013) Calvert et al. (2000) Atkinson et al. (1992) Hakola et al. (1994)
	[sesquiterpenes]↑	[OH]↑	Atkinson and Arey (2003) Winterhalter et al. (2009)
	[isoprene]↓	[OH]?, but most probably [OH]↑	Lelieveld et al. (2008) Taraborrelli et al. (2012) Wells et al. (2020)

2.7 Calculation of the formation and growth of secondary organic aerosol particles

The clustering and activation of new particles are expressed by a formation rate of neutral 2 nm sized clusters, J_2 (cm^{-3} s^{-1}), which is computed by Eq. 20, using coefficients (α_{1-3}) from Table 3, both found in Paasonen et al. (2010):

$$J_2 = \alpha_1 \times [H_2SO_4]^2 + \alpha_2 \times [H_2SO_4][OxOrg] + \alpha_3 \times [OxOrg]^2 \tag{2}$$

It is here assumed that new particles are formed via heteromolecular homogeneous nucleation between sulfuric acid and oxidised organic compounds (OxOrg) as well as via homogeneous nucleation of sulfuric acid and OxOrg alone. For simplification, we only operated with one growing aerosol mode and therefore included a unit-less correction term (KK), which determines how large a fraction of the activated clusters reaches the growing mode (Kerminen and Kulmala, 2002):

$$KK = exp\left(\eta \times [1/D_p - 1/D_{clus}]\right) \tag{3}$$

where D_p and D_{clus} are the diameters of the growing mode and clusters, respectively, and D_{clus} = 2 nm as stated above. Further, η (nm) is (Eq. 11-12 and Table 1 in Kerminen and Kulmala, 2002):

$$\eta = 1830 \text{ nm}^2 \cdot s \cdot h^{-1} \times CS/GR \tag{4}$$

where CS (s^{-1}) is the condensation sink. When used together with Eq. 3, the value of CS is that of sulfuric acid. The condensational particle diameter growth rate (GR, nm h^{-1}) of newly formed 2-3 nm particles is calculated according to Nieminen et al. (2010):

$$GR_{2-3 \text{ nm}} = 0.5 \text{ nm} \cdot h^{-1} \times CC \times 10^{-7} \text{ cm}^3 \tag{5}$$

where CC is the concentration of condensable vapours which we assumed to be the sum of sulfuric acid and OxOrg. In addition, we assumed that the molar mass of OxOrg are 3.5 times larger than that of sulfuric acid (Ehn et al., 2014), hence:

369 $CC = [H_2SO_4] + [OxOrg] \times 3.5^{1/3}$ (6)

370 It is a complex matter to model nanoparticle growth, especially in forested environments, since thousands of individual

371 molecules with different vapour pressures contribute to the growth, but particle growth rates have been observed to be strongly

372 size-dependent in the field (Hirsikko et al., 2005; Yli-Juuti et al., 2011; Häkkinen et al., 2013). Hence, we accounted for this

373 size-dependency by enhancing the growth rates of particles larger than 3 nm, as according to Hirsikko et al. (2005) and Yli-

374 Juuti et al. (2011):

375 $GR_{3-7\,nm} = 2 \times GR_{2-3\,nm}$ (7)

376 $GR_{>7\,nm} = 2.3 \times GR_{2-3\,nm}$ (8)

377 The increase in the diameter of the growing mode (D_p) is defined by the growth rate:

378 $\Delta D_p/\Delta t = GR/3600\,s \cdot h^{-1}$ (9)

379 while the increase in the number of new particles (N_p, cm^{-3}) is determined by the formation of new particles which reaches

380 the growing mode and the coagulation of particles in the growing mode by:

381 $\Delta N_p/\Delta t = J_2 \times KK - CoagS \times N_p$ (10)

382 where the coagulation sink (CoagS, s^{-1}) is calculated according to (Lehtinen et al., 2007):

383 $CoagS = CS \times \left(0.71\,nm/D_p\right)^{1.6}$ (11)

384

3 Results and discussion

3.1 Simulations of biotically stressed and non-infected forest stands throughout a growing season

387 Simulation results of one full growing season from various non-infected, and moderately and severely infected forest stands

388 are presented in Figs. 5-9. In the figures, emissions, concentrations, the isoprene-to-monoterpenes carbon concentration ratio

389 (R = [isoprene C]/[monoterpenes C] = 0.5·[isoprene]/[monoterpenes]), the formation and growth rates, and number of newly

390 formed particles are expressed as median values during 10:00-16:00 local time, while the particle diameter of the growing

391 mode is provided as the daily maximum. We underline that our modelling study is of a conceptual character and that the

392 modelling results therefore also should be treated accordingly. Modelling results are compared in detail to observations in the

393 sections below in order to put our findings into perspective.

394

3.1.1 Canopy emissions of VOCs

396 The emissions of VOCs (Figs. 5a,c,e,g, 7a,b, 8a,b, 9a-c) change throughout the season due to variations in temperature, light,

397 LAI and infection severity. The impact of leaf maturity development on emission predictions are presented in Appendix B and

398 its atmospheric relevance discussed in Sec. 3.2. Canopy emissions of VOCs are highly different from non-infected and infected

399 forest stands, due to plant stress responses, but also due to a decrease in LAI in case of larval infestations (Figs. 5a,c,e,g, 9a-

400 c). Constitutive isoprene emitters (i.e. oak and poplar) decrease their emissions of isoprene significantly during the episodes

401 of biotic stress, and a stronger reduction is observed as a function of an increase in stress severity (Figs. 5a, 7a, 8a). All

402 investigated stresses cause the plants to increase their emissions of monoterpenes greatly (Figs. 5c, 7b, 8b, 9a). The induction

403 in the emissions of monoterpenes increases as a function of stress severity per unit leaf area, but the LAI simultaneously

404 decreases in case of larval infestations, which result in smaller canopy scale emissions from severely defoliated stands

405 compared to moderately stressed stands (Figs. 5c, 9a). Also the emissions of compounds, and groups of compounds, such as

406 methyl salicylate, LOX, methanol, DMNT, sesquiterpenes and oxygenated sesquiterpenes are significantly increased as a result

407 of biotic plant stress (Figs. 5e,g, 7a,b, 8a,b, 9b,c). These compounds, together with monoterpenes, are in most cases not emitted

408 constitutively at all or only in very small abundances from the considered tree species. Though the emissions of all induced

409 VOCs increase as a function of the degree of damage, the responses to the level of stress severity are not necessarily the same

410 for all VOCs and all individual stresses. This difference can, for example, be seen in the emissions of monoterpenes (Fig. 5c)

411 and LOX compounds (Fig. 5e) from gypsy moth infested oak forests, which do not peak at the same time in the season.

412

3.1.2 Ambient concentrations of VOCs and OxOrg

414 Since the concentrations of OH and O_3 are constrained within the simulations, the VOC emission patterns are reflected in the

415 concentration patterns (Figs. 5b,d,f,h, 7c-e, 8c-e, 9e-g). All VOCs, except LOX and methanol, contribute to the formation of

416 OxOrg (Figs. 6a, 7c, 8c, 9d), but the contributions from oxidation of the individual VOCs, or groups of VOCs, vary between

417 the various stress cases and infection severity levels due to differences in emission rates and OxOrg forming yields (Appendix

418 C). For example, in herbivory infested stands, OxOrg originating from monoterpenes make up by far the largest fraction of

419 total OxOrg. This is mainly due to the fact that the induced emissions of monoterpenes are significantly higher than the

420 emissions of other VOCs which contribute to OxOrg formation (Figs. 5c,g, 9a,c). In case of oak powdery mildew infected oak,

421 HOM from monoterpenes and oxygenated organics from methyl salicylate reactions contribute about evenly to the total OxOrg.

422 The reason for this is that the canopy emissions of these VOCs are roughly similar (Fig. 7a,b), the OxOrg yield of methyl

423 salicylate is significantly higher than that of monoterpenes, but oxidation of methyl salicylate is correspondingly slower

424 (Appendix C). The main contributor to the total OxOrg in poplar rust infected poplar stands is sesquiterpenes. Contributions

425 from methyl salicylate, DMNT and α-Eudesmol to total OxOrg are individually rather small, but together, they are close to

426 matching the contribution from monoterpenes. When emissions of sesquiterpenes are omitted from simulations of a severely

427 rust infected poplar stand, the concentration of OxOrg decreases with ~46 %, while, in comparison, the concentration of OxOrg

428 decreases with ~30 % if the emissions of monoterpenes are instead excluded.

429   In the simulations, the daily median (10:00-16:00) ambient concentration of OxOrg is at maximum ~4.2×10^7 cm^{-3} in

430 a gypsy moth infested oak stand (Fig. 6a), ~1.1×10^7 cm^{-3} in an oak powdery mildew infected oak stand (Fig. 7c), ~4.2×10^7

431 cm^{-3} in a rust infected poplar stand (Fig. 8c), and ~3.3×10^7 cm^{-3} in an autumnal moth infested mountain birch stand (Fig. 9d).

432 The ambient concentration of OxOrg is much higher in gypsy moth infested oak stands, than in a non-infested oak stand,

433 during the period of stress (Fig. 6a). When the period of feeding has been concluded, the concentration of OxOrg is higher in

434 non-infested oak stands than in stands that have been exposed to stress due to a higher LAI. However, the concentration of

435 OxOrg is then only ~15-20 % of the OxOrg concentration during the period of stress and it is almost exclusively composed of

436 HOM originating from isoprene. The concentration of OxOrg increases as a function of fungal infection severity, and in our

437 simulations the concentration of OxOrg is higher in fungally infected stands by a factor of up to ~6.9 (oak powdery mildew

438 infected oak stands, Fig. 7c) and ~3.3 (poplar rust infected poplar stands, Fig. 8c). Since the investigated poplar species is a

439 great constitutive isoprene emitter, relatively high concentrations of OxOrg are predicted for the non-infected poplar stand

440 (Fig. 8c). In mountain birch stands, the concentration of OxOrg is up to 2-2.5 times higher in autumnal moth infested stands

441 during the feeding period than in a non-infested birch stand (Fig. 9d). The difference in OxOrg concentration between

442 moderately and severely infested birch stands is small, due to the combined effects of stress response (which is a function of

443 the degree of damage) and LAI reduction (Fig. 9d), but towards the conclusion of the feeding period, the concentration of

444 OxOrg is significantly higher in the less defoliated stand.

445

3.1.3 Formation of new particles

447 New particles are assumed to be formed from OxOrg and sulfuric acid (Sec. 2.7, Eq. 2). Since the concentration of sulfuric

448 acid is constrained within the simulations, the concentration pattern of OxOrg is reflected in the seasonal pattern of the

449 formation rates (Figs. 6c-e, 7f, 8f, 9h,i). Thus, in case of gypsy moth infested oak, the formation rates are much higher (increase

15

by up to a factor of ~5 (J_2), ~7 (J_3), and ~11 (J_{10})) in stressed stands than in non-infested stands during the period when the plants are exposed to stress (Figs. 6c-e). The predicted J_2 in gypsy moth infested oak stands is comparable to e.g. observations from Melpitz, Germany (~9.4 cm^{-3} s^{-1}, Paasonen et al., 2010) and San Pietro Capofiume, Italy (~13 cm^{-3} s^{-1}, Paasonen et al., 2010). Both Melpitz and San Pietro Capofiume are rural sites influenced by anthropogenic pollution (Paasonen et al., 2010). The modelled J_2 in a non-infested oak stand is comparable to observations from Hohenpeissenberg (~2.3 cm^{-3} s^{-1}, Paasonen et al., 2010) and similar or even higher than typical formation rates measured in the boreal Scots pine forest in Hyytiälä, Finland (~1-2 cm^{-3} s^{-1}, Paasonen et al., 2010; Kulmala et al., 2012, 2013; Vana et al., 2016) and in the hemiboreal forest in Järvseljä, Estonia (~1.09±1.06 cm^{-3} s^{-1}, Vana et al., 2016). By analysing data from Hyytiälä and Järvseljä, Vana et al. (2016) showed that the values of J_3 were in general about 60-80 % of those of J_2. Our simulations of a non-infested oak stand follow this threshold, thus, the predicted J_3 in a non-infested oak stand is somewhat higher than observations from Hyytiälä (~0.6 cm^{-3} s^{-1}, Kulmala et al., 2012, 2013; Nieminen et al., 2014; Vana et al., 2016) and Järvseljä (~0.8 cm^{-3} s^{-1}, Vana et al., 2016). J_3 in gypsy moth infested oak stands is high, but similar values have occasionally been observed in Hyytiälä (up to about 10 cm^{-3} s^{-1}, Nieminen et al., 2014). Formation rates of 5 nm particles (J_5=1.0±1.1 cm^{-3} s^{-1}, Yu et al., 2014) measured in an oak forest in Missouri, USA, are much less than J_{10} in our simulated infested stands, and so are e.g. also formation rates of 10 nm particles (J_{10}=1.2 cm^{-3} s^{-1}, Yli-Juuti et al., 2009) measured in a mixed forest in K-puszta, rural Hungary. Thus, the predicted formation rates in a non-infested oak stand are comparable, and in the case of gypsy moth infested oak stands, often much higher than observations from forests with intense new particle formation events.

The formation rates of new particles are always higher in oak powdery mildew infected oak stands than in a non-infected oak stand (Fig. 7f), though the fungus is not able to perturb the formation rates as strongly (increase by up to a factor of ~2.3 (J_2), ~3.0 (J_3), and ~5.3 (J_{10})) as herbivory by gypsy moth larvae.

Simulations of poplar stands suggest that particles will be formed at high rates in the range ~3.6-11.4 cm^{-3} s^{-1} (J_2) and ~2.7-10.6 cm^{-3} s^{-1} (J_3) during the late summer when the full leaf state has been attained, and our simulations suggest that new particles will be formed the fastest in severely rust infected stands (increase by up to a factor of ~3.2 (J_2), and ~3.9 (J_3)).

In our simulations, herbivory by autumnal moth increases the formation rates of new particles in mountain birch stands by up to a factor of ~2.5 (J_2) and ~2.6 (J_3). The formation rates of 2 and 3 nm particles are predicted to vary between 0.38 cm^{-3} s^{-1} and 2.5 cm^{-3} s^{-1} (J_2), and 0.31 cm^{-3} s^{-1} and 2.5 cm^{-3} s^{-1} (J_3) in stressed stands, and between 0.32 cm^{-3} s^{-1} and 1.1 cm^{-3} s^{-1} (J_2), and 0.26 cm^{-3} s^{-1} and 0.99 cm^{-3} s^{-1} (J_3) in non-infested stands. The higher end of these values is comparable to rates observed in Hohenpeissenberg and Hyytiälä (see above). Kyrö et al. (2014) reported that the monthly averaged formation rate of 3 nm particles during 2005 - 2011, at the SMEAR I station in Värriö, varied throughout the year by 0.04-0.45 cm^{-3} s^{-1}, and by 0.16-0.23 cm^{-3} s^{-1} during the summer months. Analysis of years 2013 and 2014, also in Värriö, led to a median formation rate of 0.14±0.05 cm^{-3} s^{-1} (J_3) (Vana et al., 2016). Thus, the predicted formation rates in, especially, non-infested mountain birch stands in Lapland are generally within range, but often somewhat higher than observations from the same location. It should, though, be mentioned that these literature values cannot be used to validate our simulation results, since Scots pines, and not mountain birches, dominate the SMEAR I site (Kyrö et al., 2014), and the LAI of mountain birches at the station is significantly less than 2 m^2 m^{-2} (Ylivinkka et al., 2020). The modelled formation rates are not compared to observations from the mountain birch dominated areas in Lapland, since such observations do not, to our knowledge, exist.

A very recent investigation of long-term field observations (25 years) from the SMEAR I station (Ylivinkka et al., 2020), where autumnal moth larvae are prominent defoliators of mountain birches, did, however, not find any evidence that herbivory by autumnal moth would enhance the formation, nor growth, of atmospheric aerosol particles during the summer of infestation. Instead there was some evidence of elevated total particle concentrations for a few years after summers with larval infestation, which was speculated to be caused by delayed defense responses of mountain birches. It is, however, possible that the total foliage mass of mountain birches in the area is too small, or that the level of infestation was too low during the investigated time period, in order to cause detectable changes in aerosol variables (Ylivinkka et al., 2020).

The amount of newly formed particles is predicted to be up to about one order of magnitude higher in a gypsy moth infested oak stand than in a non-infested oak stand, with a 10:00-16:00 median of up to ~1.4×10^5 cm^{-3} in an infested stand (Fig. 6f). Such a high production of new particles is comparable to observations from e.g. Melpitz (Größ et al., 2018). The number of produced particles in a non-infested oak stand (~1.1×10^4 cm^{-3}; Fig. 6f) is comparable to e.g. the number of new particles produced during a typical new particle formation event in Hyytiälä (~$1-2\times10^4$ cm^{-3}; Dal Maso et al., 2008; Nieminen et al., 2014), but significantly higher than observations from a Missouri oak forest, where sub-5 nm particles were measured to be up to ~2×10^4 cm^{-3}, and 5-25 nm particles to ~3000 cm^{-3}, during typical new particle formation events (Yu et al., 2014). After the period of stress, the number of particles in the growing mode is predicted to range between ~7×10^3 cm^{-3} and ~17×10^3 cm^{-3} in a non-infested stand, ~6×10^3 cm^{-3} and ~12×10^3 cm^{-3} in a 30 % defoliated stand and between ~3×10^3 cm^{-3} and ~5×10^3 cm^{-3} in a 80 % defoliated oak stand (Fig. 6f). Oak powdery mildew is predicted to enhance the number of particles in the growing mode by up to a factor of ~4 compared to the corresponding non-infected stand, resulting in a maximum of ~1.7×10^4 cm^{-3} in an infected stand, under the used border conditions (Fig 7g). Under the same environmental conditions, a severely poplar rust infected poplar stand is predicted to produce up to about five times as many new particles as a non-infected poplar stand, leading to a maximum of about 1.1×10^5 cm^{-3} in a severely infected stand (Fig 8h). Finally, it is predicted that herbivory by autumnal moth enhances the amount of produced particles by up to a factor of ~2.7, with a maximum number of particles in the growing mode of ~3×10^4 cm^{-3} in an infested birch stand (Fig. 9j). The predicted amount of particles in a non-infested mountain birch stand is in the same order as observations from Finnish Lapland (Komppula et al., 2006).

3.1.4 New particle growth

New particles are assumed to grow by sulfuric acid and OxOrg (Sec. 2.7, Eq. 5-8), hence the seasonal patterns of formation rates and OxOrg concentration are reflected in the pattern of the growth rates (Figs. 6g, 7h, 8g, 9k), and therefore also in the season pattern of the number (Figs. 6f, 7g, 8h, 9j) and size (Figs. 6h, 7g, 8g, 9l) of the growing particle mode. We predict that the 10:00-16:00 median growth rate in a gypsy moth infested oak stand is at maximum ~5.9 nm h^{-1} under the assumed boundary conditions, whereas the corresponding growth rate in a non-infested oak stand is around 1.6 nm h^{-1}, when the full leaf state has been attained (Fig. 6g). For comparison, the growth rate of new particles has been reported to range from 0.5 to 12 nm h^{-1} in Hyytiälä (Dal Maso et al., 2007), with median values of 2.1 nm h^{-1} (Vana et al., 2016), 2.5 nm h^{-1} (Dal Maso et al., 2007), and 3.3 nm h^{-1} (Paasonen et al., 2010), depending on which years the data covered. Dal Maso et al. (2007) reported that the growth rate of new small particles in Aspvreten, a rural site in Sweden dominated by deciduous and conifer forests and some farmlands, ranged between 1 and 11 nm h^{-1}, with a median value of 3.4 nm h^{-1}. The growth rate was found to range from 2.1 to 22.9 nm h^{-1}, with a median value of 7.25 nm h^{-1} during spring in a mixed deciduous forest area close to Heidelberg in Germany, under influence of anthropogenic pollution (Fiedler et al., 2005). Growth rates from an oak forest in Missouri, USA, were in the range 1.6-11.2 nm h^{-1} (Yu et al., 2014). Median values for the growth rate have been reported to be 4.2 nm h^{-1} in Melpitz (Paasonen et al., 2010), 4.6 nm h^{-1} in Järvseljä (Vana et al., 2016), 4.8 nm h^{-1} in Hohenpeißenberg (Paasonen et al., 2010) and 9.5 nm h^{-1} in San Pietro Capofiume (Paasonen et al., 2010). Thus, we can conclude that our predicted growth rates are comparable to atmospheric observations from several different rural sites. Growth rates obtained from areas influenced by anthropogenic pollution are generally higher than our simulated rates, but this is expected, since our model is constrained by conditions representative for rural sites.

Growth rates are predicted to be lower in an oak powdery mildew infected oak forest, than in a gypsy moth infested oak forest. The rates are predicted to, at maximum, be ~2.0 nm h^{-1} (80 % of leaf area covered by mildew), ~1.6 nm h^{-1} (30 % of leaf area covered by mildew) and ~1.2 nm h^{-1} (non-infected, in the same environmental conditions as the infected trees) (Fig. 7h). Thus, the growth rates are similar to the lower end of the observed range.

The growth of small particles in non-infected and rust infected poplar stands are predicted to range between ~2.1 nm h^{-1} and ~5.7 nm h^{-1}, during the late summer when the full leaf state has been attained, with the fastest growth in a heavily rust infected forest stand (Fig. 8g). This range in growth rates is thus similar to simulation results of herbivory infested oak (see above; Fig. 6g).

The predicted growth rates are smallest in simulations of non-infested mountain birch stands in Lapland. The 10:00-16:00 median growth rate is at maximum predicted to be ~1.4 nm h^{-1} in an infested stand and varies between ~0.6 nm h^{-1} and ~2.0 nm h^{-1} in a non-infested stand (Fig. 9k). These values are in line with observations from Värriö (median: 1.6±0.9 nm h^{-1}, Vana et al., 2016; monthly summer mean: 3.7-4.4 nm h^{-1}, Kyrö et al., 2014; range: 1-10 nm h^{-1}, median: 2.4 nm h^{-1}, Dal Maso et al., 2007) and from Pallas, Finnish Lapland (median: 2.0 nm h^{-1}, daily range: 0.5-11 nm h^{-1}, Dal Maso et al., 2007; monthly range: 1.9-4.6 nm h^{-1}, Asmi et al., 2011).

According to our predictions, new particles will grow up to about 46 nm larger in an oak gypsy moth infested oak stand compared to a non-infested oak stand within one day (Fig. 6h). Simulation results for the other species/stressors show that new particles will grow up to about 8 nm more in an oak powdery mildew infected stand (Fig. 7g), ~28 nm more in a poplar rust infected poplar stand (Fig. 8g), and ~26 nm larger in an autumnal moth infested mountain birch stand (Fig. 9l), within one day, compared to their corresponding non-infected stands. In our simulations, the newly formed particles in non-infected oak stands are always mainly formed and grown by sulfuric acid (Figs. 6h, 7g), but in modelling of non-infected poplar, more than half of the formation and growth is due to HOM originating from isoprene (Fig. 8g), while HOM formed from monoterpenes account for a large fraction of the predicted formation and growth in non-infested birch stands (Fig. 9l).

3.1.5 R: the isoprene-to-monoterpenes carbon concentration ratio

Previous chamber studies (Kiendler-Scharr et al., 2009, 2012; McFiggans et al., 2019; Heinritzi et al., 2020) have suggested that isoprene suppresses the formation of new particles from monoterpenes when the isoprene-to-monoterpene carbon concentration ratio (R) becomes too high. New particle formation has rarely been observed in the field when R>1 (e.g. Kanawade et al., 2011; Pöschl et al., 2010; Pöhlker et al., 2012; Lee et al., 2016). For example, Yu et al. (2014) observed formation of sub-5 nm particles during 64 % of the measured days in an oak forest, though R was 15.3 ± 7.2 during the campaign period. However, since the formation of new particles occurs on a regional scale, the authors suggested that the detected particles could have been formed at lower R and advected to their measurement site. Contrarily, it has earlier been proposed that oxidation products of isoprene (e.g. IEPOX) promote the growth of existing new particles (D_p>3 nm, e.g. Surratt et al., 2010; Lin et al., 2013), while Heinritzi et al. (2020) observed the growth of particles above 3.2 nm to be unaffected by the concentration of isoprene. It is thus likely that the zone of R values, inside which the probability for new particle formation to occur changes, is influenced by other environmental factors and is therefore location and/or season dependent.

New particle formation has also been observed in the upper troposphere in tropical regions (Andreae et al., 2018; Williamson et al., 2019) where isoprene dominates the emission spectrum greatly. The hypothesis is that isoprene is vertically transported via strong convection and new particles are formed from isoprene oxidation products, which is possible due to lower temperature conditions in the upper troposphere.

The concentration ratio of isoprene-to-monoterpene carbon is very high in non-infected oak and poplar stands and in oak stands which are no longer exposed to herbivory (Figs. 6b, 7d, 8d), and it is therefore questionable whether particles will be formed at all in the atmospheric boundary layer from these stands when they are not experiencing stress. Biotic stress greatly reduces R in all three cases. R is most significantly decreased to a minimum 10:00-16:00 median value of 0.004 in simulations of gypsy moth infested oak stands (Fig. 6b), but the period with low R values is rather short. For example, R < 1 during only 11 and 4 days, respectively, while R < 22.5 (probably the highest ratio at which new particles formation has been observed in the field, Yu et al., 2014) during 32 and 21 days, respectively, in our simulations of a severely and moderately European gypsy

moth infested oak stand (Fig. 12e). R is predicted to be close to 1, though never below 1, in simulations of both oak powdery mildew infected oak stands and rust infected poplar stands. The duration where R is e.g. less than 22.5 is 39 days in a severely mildew infected oak stand, 31 days in a moderately mildew infected oak stand, and 27 days in a severely rust infected poplar stand (Fig. 12e). For comparison, R is never predicted to be less than 22.5 in a moderately infected poplar stand (Fig. 8d). Even if new particles are not formed from oak powdery mildew or poplar rust infected stands in the boundary layer, then both the potential to form new particles in the upper troposphere (Figs. 7f,g, 8f,h) and the potential to grow already existing particles, which are formed in nearby stands and horizontally transported to the infected stands (Figs. 7g,h, 8g), are still predicted to be greater than in our simulations of the correspondingly non-infected stands. R is not relevant in the case of mountain birch, since this tree species does not emit isoprene constitutively, nor in response to herbivory stress by autumnal moth larvae (Yli-Pirilä et al., 2016; Rieksta et al., 2020).
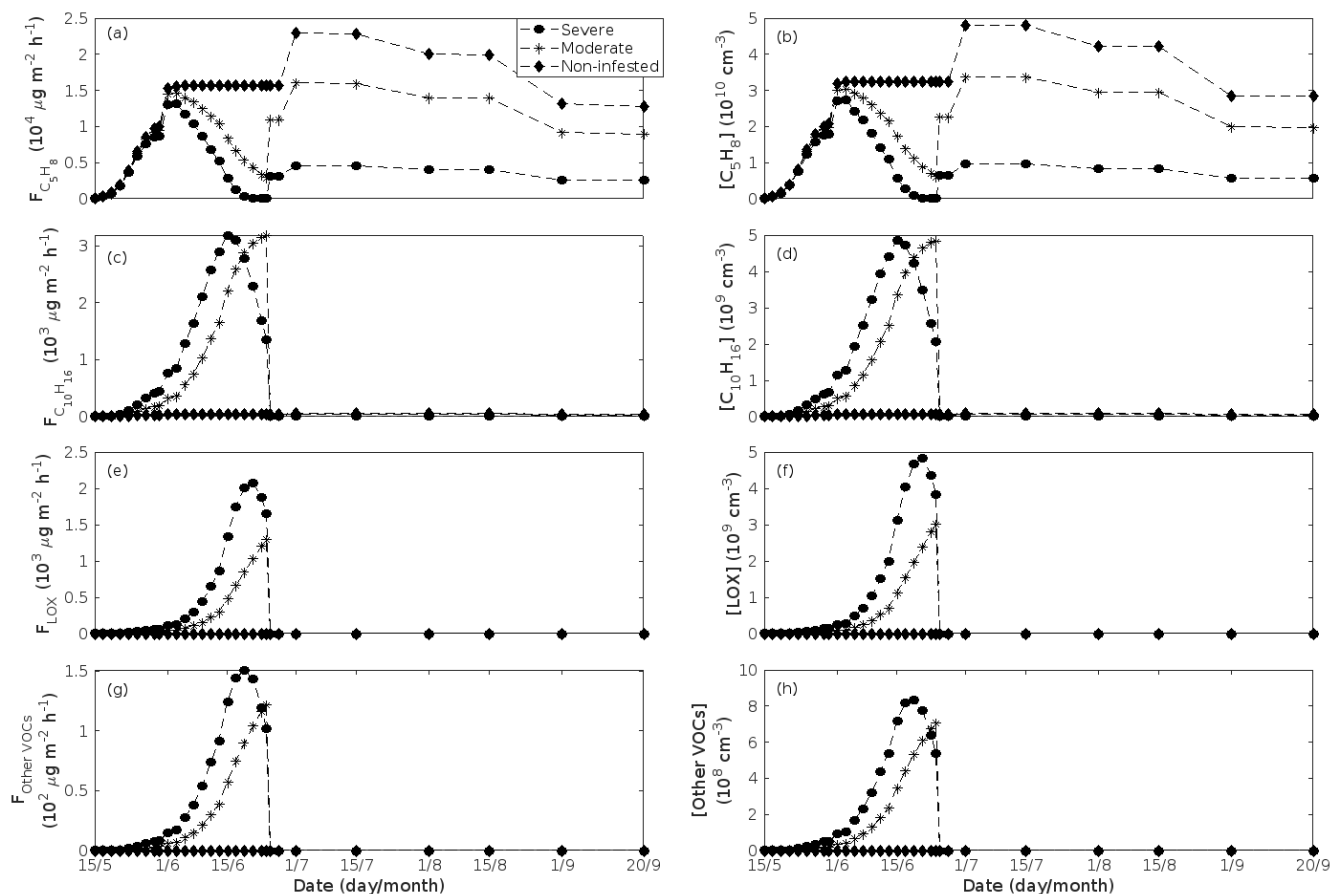
Figure 5. A pure oak stand infested with European gypsy moth larvae in comparison to a non-infested pure oak stand. Canopy emissions of **(a)** isoprene, **(c)** monoterpenes, **(e)** lipoxygenase pathway volatiles (LOX), and **(g)** the sum of other VOCs which contribute to OxOrg formation (here i.e. methyl salicylate and dimethyl-nonatriene). Atmospheric concentrations of **(b)** isoprene, **(d)** monoterpenes, **(f)** lipoxygenase pathway volatiles, and **(h)** the sum of other VOCs which contribute to OxOrg formation. "Moderately" and "severely" refer to 30 % and 80 %, respectively, of the leaf area that has been consumed by the end of the feeding period.
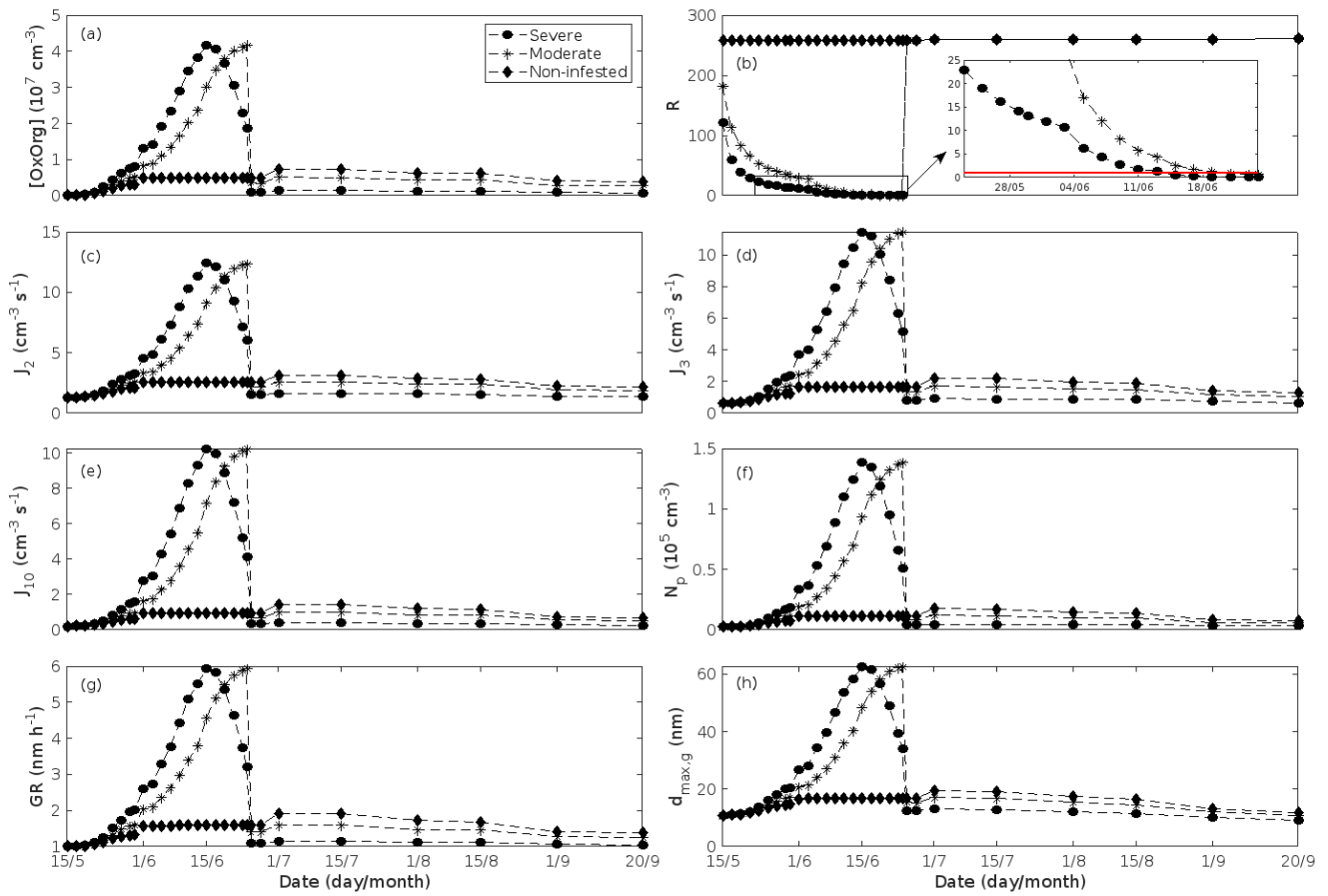
19

**Figure 6.** A pure oak stand infested with European gypsy moth larvae in comparison to a non-infested pure oak stand. **(a)** atmospheric concentrations of OxOrg. **(b)** the ratios of isoprene-to-monoterpenes carbon concentrations, where the red line indicates R = 1. Formation rates of **(c)** 2, **(d)** 3 and **(e)** 10 nm particles. **(f)** number concentrations of formed particles, **(g)** growth rates of newly formed particles, and **(h)** the daily maxima diameter of the growing particle mode. "Moderately" and "severely" refer to 30 % and 80 %, respectively, of the leaf area that has been consumed by the end of the feeding period.

20

601

602
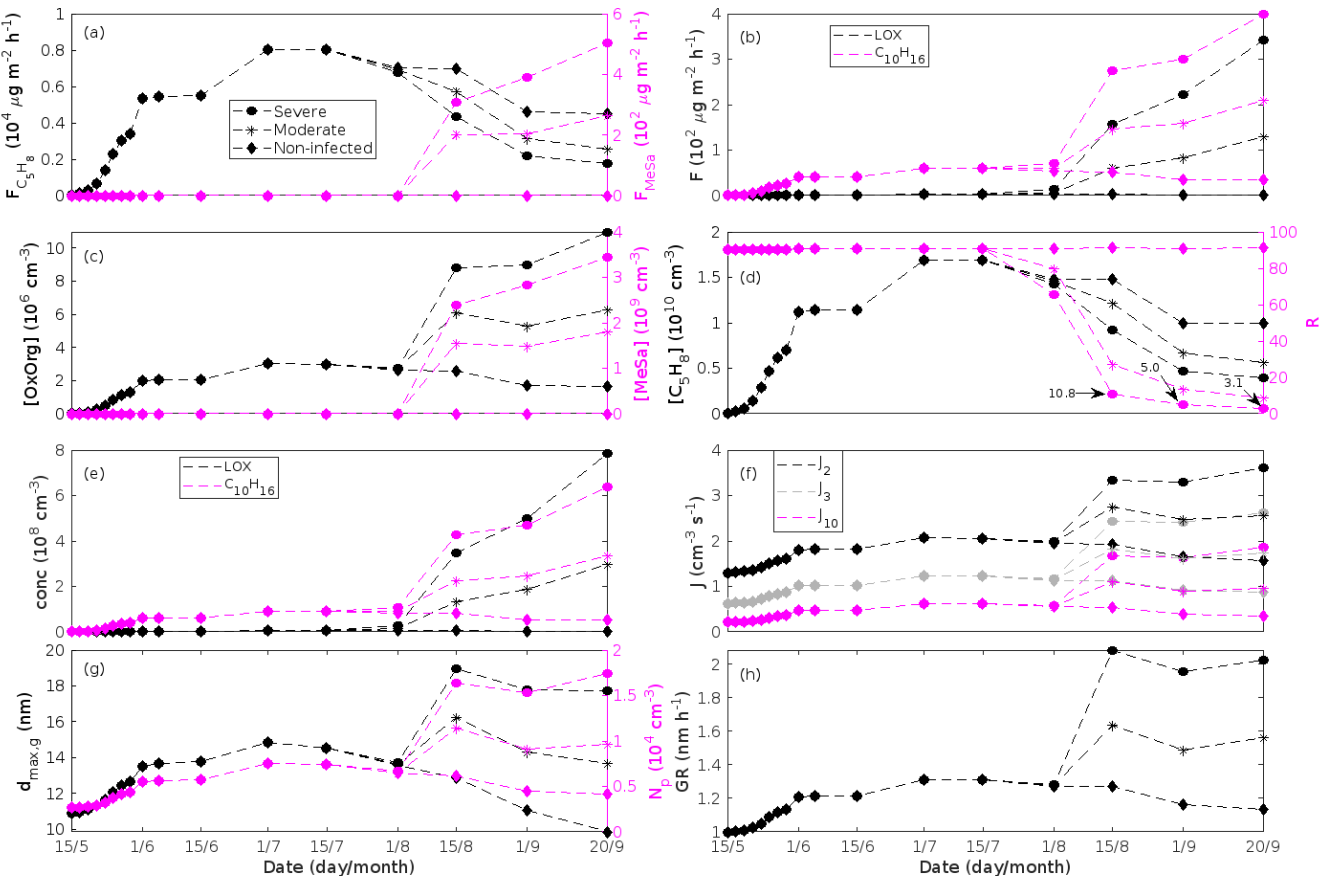
Figure 7. A pure oak stand infected by oak powdery mildew in comparison to a non-infected pure oak stand. Canopy emissions of **(a, left axis)** isoprene, **(a, right axis)** methyl salicylate, **(b)** lipoxygenase pathway volatiles and monoterpenes. Atmospheric concentrations of **(c, left axis)** OxOrg, **(c, right axis)** methyl salicylate, **(d, left axis)** isoprene, and **(e)** lipoxygenase pathway volatiles and monoterpenes. **(d, right axis)** the ratios of isoprene-to-monoterpene carbon concentrations. **(f)** formation rates of 2, 3 and 10 nm particles. **(g, left axis)** daily maxima diameter of the growing particle mode, and **(g, right axis)** number concentrations of formed particles. **(h)** growth rates of newly formed particles. "Moderately" and "severely" refer to 30 % and 80 %, respectively, of the leaf area that has been infected by fungi by the onset of senescence.

21

610
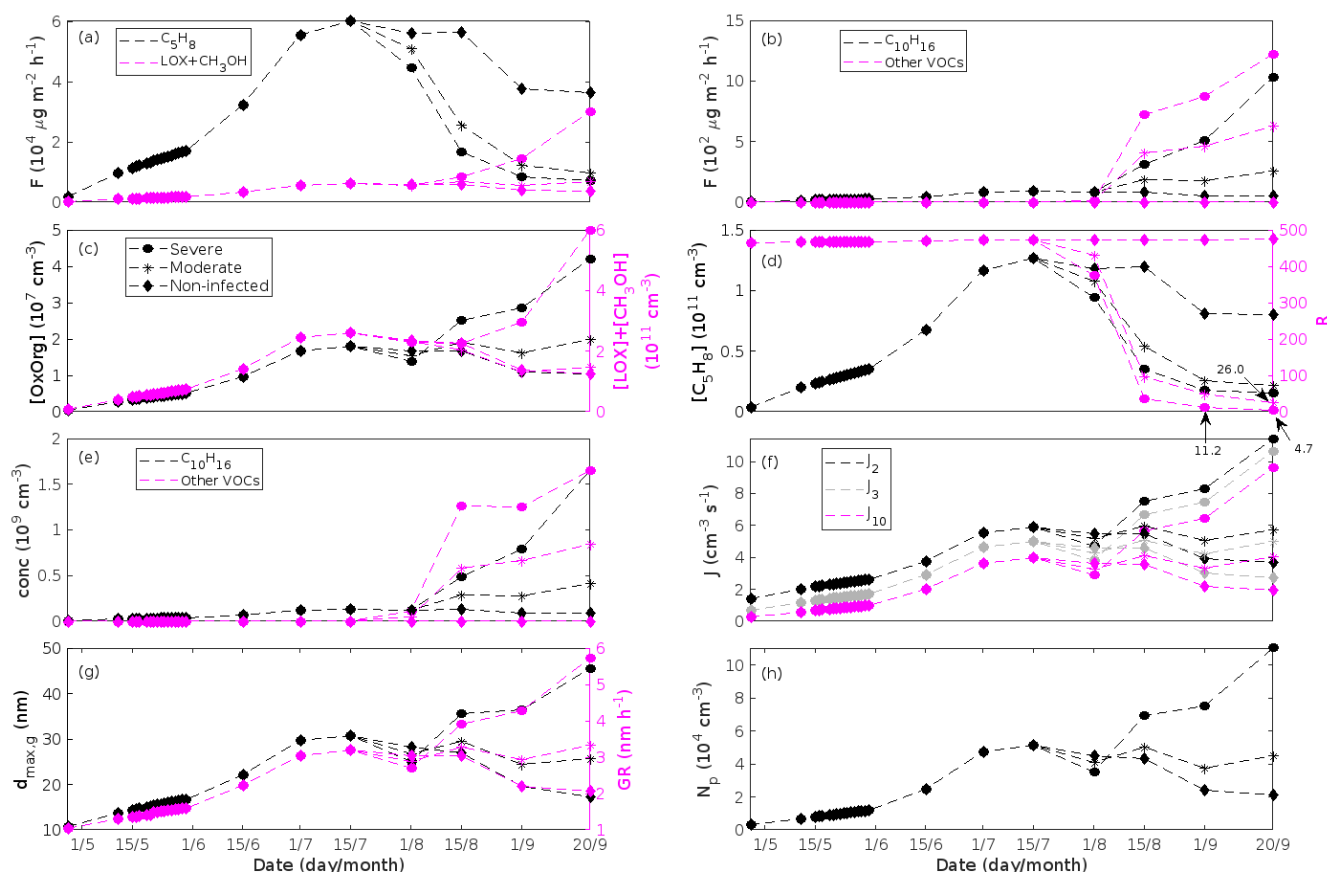
611

Figure 8. A pure poplar stand infected by rust fungi in comparison to a non-infected pure poplar stand. Canopy emissions of
(a) isoprene and the sum of lipoxygenase pathway volatiles and methanol, **(b)** monoterpenes and the sum of other VOCs which
contribute to OxOrg formation (here i.e. methyl salicylate, dimethyl-nonatriene, α-Eudesmol and sesquiterpenes). Atmospheric
concentrations of **(c, left axis)** OxOrg, **(c, right axis)** the sum of lipoxygenase pathway volatiles and methanol, **(d, left axis)**
isoprene, and **(e)** monoterpenes and the sum of other VOCs which contribute to OxOrg formation. **(d, right axis)** the ratios of
isoprene-to-monoterpene carbon concentrations. **(f)** formation rates of 2, 3 and 10 nm particles. **(g, left axis)** daily maxima
diameter of the growing particle mode, and **(g, right axis)** growth rates of newly formed particles. **(h)** number concentrations
of formed particles. "Moderately" and "severely" refer to 30 % and 80 %, respectively, of the leaf area that has been infected
by fungi by the onset of senescence.

621
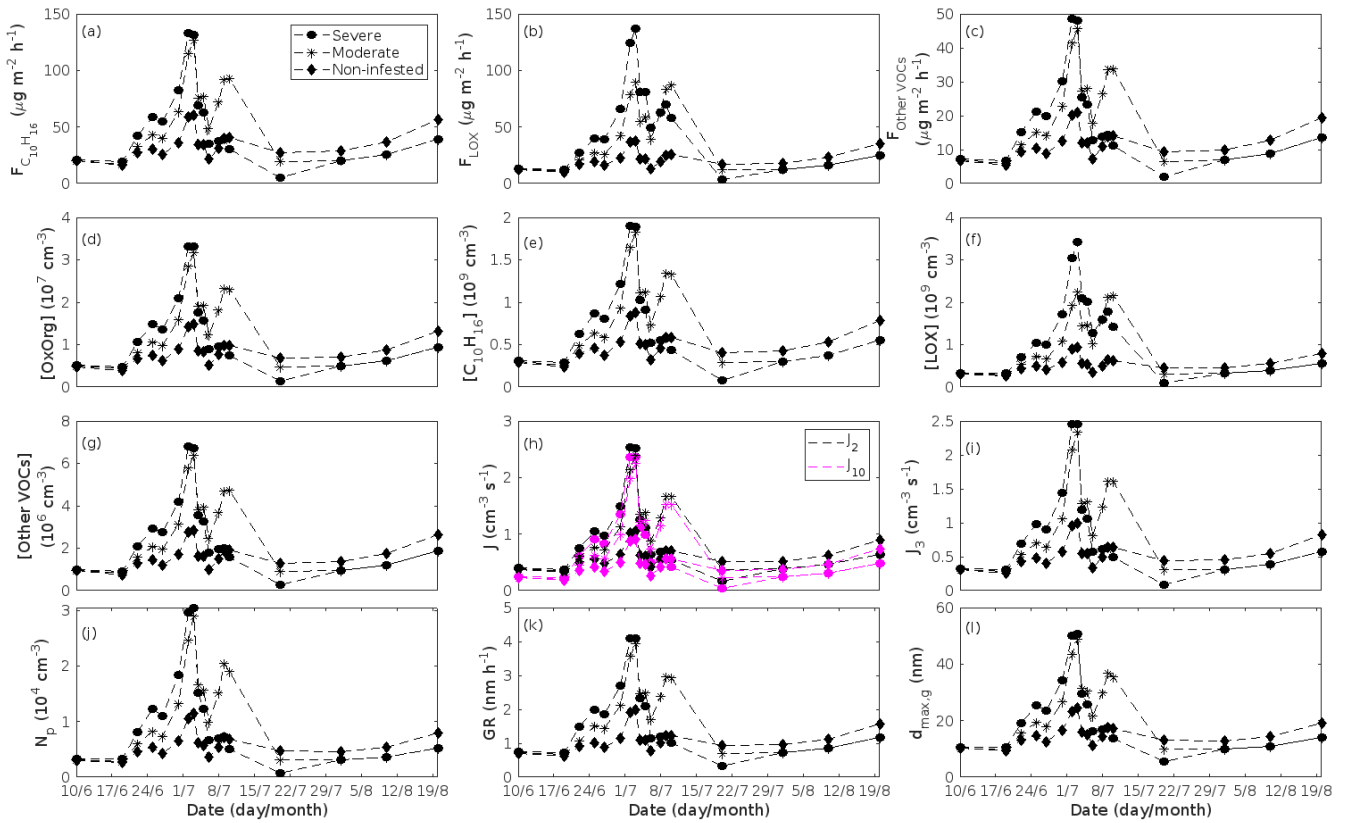
Figure 9. A pure mountain birch stand infested with autumnal moth larvae in comparison to a non-infested pure mountain birch stand. Canopy emissions of **(a)** monoterpenes, **(b)** lipoxygenase pathway volatiles, and **(c)** the sum of other VOCs which contribute to OxOrg formation (here i.e. dimethyl-nonatriene and sesquiterpenes). Atmospheric concentrations of **(d)** OxOrg, **(e)** monoterpenes, **(f)** lipoxygenase pathway volatiles, and **(g)** the sum of other VOCs which contribute to OxOrg formation. Formation rates of **(h)** 2, 10 and **(i)** 3 nm particles. **(j)** number concentrations of formed particles. **(k)** growth rates of newly formed particles. **(l)** daily maxima diameter of the growing particle mode. "Moderately" and "severely" refer to 30 % and 80 %, respectively, of the leaf area that has been consumed by the end of the feeding period.

3.2 Estimating the reliability of our results

Since aerosol processes are very sensitive to changes in environmental conditions - conditions which can vary greatly, both interannually, but also from day to day, we investigated the influence of a wide range of realistic and relevant environmental conditions (Table D1 in Appendix D) on our model predictions (Figs. 10-11, D1-2 in Appendix D). Nine different sensitivity tests (ST1-9) were conducted for all plant species and infections, where only one parameter was changed at a time (Table D1). For these simulations, the default values listed in Table 2 were used, while the default maximum daily temperature at Hohenpeissenberg and SMEAR I were assigned to 25 ℃ and 20 ℃, respectively, and the default LAI for oak/poplar and birch was assumed to be 5 $m^2 m^{-2}$ and 2 $m^2 m^{-2}$, respectively. All aerosol parameters (formation and growth rates, diameter, number of particles) show a similar response to changes in the considered environmental parameters, thus only the impact on the number of newly formed particles (Figs. 10-11) and the rate at which new small particles grow (Figs. D1-2) is displayed.

As is also observed in nature, certain conditions suppress or prevent the formation of new particles, such as for example a high condensation sink (Fig. 11d,i,n,s; e.g. Hyvönen et al., 2005; Nieminen et al., 2015; Vana et al., 2016) and low sulfuric acid concentration (Fig. 11c,h,m,r; e.g. Boy et al., 2005; Nieminen et al., 2014), making the atmospheric relevance of the forest stands minor. Since we have assumed realistic conditions, but at the same time conditions which do not prevent the formation of new particles, in our simulations, the number of predicted days with occurring new particle formation is the theoretical maximum for clean environments, which our aerosol theory is based on (Sec. 2.7). Though the absolute number of

23

predicted new particles depend highly on the assumed environmental conditions (Figs. 10-11), the relative difference between non-infected and stressed stands of the same tree species is not impacted: e.g. the number of new particles is always significantly higher in gypsy moth infested, and oak powdery mildew infected, oak stands, than in non-infected oak stands, when the environmental conditions are assumed to be the same in all stands (Figs. 10a-h, 11a-j). Likewise, more particles are always formed in moderately, than severely, moth infested oak and birch stands, since the decrease in LAI is stronger than the increase in the stress-induced emission response per unit leaf area (Figs. 10a-d,m-p, 11a-e,p-t). This is emphasised in very severely infested mountain birch stands (e.g. 80 % defoliation), where the number of produced particles is always less than in its corresponding non-infested stand (Figs. 10m-p, 11p-t).

Sensitivity tests were also carried out in order to assess whether the simplifications made in the model are valid: (1) As mentioned earlier (Sec. 2.4), we did not incorporate a full canopy environment in the model - an approach which has also been taken by other investigators (e.g. Simpson et al., 1999, 2012; Bergström et al., 2014). In ST2 (Table D1, Figs. 10b,f,j,n, D1b,f,j,n) changes in light conditions exclusively impact the predicted emissions of VOCs. From Figs. 10b,f,j,n, D1b,f,j,n it is clear that even assuming extremely different light environments would not change our conclusions about the atmospheric importance of biotic plant stresses, since our results show that stressed forest with a maximum light availability down to 200 μmol m^{-2} s^{-1} would still produce more new particles than its correspondingly non-infected stand at theoretically clear sky conditions (Fig. 10b,f,j,n). A highly autumnal moth stressed mountain birch stand (80 % defoliation) would possibly produce slightly more particles than a non-infested stand, if a full canopy environment would be considered. For example, the number of produced particles is slightly higher in a birch stand experiencing a stress level of 80 % under 1000 μmol m^{-2} s^{-1} than a non-infested stand under 400 μmol m^{-2} s^{-1} (Fig. 10n). However, the LAI of mountain birch stands is usually rather low (Heiskanen, 2006), making the difference in light environment between a non-infested and a highly defoliated stand small. Since mildew and rust do not decrease the leaf area of their host, a different treatment of the light environment would not influence the relative atmospheric importance of fungally infected oak and poplar vs their correspondingly non-infected stands (Fig. 10f,j).

(2) In ST3 (Table D1, Figs. 10c,g,k,o, D1c,g,k,o) and in our seasonal simulations (Figs. 5-9), the change of temperature only impacts the emission rates of VOCs. In reality, the vapour pressures of oxidised compounds increase non-linearly with an increase in temperature (e.g Bilde et al., 2015), and less HOM, and other oxidised organic compounds, will therefore condense at higher temperatures, whereby the formation and subsequent growth of particles will decrease (Stolzenburg et al., 2018; Simon et al., 2020). Gas phase chemistry, including the formation of HOM, is also in reality temperature dependent (e.g. Quéléver et al., 2019). These effects have not been included in the model. Since the range of daily maximum temperatures throughout the growing season is assumed to be rather narrow (Fig. 4), this effect does not greatly impact our results (Sec. 3.1), but it means that the number of particles produced at high temperatures (Fig. 10c,g,k,o), and the growth rate at which they are produced (Fig. D1c,g,k,o), are overestimated for both non-infected and stressed forests.

(3) The concentrations of ozone and OH were unaltered between simulations of non-infected forests and forests under varying degrees of infection (Sec. 2.6), though in reality, the atmospheric oxidation capacity is controlled by changes in the concentration of atmospheric trace gases, including VOCs. The total emission of VOCs from oak and poplar stands is greatly dominated by isoprene, but the emission of isoprene decreases as a function of biotic stress severity (Figs. 5a, 7a, 8a). In contrast, the emission of LOX, methyl salicylate, methanol, monoterpenes and sesquiterpenes increases as the level of stress increases (Figs. 5c,e,g, 7a,b, 8a,b). The oxidation of isoprene, LOX, methyl salicylate and methanol is primarily driven by reactions with OH, and also monoterpenes react with OH, which all leads to reductions in the concentration of OH (Table 3), though e.g. ozonolysis of monoterpenes also produce OH, which thus counters part of the reduction. When considering the reaction rates and emission rates of the considered VOCs in simulations of oak and poplar stands, the concentration of OH is mainly controlled by changes in the emission of isoprene. Thus, we expect that the concentration of OH will increase as the degree of stress increases, but even a strong shift in the concentration of OH, will not change the conclusion about the relative atmospheric importance of stressed vs stress-free oak and poplar forests (Figs. 11b,g,l,q, D2b,g,l,q). The absolute number of predicted new particles in herbivory stressed oak stands will, however, be predicted to be smaller at higher levels of OH (Fig.

24

11b), because the oxidation of monoterpenes is then more strongly controlled by OH, which leads to a smaller production of HOM, as monoterpenes typically form HOM at a considerably lower yield from reactions with OH than ozone (Appendix C). A similar shift in the oxidation of monoterpenes is happening in case of oak powdery mildew infected oak, but the effect is counted by an increase in the formation of oxidised organic compounds from oxidation of methyl salicylate at high levels of OH, leading totally to higher predicted particle number concentrations (Fig. 11g). Considering the emissions from biotically stressed and non-infested mountain birch, we estimate that the concentration of OH should stay largely the same, or potentially decrease slightly at higher levels of infestation, which will enhance the oxidation of monoterpenes by ozone, which will lead to a larger production of HOM and thereby a slightly higher predicted number of new particles (Fig. 11q). In the atmosphere, the production of sulfuric acid is limited by the availability of OH, and it is therefore possible that the effects of changes in the concentration of OH (Fig. 11b,q) and sulfuric acid (Fig. 11c,r), in herbivory stressed stands, on the absolute number of predicted new particles, will cancel out or even lead to a stronger particle production than predicted. In case of oak powdery mildew infected oak, the two effects will enhance each other and result in an even higher number of predicted particles. In clean, low NO_X environments, which we aimed to simulate, the concentration of ozone is largely unaffected by the ambient concentration of isoprene (e.g. Jenkin et al., 2015). However, isoprene forms ozone progressively with an increased availability of NO_X (e.g. Jenkin and Clemitshaw, 2000). Higher ozone levels support enhanced formation of HOM, and thus aerosol processes, but the production of HOM is also known to decrease as a function of increased NO_X concentration (e.g. Ehn et al., 2014), whereby the formation and growth of new particles becomes suppressed (e.g. Yan et al., 2020; Pullinen et al., 2020).

(4) As mentioned earlier (Sec. 2.6), many HOM yields have not been investigated for the exact compounds which are emitted from the tree species, which are the focus of this study. From Fig. 11e,j,o,t it is obvious, that even if all the OxOrg yields used for simulations of only biotically stressed forests were to be decreased significantly - in case of moderately herbivory infested oak (30 % of leaf area defoliated) by down to about 95 % - biotically stressed oak, poplar and mountain birch forests would still, in most cases, produce more particles than non-infected forests of the same tree species. The yields, at which HOM are formed, have been treated as fixed values (Appendix C) in the seasonal simulations (Sec. 3.1), but the yields actually depend on several factors, such as e.g. the concentration of NO_X (point 3 above; Ehn et al., 2014), temperature (point 3 above; Quéléver et al., 2019; Simon et al., 2020) and the ambient blend of VOCs (Sec. 3.1.5; McFiggans et al., 2019). Exactly how the formation and growth of new particles depend on the VOC blend is still uncertain, but it has recently been demonstrated that a linear addition of the yields from the individual yields of components in the VOC mixture will result in an overestimation of both the number and size of particles (McFiggans et al., 2019). As we have followed a similar procedure, this effect might cause our predicted aerosol processes (Sec. 3.1) to be overestimated, but since the ratio of isoprene-to-monoterpenes carbon concentration is much higher in non-infected oak and poplar stands than in the correspondingly stressed stands (Figs. 6b, 7d, 8d), the overestimation is expected to be more pronounced in the non-infected stands (McFiggans et al., 2019). The difference in the atmospheric importance of non-infected and biotically stressed oak and poplar stands thereby widens (Fig. 11e,j,o).

It is well known that the potential for foliage to emit VOCs depends on the age of the foliage: emerging and growing foliage usually emits isoprene at reduced rates (e.g. Guenther et al., 1991, 2012; Goldstein et al., 1998; Petron et al., 2001) and monoterpenes at enhanced rates (e.g. Guenther et al., 1991, 2012; Aalto et al., 2014; Taipale et al., 2020) compared to that of its corresponding mature foliage. Old leaves do usually additionally emit isoprene at decreased rates (Monson et al., 1994; Schnitzler et al., 1997; Sun et al., 2012). These effects were not considered in our simulations (Sec. 3.1), since the effect of leaf age on biotic plant stress emissions is unexplored. Considering a similar treatment of the impact of leaf maturity on the emissions of VOCs as Gunther et al. (2012) (see Appendix B) would only influence the predicted number and size of particles in herbivory stressed and non-infested oak forests insignificantly (Fig. B2). However, it would decrease the ratio of isoprene-to-monoterpenes carbon so significantly in gypsy moth infested oak stands, that the possible suppression of aerosol processes by isoprene would disappear during most, or even the entire, duration of stress (Fig. B2b). Applying a similar leaf age effect as described in Gunther et al. (2012) on simulations of fungally infected oak and poplar forests would not decrease the ratio of

isoprene-to-monoterpenes carbon sufficiently in order to avoid the possible suppression effect of isoprene, since Guenther et al. (2012) only assume a reduction of 10 % on the emissions of isoprene from old leaves. We investigated that the emission of isoprene from mildew infected oak would need to decrease by ~68-96 % (severity of stress ranging from 80 to 9 %), in comparison to simulations where the leaf age effect is not considered, in order to reach R≤1, whereas the emission of isoprene from non-infected oak would need to decrease by ~99 % (Fig. B3a). In comparison, the emission of isoprene from a non-infected poplar stand would need to decline by 99.8 %, and from a rust infected poplar stand by at least 79 %, in order to attain R≤1 (Fig. B4a). In order to reach R≤22.5, the upper limit at which new particle formation has been observed in the atmosphere (Yu et al., 2014), the emission of isoprene from a non-infected poplar stand would need to decrease by ~95 %, whereas heavily rust infected poplar forest would already be below this limit without considering an age dependent reduction of the emission potential (Fig B4a). Simulations were not done for mountain birch forest stands, since no emissions are suppressed upon herbivory stress of mountain birch (Yli-Pirilä et al., 2016) and since Yli-Pirilä et al. (2016) did not provide age information on the leaves they measured.
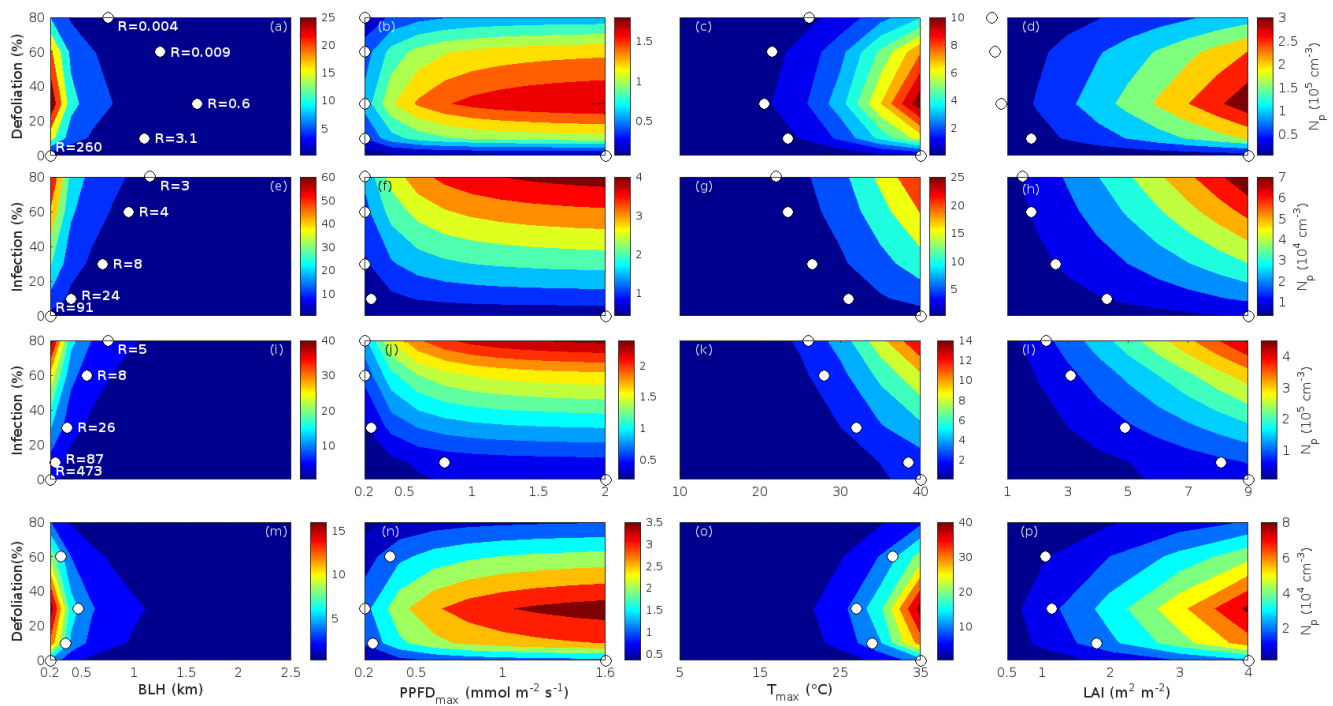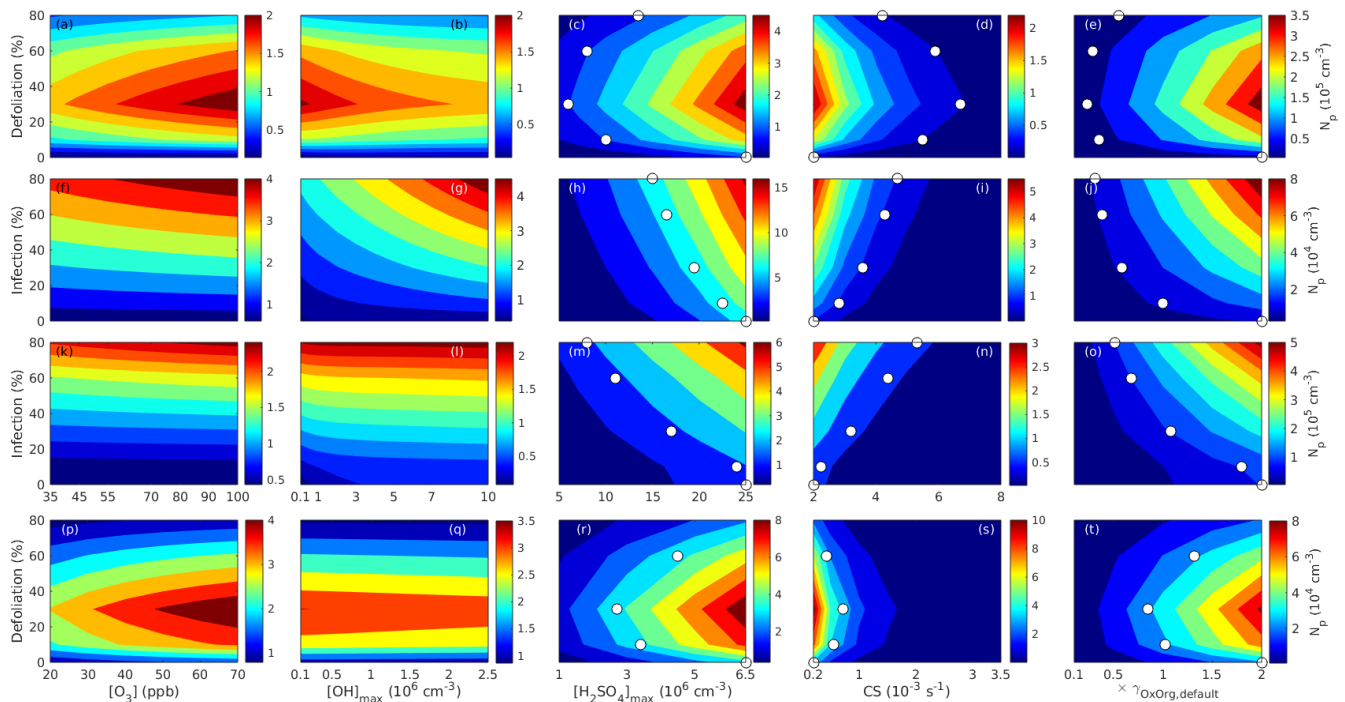

Figure 10. Impact of changed boundary conditions on the number concentrations of newly formed particles in non-infected and biotically stressed forest stands. The number concentration of newly formed particles is expressed as a function of changes in the boundary layer height **(a, e, i, m)**, light **(b, f, j, n)**, temperature **(c, g, k, o)** and leaf area index **(d, h, l, p)** for non-infected and infected oak **(a-d**, gypsy moth, **e-h**, powdery mildew), poplar **(i-l)** and birch **(m-p)** stands. Light **(b, f, j, n)** and temperature **(c, g, k, o)** are given as the daily maxima, but in the simulations the parameters follow a daily cycle. The displayed LAI **(d, h, l, p)** is that of a non-infected stand, hence e.g. at LAI = 7 m^2 m^{-2}, the simulation for a larval infestation level of 80 % has been conducted with LAI = 1.4 m^2 m^{-2}, which is 20 % of the non-infected stand LAI value. Optimal conditions (i.e. leading to highest number concentrations) for non-infected stands are indicated with white markers at an infection level of 0 %. White markers located at various infection levels mark the conditions at which an identical or slightly higher number concentration, as produced by a non-infected forest stand at optimal conditions, is reached. No markers are used for 80 % defoliated mountain birch **(m-p)**, since the corresponding number concentrations are always lower than in a non-infested birch stand at optimal conditions. Be aware that white markers in **d** and **p** are not located at the LAI of a non-infected stand, but instead at the values used for the simulations. R values **(a, e, i)** indicate the ratio of isoprene carbon / monoterpene carbon at the locations of the write markers. Be aware that the x-axes are different for simulations in Hohenpeißenberg **(a-l)** and SMEAR I conditions **(m-p)** except in the case of changing boundary layer height **(a, e, i, m)**.

26

Figure 11. Impact of changed boundary conditions on the number concentrations of newly formed particles in non-infected and biotically stressed forest stands. The number concentration of newly formed particles is expressed as a function of changes in the concentration of ozone **(a, f, k, p)**, OH **(b, g, l, q)** and sulfuric acid **(c, h, m, r)**, the condensation sink **(d, i, n, s)** and OxOrg yields **(e, j, o, t)** for non-infected and infected oak **(a-e**, gypsy moth, **f-j**, powdery mildew), poplar **(k-o)** and birch **(p-t)** stands. The concentrations of OH **(b, g, l, q)** and sulfuric acid **(c, h, m, r)** are given as the daily maxima, but in the simulations the parameters follow a daily cycle. White markers are used in a similar way as in Fig. 10. Be aware that the x-axes are different for simulations in Hohenpeißenberg **(a-o)** and SMEAR I conditions **(p-t)** except in the case of changing Oxorg yields **(e, j, o, t)**.

3.3 Implications and remaining issues to be explored

Our simulation results (Figs. 5-9) illustrate that biotic plant stresses are capable of substantially perturbing both the number and size of atmospheric aerosol particles throughout a significant fraction of the year (summarised in Fig. 12). Considering that we calculated *daily* new particle growth, our results point to the direction that induced plant emissions will subsequently lead to more efficient CCN production in the atmosphere (Fig. 12), which will moreover affect cloud properties, such as cloud albedo and lifetime (Twomey, 1977; Albrecht, 1989; Gryspeerdt et al., 2014; Rosenfeld et al., 2014). The amplitude of the enhancement, however, depends strongly on the specific stressor and tree species which are attacked.

Naturally, both the duration of stress (Fig. 12e) and the predicted number (Fig. 12d) and size (Fig. 12c) of new particles depend highly on our assumptions about e.g. when the fungi start to attack their host, how fast the fungi spread, whether the larval eggs hatch simultaneously with budburst, how fast larval development occurs, and when senescence onsets - all which depend strongly on environmental conditions. It is furthermore probable that emissions are also induced from fungally infected leaves during senescence, which was not simulated here. The duration of stress can, thus, be significantly longer than what is summarised in Fig. 12e, whereby also the post-defoliation period, in case of herbivory infestations, will be shorter, and the atmospheric importance of the stresses stronger.

We have also shown that it can be more important to account for biotic plant stresses in models for local and regional predictions of new particle formation and growth during the time of infestation/infection than significant variations in those environmental parameters which predictions of VOC emissions are currently controlled by, e.g. light conditions (Fig.

10b,f,j,n), temperature (Fig. 10c,g,k,o) and LAI (Fig. 10d,h,l,p). Considering changes in the emissions of VOCs caused by stress also seems to be more crucial than accounting for large changes in the concentrations of O_3 (Fig. 11a,f,k,p) and OH (Fig. 11b,g,l,q).

Considering the frequency and scale of the investigated biotic stresses is important in order to properly evaluate the impact of the stresses on the atmosphere and climate: Fungi are largely ubiquitous and e.g. yearly account for ~10 % of all recorded damage symptoms on trees growing in European forests (ICP Forests, 2020). To put that number in perspective, ~87 % of all investigated broadleaved trees (>50000) are yearly reported to have damage symptoms in European forests (ICP Forests, 2020). Considering the duration of stress, and the predicted increase in the number and size of atmospheric aerosol particles in response to fungal infections, together with the fact that especially oak powdery mildew is one of the most common plant diseases, with e.g. ~9 % of pedunculate and sessile oak reported to be infected by powdery mildew in Europe yearly (ICP Forests, 2020), our findings call for initiatives to account for fungal stress emission responses in numerical models in a robust manner. Though larvae are present every summer, the population density of both gypsy and autumnal moths is cyclic, with 8-10 years or 4-5 years between gypsy moth outbreaks, depending on the forest type (mesic vs xeric sites; Johnson et al., 2006), and 9-11 years between autumnal moth outbreaks (Haukioja et al., 1988; Ruohomäki et al., 2000; Ylivinkka et al., 2020). Gypsy moth, in North America alone, is estimated to have defoliated >38 million ha of forest during years 1920 to 2020 (Coleman et al., 2020), and yearly, gypsy moth larvae are usually reported to defoliate between ~0.2-0.8 million ha of forested land in the US, but with values as high as ~5 million ha/year (Karel and Man, 2017). In comparison, the total area of forested land in the US is ~333 million ha (www.fs.usda.gov.). In European forests, the mean level of defoliation of pedunculate and sessile oak is yearly reported to be ~27 %, while most of the trees are 10-25 % (~39 % of trees) or 25-40 % defoliated (~28 % of trees, ICP Forests, 2020). In comparison, only ~19 % of deciduous temperate oak trees in European forests are yearly reported to not be defoliated at all or that less than 10 % of the trees' foliage have been defoliated by herbivores (ICP Forests, 2020). Since European gypsy moth is one of the major defoliating insects feeding on pedunculate oak (https://www.cabi.org/isc/datasheet/31807#tohostsOrSpeciesAffected, last accessed 11th of June, 2021), it must be reasonable to assume that a significant fraction of the reported defoliation is caused by feeding by gypsy moth larvae, and thus it is likely that accounting for stress emissions in response to feeding by gypsy moth larval is important for realistic predictions of new particle formation and growth. It is also likely that the reported defoliation which is not caused by gypsy moth larvae, but other herbivores, also impacts new particle formation, though to which direction and with which amplitude is currently unknown. When the larval density of autumnal moth in Fennoscandinavia is low, the level of defoliation usually remains less than 15 % (Bylund 1995), but during outbreak years, large areas (in the order of several thousands of square kilometres) can become either completely or severely defoliated (e.g., Ruohomäki et al., 2000; Tenow 1975; Nikula 1993). Thus, considering the scale of autumnal moth infestation combined with our findings about both the order of the increase in atmospheric new particle formation and growth caused by autumnal moth infestations, and also the absolute number and size of newly formed particles, it could seem that the importance of accounting for autumnal moth infestation in models to predict aerosol formation is minor. It should, however, be emphasised that in our simulations we did not accounted for delayed defense responses, which mountain birches are known to possess (e.g., Kaitaniemi et al., 1998; Ruuhola et al., 2007), and which possibly cause elevated total particle concentrations for a few years after larval infestation (Ylivinkka et al., 2020). Also, we did not take multiple co-occurring stresses into account, which are often the rule in nature and which generally enhances the already induced emission response due to biotic plant stress (e.g. Blande et al., 2007; Vapaavuori et al., 2009; Holopainen and Gershenzon, 2010; Kivimäenpää et al., 2016; Ghimire et al., 2017). For example, Li et al. (2019) recently showed that warming significantly amplifies the emission response due to autumnal moth feeding. Thus, there is a great need for new field observations in order to validate modelling studies such as ours, and in general to quantify the role of stress emissions in the formation and subsequent growth of new particles. Especially because enclosure studies, which currently are close to the only published measurements studies which have investigated the ability of biotic plant stress to influence aerosol processes, often do not accurately represent what is observed on canopy to landscape scales. In addition to this, robust representations of stress

emissions, and the drivers of the emissions, are needed before it is possible to integrate stress emissions into large scale models

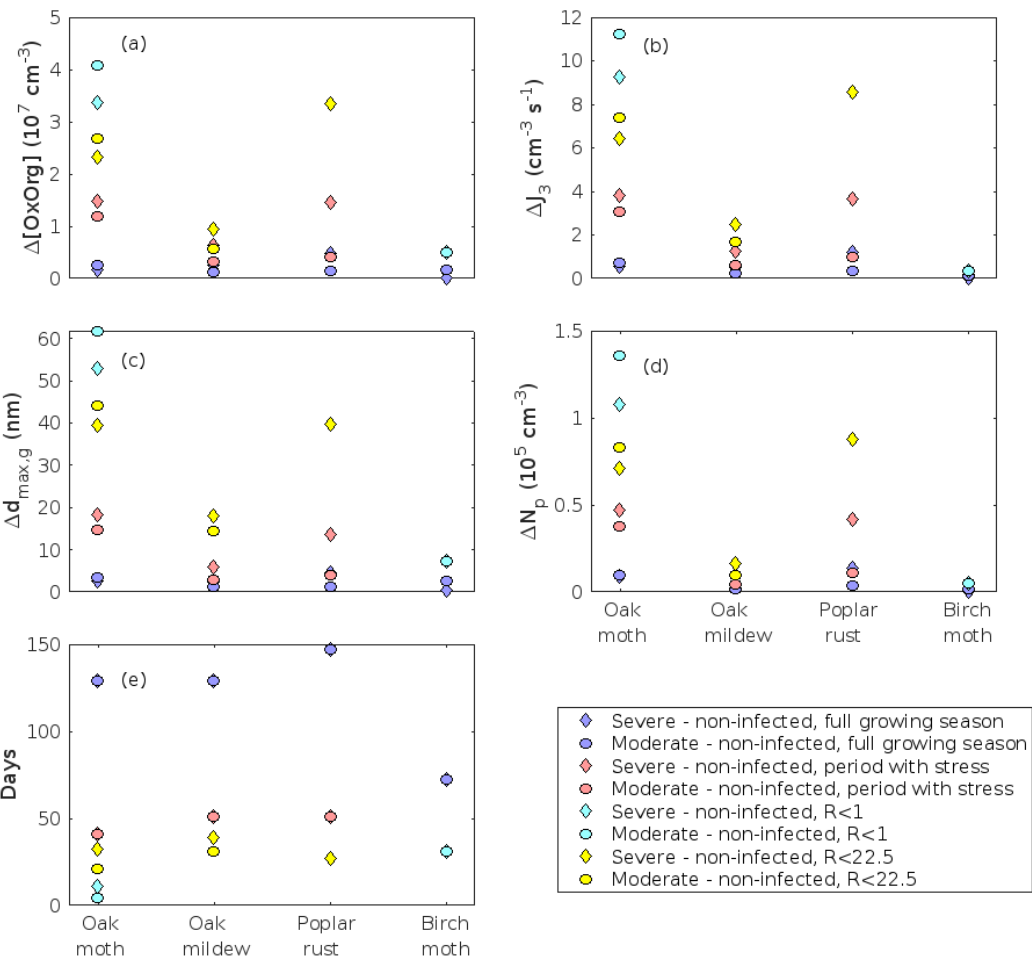837 without introducing errors in the models.

838

839

840 **Figure 12.** Differences in atmospheric response from various non-infected and biotically stressed plant species. **(a)**
841 atmospheric concentrations of OxOrg, **(b)** formation rates of 3 nm particles, **(c)** daily maximum diameter of the growing
842 particle mode, **(d)** number concentration of formed particles, and **(e)** amount of days considered. **a-d** are provided as the
843 differences between the averaged parameter in a stressed and stress-free forest stand of the same plant species type. Differences
844 and averages are considered based on the complete growing season, the period with stress, when the ratio of isoprene-to-
845 monoterpenes carbon concentration is less than 1 or less than 22.5. Be aware that R is always zero in simulations of birch. In
846 cases where R does not reach less than 1 or less than 22.5 in the atmosphere surrounding a non-infected forest stand, but it
847 does in the case of the corresponding stressed stand, it is assumed that the atmospheric parameter in the non-infected stand is
848 zero and hence the difference is given as the value of the stressed stand. The concentration differences of OxOrg, formation
849 rates and number concentrations are calculated based on an average, for the period of interest, of the median values during
850 10:00-16:00 local time. "Severe" and "moderate" refer to that 80 % or 30 % of the total leaf area has been consumed or infected
851 by the end of the feeding/infection period, respectively. Southern Germany has been used as border conditions for simulations
852 of oak and poplar, while SMEAR I, Finnish Lapland, has been used for modelling of birch.

853

4 Conclusions

We constructed a conceptual model to simulate new particle formation and growth in various broadleaved forest stands, in clean low NO_X environments, under biotically stressed and stress-free conditions, throughout a full growing season. Unsurprisingly, we found that the predicted atmospheric importance of biotic plant stress highly depends on the specific individual stressor and tree species which are attacked. Thus, the amount of newly formed particles was predicted to be up to about one order of magnitude higher in a gypsy moth infested oak stand than in a non-infested oak stand. In comparison, the number of new particles was simulated to be up to about a factor of 3, 4 and 5 higher in autumnal moth, oak powdery mildew and poplar rust infected mountain birch, pedunculate oak and balsam poplar stands, respectively. We furthermore predicted that the new particles will grow up to about 46, 28, 26 and 8 nm larger in an oak gypsy moth, poplar rust, autumnal moth and oak powdery mildew infected stand, respectively, compared to their corresponding non-infected stands within one day. To our knowledge, this study is the first to investigate the atmospheric impact of biotic plant stresses throughout a full growing season.

Our modelling results generally indicate that all the investigated plant stresses are capable of substantially perturbing both the number and size of atmospheric aerosol particles, and it is thus likely that the induced emissions will subsequently lead to more efficient CCN production in the atmosphere. We also showed that it can be more important to account for biotic plant stresses in models for local and regional predictions of new particle formation and growth during the time of infestation/infection than significant variations in e.g. LAI, and temperature and light conditions, which are currently the main parameters controlling predictions of VOC emissions. Considering our findings together with the fact that insect outbreaks and fungal diseases are generally expected to increase in both frequency and severity in the future, our study underlines the need for new field measurements to quantify the role of stress emissions in atmospheric aerosol processes and for making integration of biotic plant stress emission responses into numerical models possible.

Data availability. The model code is available upon reasonable request by contacting ditte.taipale[at]helsinki.fi. SMEAR I mountain birch leafing data can be obtained by contacting vesa.haataja[at]helsinki.fi. All other data used to constrain the model is publicly available following the provided references.

Author contributions. Idea and concept by ÜN. ÜN standardised the published emission rates. VM, MK and ME developed the theory for the aerosol module. DT developed the model code, conducted the simulations, and wrote the manuscript, with inputs from all authors. All authors discussed the results, and commented and edited the manuscript.

Competing interests. The authors declare that they have no conflict of interest.

References

Aalto, J., Kolari, P., Hari, P., Kerminen, V.-M., Schiestl-Aalto, P., Aaltonen, H., Levula, J., Siivola, E., Kulmala, M., and Bäck, J.: New foliage growth is a significant, unaccounted source for volatiles in boreal evergreen forests, Biogeosciences, 11, 1331–1344, https://doi.org/10.5194/bg-11-1331-2014, 2014.

895

896 Aalto, P., Aalto, T., and Keronen, P. SMEAR I Värriö forest meteorology, air quality and soil, Institute for Atmospheric and
897 Earth System Research, urn:nbn:fi:att:2a9c28bd-ca13-4a17-8b76-922bafa067a7, 2019.

898

899 Åhman, I: Rust scorings in a plantation of Salix viminalis clones during ten consecutive years, Eur. J. For. Path., 28, 251-258,
900 https://doi.org/10.1111/j.1439-0329.1998.tb01180.x, 1998.

901

902 Albrecht, B. A.: Aerosols, cloud microphysics, and fractional cloudiness, Science, 245, 1227-1230, DOI:
903 10.1126/science.245.4923.1227, 1989.

904

905 Ammunét, T., Klemola, T., and Saikkonen, K.: Impact of host plant quality on geometrid moth expansion on environmental
906 and local population scales, Ecogeg., 34, 848-855, doi: 10.1111/j.1600-0587.2011.06685.x, 2011.

907

908 Andreae, M. O., Afchine, A., Albrecht, R., Holanda, B. A., Artaxo, P., Barbosa, H. M. J., Borrmann, S., Cecchini, M. A.,
909 Costa, A., Dollner, M., Fütterer, D., Järvinen, E., Jurkat, T., Klimach, T., Konemann, T., Knote, C., Krämer, M., Krisna, T.,
910 Machado, L. A. T., Mertes, S., Minikin, A., Pöhlker, C., Pöhlker, M. L., Pöschl, U., Rosenfeld, D., Sauer, D., Schlager, H.,
911 Schnaiter, M., Schneider, J., Schulz, C., Spanu, A., Sperling, V. B., Voigt, C., Walser, A., Wang, J., Weinzierl, B., Wendisch,
912 M., and Ziereis, H.: Aerosol characteristics and particle production in the upper troposphere over the Amazon Basin, Atmos.
913 Chem. Phys., 18, 921–961, https://doi.org/10.5194/acp-18-921-2018, 2018.

914

915 Aphalo, P. J., Lahti, M., Lehto, T., Repo, T., Rummukainen, A., Mannerkoski, H., and Finér, L.: Responses of silver birch
916 saplings to low soil temperature, Silva Fenn., 40, 429-444, https://doi.org/10.14214/sf.328, 2006.

917

918 Arimura, G.-I., Köpke, S., Kunert, M., Volpe, V., David, A., Brand, P., Dabrowska, P., Maffei, M. E., and Boland, W.: Effects
919 of feeding Spodoptera littoralis on lima bean leaves. IV. Diurnal and nocturnal damage differentially initiate plant volatile
920 emission, Plant Physiol., 146, 965-973, https://doi.org/10.1104/pp.107.111088, 2008.

921

922 Asmi, E., Kivekäs, N., Kerminen, V.-M., Komppula, M., Hyvärinen, A.-P., Hatakka, J., Viisanen, Y., and Lihavainen, H.:
923 Secondary new particle formation in Northern Finland Pallas site between the years 2000 and 2010, Atmos. Chem. Phys., 11,
924 12959–12972, https://doi.org/10.5194/acp-11-12959-2011, 2011.

925

926 Atkinson, R., and Arey, J.: Atmospheric degradation of volatile organic compounds, Chem. Rev., 103, 4605-4638,
927 https://doi.org/10.1021/cr0206420, 2003.

928

929 Atkinson, R., Aschmann, S. M, Arey, J., and Shorees, B.: Formation of OH radicals in the gas phase reactions of O_3 with a
930 series of terpenes, J. Geophys. Res. A, 97, 6065-6073, https://doi.org/10.1029/92JD00062, 1992.

931

932 Ayres, M. P., and MacLean, Jr. S. F.: Molt as a component of insect development: Galerucella sagittariae (Chrysomelidae)
933 and Epirrita autumnata (Geometridae), Oikos 48, 273-279, doi:10.2307/3565514, 1987.

934

935 Bale, J. S., Masters, G. J., Hodkinson, I. D., Awmack, C., Bezemer, T. M., Brown, V. K., Butterfield, J., Buse, A., Coulson, J.
936 C., Farrar, J., Good, J. E. G., Harrington, R., Hartley, S., Jones, T. H., Lindroth, R. L., Press, M. C., Symrnioudis, I., Watt, A.
937 D., and Whittaker, J. B.: Herbivory in global climate change research: direct effects of rising temperature on insect herbivores,
938 Glob. Change Biol., 8, 1-16, https://doi.org/10.1046/j.1365-2486.2002.00451.x, 2002.

939

940 Berg, A. R., Heald, C. L., Huff Hartz, K. E., Hallar, A. G., Meddens, A. J. H., Hicke, J. A., Lamarque, J.-F., and Tilmes, S.:

941 The impact of bark beetle infestations on monoterpene emissions and secondary organic aerosol formation in western North

942 America, Atmos. Chem. Phys., 13, 3149–3161, https://doi.org/10.5194/acp-13-3149-2013, 2013.

943

944 Bergström, R., Hallquist, M., Simpson, D., Wildt, J., and Mentel, T. F.: Biotic stress: a significant contributor to organic

945 aerosol in Europe?, Atmos. Chem. Phys., 14, 13643–13660, https://doi.org/10.5194/acp-14-13643-2014, 2014.

946

947 Berndt, T., Richters, S., Jokinen, T., Hyttinen, N., Kurtén, T., Otkjær, R. V., Kjaergaard, H. G., Stratmann, F., Herrmann, H.,

948 Sipilä, M., Kulmala, M., and Ehn, M.: Hydroxyl radical-induced formation of highly oxidized organic compounds, Nat.

949 Commun., 7 13677, https://doi.org/10.1038/ncomms13677, 2016.

950

951 Berresheim, H., Elste, T., Plass-Dülmer, C., Eisele, F. L., and Tanner, D. J.: Chemical ionization mass spectrometer for long-

952 term measurements of atmospheric OH and H2SO4, Int. J. Mass. Spectrom., 202, 91-109, https://doi.org/10.1016/S1387-

953 3806(00)00233-5, 2000.

954

955 Bert, D., Lasnier, J.-B., Capdevielle, X., Dugravot, A., and Desprez-Loustau, M.-L.: Powdery mildew decreases the radial

956 growth of oak trees with cumulative and delayed effects over years, PLoS ONE, 11, e0155344, doi:10.1371/journal.

957 pone.0155344, 2016.

958

959 Bianchi, F., Kurtén, T., Riva, M., Mohr, C., Rissanen, M. P., Roldin, P., Berndt, T., Crounse, J. D., Wennberg, P. O., Mentel,

960 T. F., Wildt, J., Junninen, H., Jokinen, T., Kulmala, M., Worsnop, D. R., Thronton, J. A., Donahue, N., Kjaergaard, H. G., and

961 Ehn, M.: Highly oxygenated organic molecules (HOM) from gas-phase autoxidation involving peroxy radicals: A key

962 contributor to atmospheric aerosol, Chem. Rev., 119, 3472–3509, https://doi.org/10.1021/acs.chemrev.8b00395, 2019.

963

964 Bilde, M., Barsanti, K., Booth, M. D., Cappa, C. D., Donahue, N. M., McFiggans, G., Krieger, U. K., Marcolli, C., Topping,

965 D., Ziemann, P., Barley, M., Clegg, S., Dennis-Smither, B., Emanuelsson, E. U., Hallquist, M., Hallquist, Å. M., Khlystov,

966 A., Kulmala, M., Mogensen, D., Percival, C. P., Pope, F., Reid, J. R., Ribeiro da Silva, M. A. V., Rosenoern, T., Salo, K.,

967 Soonsin, V. P., Yli-Juuti, T., Prisle, N. L., Pagels, J., Rarey, J., Zardini, A. A., and Riipinen, I.: Saturation vapor pressures and

968 transition enthalpies of low-volatility organic molecules of atmospheric relevance: from dicarboxylic acids to complex

969 mixtures, Chem. Rev., 115, 3679-4570, https://doi.org/10.1021/cr5005502, 2015.

970

971 Birmili, W., Berresheim, H., Plass-Dülmer, C., Elste, T., Gilge, S., Wiedensohler, A., and Uhrner, U.: The Hohenpeissenberg

972 aerosol formation experiment (HAFEX): a long-term study including size-resolved aerosol, H2SO4, OH, and monoterpenes

973 measurements, Atmos. Chem. Phys., 3, 361–376, https://doi.org/10.5194/acp-3-361-2003, 2003.

974

975 Blande, J. D., Tiiva, P., Oksanen, E., and Holopainen, J. K.: Emission of herbivore-induced volatile terpenoids from two hybrid

976 aspen (Populus tremula×tremuloides) clones under ambient and elevated ozone concentrations in the field, Glob. Chang. Biol.,

977 13, 2538-2550, 10.1111/j.1365-2486.2007.01453.x, 2007.

978

979 Blande, J. D., Turunen, K., and Holopainen, J. K.: Pine weevil feeding on Norway spruce bark has a stronger impact on needle

980 VOC emissions than enhanced ultraviolet-B radiation, Environ. Pollut., 157, 174-180, 10.1016/j.envpol.2008.07.007, 2009.

981

982 Boy, M., Kulmala, M., Ruuskanen, T. M., Pihlatie, M., Reissell, A., Aalto, P. P., Keronen, P., Dal Maso, M., Hellen, H.,
983 Hakola, H., Jansson, R., Hanke, M., and Arnold, F.: Sulphuric acid closure and contribution to nucleation mode particle growth,
984 Atmos. Chem. Phys., 5, 863–878, https://doi.org/10.5194/acp-5-863-2005, 2005.

986 Boyd, I. L., Freer-Smith, P. H., Gilligan, C. A., and Godfray, H. C. J: The consequence of tree pests and diseases for ecosystem
987 services, Science, 342, 1235773, doi: 10.1126/science.1235773, 2013.

989 Brilli, F., Ciccioli, P., Frattoni, M., Prestininzi, M., Spanedda, A. F., and Loreto, F.: Constitutive and herbivore-induced
990 monoterpenes emitted by Populus × euroamericana leaves are key volatiles that orient Chrysomela populi beetles, Plant Cell
991 Environ., 32, 542-552, 10.1111/j.1365-3040.2009.01948.x, 2009.

993 Bylund, H.: Long-term interactions between the autumnal moth and mountain birch: The roles of resources, competitors,
994 natural enemies, and weather (PhD Thesis). Swedish University Agricultural Sciences, 1995.

996 Cannon, R. J. C.: The implications of predicted climate change for insect pests in the UK, with emphasis on non-indigenous
997 species, Glob. Chang. Biol., 4, 785-796, 10.1046/j.1365-2486.1998.00190.x, 1998.

999 Calvert, J., Atkinson, R., Kerr, J. A., Madronich, S., Moortgat, G. K., Wallington, T. J., and Yarwood, G.: The Mechanisms
1000 of Atmospheric Oxidation of the Alkenes, Oxford University Press, Oxford, UK, 2000.

1002 Coleman, T. W., Haavik, L. J., Foelker, C., and Liebhold, A. M.: Forest Insect & Disease Leaflet 162 April 2020, US Forest
1003 Service.

1005 Copolovici, L., Väärtnõu, F., Portillo Estrada, M., and Niinemets, Ü.: Oak powdery mildew (Erysiphe alphitoides)-induced
1006 volatile emissions scale with the degree of infection in Quercus robur, Tree Physiol., 34, 1399-1410,
1007 https://doi.org/10.1093/treephys/tpu091, 2014.

1009 Copolovici, L., Pag, A., Kännaste, A., Bodescu, A., Tomescu, D., Copolovici, D., Soran, M.-L., and Niinemets, Ü.:
1010 Disproportionate photosynthetic decline and inverse relationship between constitutive and induced volatile emissions upon
1011 feeding of Quercus robur leaves by large larvae of gypsy moth (Lymantria dispar), Environ. Exp. Bot. 138 184-192,
1012 https://doi.org/10.1016/j.envexpbot.2017.03.014, 2017.

1014 Covarelli, L., Beccari, G., Tosi, L., Fabre, B., and Frey, P.: Three-year investigations on leaf rust of poplar cultivated for
1015 biomass production in Umbria, Central Italy, Biomass Bioenerg., 49, 315-322,
1016 https://doi.org/10.1016/j.biombioe.2012.12.032, 2013.

1018 Dahlberg, U., Berge, T. W., Petersson, H., and Vencatasawmy, C. P.: Modelling biomass and leaf area index in a sub-arctic
1019 Scandinavian mountain area, Scand. J. Forest Res., 19, 60-71, https://doi.org/10.1080/02827580310019266, 2004.

1021 Dal Maso, M., Sogacheva, L., Aalto, P. P., Riipinen, I., Komppula, M., Tunved, P., Korhonen, L., Suur-Uski, V., Hirsikko,
1022 A., Kurtén, T., Kerminen, V.-M., Lihavainen, H., Viisanen, Y., Hansson, H.-C., and Kulmala, M.: Aerosol size distribution
1023 measurements at four Nordic field stations: identification, analysis and trajectory analysis of new particle formation bursts,
1024 Tellus B, 59, 350-361, doi: 10.1111/j.1600-0889.2007.00267.x, 2007.

1025

Dal Maso, M., Hyvärinen, A., Komppula, M., Tunved, P., Kerminen, V.-M., Lihavainen, H., Viisanen, Y., Hansson, H.-C., and Kulmala, M.: Annual and interannual variation in boreal forest aerosol particle number and volume concentration and their connection to particle formation, Tellus 60B, 495-508, https://doi.org/10.1111/j.1600-0889.2008.00366.x, 2008.

Desprez-Loustau, M. L., Feau, N., Mougou-Hamdane, A., and Dutech, C.: Interspecific and intraspecific diversity in oak powdery mildews in Europe: coevolution history and adaptation to their hosts, Mycoscience, 52, 165-173, https://doi.org/10.1007/s10267-010-0100-5, 2011.

Di Carlo, P., Brune, W. H., Martinez, M., Harder, H., Lesher, R., Ren, X., Thornberry, T., Carroll, M. A., Young, V., Shepson, P. B., Riemer, D., Apel, E., and Campbell, C.: Missing OH reactivity in a forest: Evidence for unknown reactive biogenic VOCs, Science, 304, 722–725, doi: 10.1126/science.1094392, 2004.

Donahue, N. M., Ortega, I. K., Chuang, W., Riipinen, I., Riccobono, F., Schobesberger, S., Dommen, J., Baltensperger, U., Kulmala, M., Worsnop, D. R., Vehkamäki, H.: How do organic vapors contribute to new-particle formation?, Faraday Discuss., 165, 91-104, 10.1039/C3FD00046J, 2013.

Douma, J. C., Ganzeveld, L. N., Unsicker, S. B., Boeckler, A., and Dicke, M.: What makes a volatile organic compound a reliable indicator of insect herbivory?, Plant Cell Environ., 42, 3308-3325, https://doi.org/10.1111/pce.13624, 2019.

Dunne, E. M., Gordon, H., Kürten, A., Almeida, J., Duplissy, J., Williamson, C., Ortega, I. K., Pringle, K. J., Adamov, A., Baltensperger, U., Barmet, P., Benduhn, F., Bianchi, F., Breitenlechner, M., Clarke, A., Curtius, J., Dommen, J., Donahue, N. M., Ehrhart, S., Flagan, R. C., Franchin, A., Guida, R., Hakala, J., Hansel, A., Heinritzi, M., Jokinen, T., Kangasluoma, J., Kirkby, J., Kulmala, M., Kupic, A., Lawler, M. J., Lehtipalo, K., Makhmutov, V., Mann, G., Mathot, S., Merikanto, J., Miettinen, P., Nenes, A., Onnela, A., Rap, A., Reddington, C. L. S., Riccobono, F., Richards, N. A. D., Rissanen, M. P., Rondo, L., Sarnela, N., Schobesberger, S., Sengupta, K., Simon, M., Sipilä, M., Smith, J. N., Stozkhov, Y., Tomé, A., Tröstl, J., Wagner, P. E., Wimmer, D., Winkler, P. M., Worsnop, D. R., and Carslaw, K. S.: Global atmospheric particle formation from CERN CLOUD measurements, Science, 354, 1119-1124, DOI: 10.1126/science.aaf2649, 2016.

Ehn, M., Kleist, E., Junninen, H., Petäjä, T., Lönn, G., Schobesberger, S., Dal Maso, M., Trimborn, A., Kulmala, M., Worsnop, D. R., Wahner, A., Wildt, J., and Mentel, Th. F.: Gas phase formation of extremely oxidized pinene reaction products in chamber and ambient air, Atmos. Chem. Phys., 12, 5113–5127, https://doi.org/10.5194/acp-12-5113-2012, 2012.

Ehn, M., Thornton, J. A., Kleist, E., Sipilä, M., Junninen, H., Pullinen, I., Springer, M., Rubach, F., Tillmann, R., Lee, B., Lopez-Hilfiker, F., Andres, S., Acir, I-H., Rissanen, M., Jokinen, T., Schobesberger, S., Kangasluoma, J., Kontkanen, J., Nieminen, T., Kurtén, T., Nielsen, L. B., Jørgensen, S., Kjaergaard, H. G., Canagaratna, M., Maso, M. D., Berndt, T., Petäjä, T., Wahner, A., Kerminen, V.-M., Kulmala, M., Worsnop, D. R., Wildt, J., and Mentel, T. F.: A large source of low-volatility secondary organic aerosol, Nature 506, 476-479, https://doi.org/10.1038/nature13032, 2014.

El-Ghany, T. M. A., Eman, M. E., and EI-Sheikh, H. H.: Efficacy of fungal rust disease on willow plant in Egypt, Aust. J. Basic Appl. Sci., 3, 1527-1539, 2009.

Faiola, C. and Taipale, D.: Impact of insect herbivory on plant stress volatile emissions from trees: A synthesis of quantitative measurements and recommendations for future research, Atmos. Environ. X, 5, 100060, https://doi.org/10.1016/j.aeaoa.2019.100060, 2020.

1070

1071 Faiola, C. L., Buchholz, A., Kari, E., Yli-Pirilä, P., Holopainen, J. K., Kivimäenpää, M., Miettinen, P., Worsnop, D. R.,

1072 Lehtinen, K. E. J., Guenther, A. B., and Virtanen, A.: Terpene composition complexity controls secondary organic aerosol

1073 yields from Scots pine volatile emissions, Sci. Rep., 8, 3053, 10.1038/s41598-018-21045-1, 2018.

1074

1075 Faiola, C. L., Pullinen, I., Buchholz, A., Khalaj, F., Ylisirniö, A., Kari, E., Miettinen, P., Holopainen, J. K., Kivimäenpää, M.,

1076 Schobesberger, S., Yli-Juuti, T., and Virtanen, A.: Secondary Organic aerosol formation from healthy and aphid-stressed Scots

1077 pine emissions, ACS Earth Space Chem., 3, 1756-1772, https://doi.org/10.1021/acsearthspacechem.9b00118, 2019.

1078

1079 Fiedler, V., Dal Maso, M., Boy, M., Aufmhoff, H., Hoffmann, J., Schuck, T., Birmili, W., Hanke, M., Uecker, J., Arnold, F.,

1080 and Kulmala, M.: The contribution of sulphuric acid to atmospheric particle formation and growth: a comparison between

1081 boundary layers in Northern and Central Europe, Atmos. Chem. Phys., 5, 1773–1785, https://doi.org/10.5194/acp-5-1773-

1082 2005, 2005.

1083

1084 Gérard, P. R., Husson, C., Pinon, J., and Frey, P.: Comparison of genetic and virulence diversity of Melampsora larici-populina

1085 populations on wild and cultivated poplar and influence of the alternate host, Phytopathology, 96, 1027-1036, doi:

1086 10.1094/PHYTO-96-1027, 2006.

1087

1088 Ghimire, R. P., Kivimäenpää, M., Kasurinen, A., Häikiö, E., Holopainen, T., and Holopainen, J. K.: Herbivore-induced BVOC

1089 emissions of Scots pine under warming, elevated ozone and increased nitrogen availability in an open-field exposure, Agric.

1090 For. Meteorol., 242, 21-32, 10.1016/j.agrformet.2017.04.008, 2017.

1091

1092 Ghirardo, A., Koch, K., Taipale, R., Zimmer, I., Schnitzler, J.-P., and Rinne, J.: Determination of de novo and pool emissions

1093 of terpenes from four common boreal/alpine trees by $^{13}CO_2$ labelling and PTR-MS analysis, Plant Cell Environ., 33, 781-792,

1094 https://doi.org/10.1111/j.1365-3040.2009.02104.x, 2010.

1095

1096 Gill, A. L., Gallinat, A. S., Sanders-DeMott, R., Rigden, A. J., Short Gianotti, D. J., Mantooth, J. A., and Templer, P. H.:

1097 Changes in autumn senescence in northern hemisphere deciduous trees: a meta-analysis of autumn phenology studies. Ann.

1098 Bot. 116, 875-888, doi: 10.1093/aob/mcv055, 2015.

1099

1100 Glawe, D. A.: The powdery mildews: a review of the world's most familiar (yet poorly known) plant pathogens, Annu. Rev.

1101 Phytopathol., 46, 27-51, doi: 10.1146/annurev.phyto.46.081407.104740, 2008.

1102

1103 Goldstein, A., Goulden, M., Munger, J. W., Wofsy, S., and Geron, C.: Seasonal course of isoprene emissions from a midlatitude

1104 forest, J. Geophys. Res., 103, 31 045–31 056, https://doi.org/10.1029/98JD02708, 1998.

1105

1106 Größ, J., Hamed, A., Sonntag, A., Spindler, G., Manninen, H. E., Nieminen, T., Kulmala, M., Hõrrak, U., Plass-Dülmer, C.,

1107 Wiedensohler, A., and Birmili, W.: Atmospheric new particle formation at the research station Melpitz, Germany: connection

1108 with gaseous precursors and meteorological parameters, Atmos. Chem. Phys., 18, 1835–1861, https://doi.org/10.5194/acp-18-

1109 1835-2018, 2018.

1110

1111 Grote, R., Monson, R. K., Niinemets, Ü.: Leaf-level models of constitutive and stress-driven volatile organic compound

1112 emissions, Biology, Controls and Models of Tree Volatile Organic Compound Emissions, Tree Physiology, Springer,

1113 Dordrecht, 315-355, 10.1007/978-94-007-6606-8_12, 2013.

1114

1115 Grote, R., Sharma, M., Ghirardo, A., Schnitzler, J.-P.: A new modeling approach for estimating abiotic and biotic stress-
1116 induced de novo emissions of biogenic volatile organic compounds from plants, Front. For. Glob. Change, 2, 26, doi:
1117 10.3389/ffgc.2019.00026, 2019.

1118

1119 Gryspeerdt, E., Stier, P., and Partridge, D. G.: Satellite observations of cloud regime development: the role of aerosol processes,
1120 Atmos. Chem. Phys., 14, 1141–1158, https://doi.org/10.5194/acp-14-1141-2014, 2014.

1121

1122 Guenther, A.: Seasonal and spatial variations in natural volatile organic compound emissions, Ecol. Appl., 7, 34-45,
1123 https://doi.org/10.1890/1051-0761(1997)007[0034:SASVIN]2.0.CO;2, 1997.

1124

1125 Guenther, A. B., Monson, R. K., and Fall, R.: Isoprene and monoterpene emission rate variability: Observations with
1126 eucalyptus and emission rate algorithm development, J. Geophys. Res., 96, 10799-10808, https://doi.org/10.1029/91JD00960,
1127 1991.

1128

1129 Guenther, A., Zimmerman, P., and Wildermuth, M.: Natural volatile organic compound emission rate estimates for U.S.
1130 woodland landscapes, Atmos. Environ., 28, 1197-1210, https://doi.org/10.1016/1352-2310(94)90297-6, 1994.

1131

1132 Guenther, A., Karl, T., Harley, P., Wiedinmyer, C., Palmer, P. I., and Geron, C.: Estimates of global terrestrial isoprene
1133 emissions using MEGAN (Model of Emissions of Gases and Aerosols from Nature), Atmos. Chem. Phys., 6, 3181–3210,
1134 https://doi.org/10.5194/acp-6-3181-2006, 2006.

1135

1136 Guenther, A. B., Jiang, X., Heald, C. L., Sakulyanontvittaya, T., Duhl, T., Emmons, L. K., and Wang, X.: The Model of
1137 Emissions of Gases and Aerosols from Nature version 2.1 (MEGAN2.1): an extended and updated framework for modeling
1138 biogenic emissions, Geosci. Model Dev., 5, 1471–1492, https://doi.org/10.5194/gmd-5-1471-2012, 2012.

1139

1140 Hajji, M., Dreyer, M., and Marçais, B.: Impact of Erysiphe alphitoides on transpiration and photosynthesis in Quercus robur
1141 leaves, Eur. J. Plant. Pathol., 125, 63-72, https://doi.org/10.1007/s10658-009-9458-7, 2009.

1142

1143 Häkkinen, S. A. K., Manninen, H. E., Yli-Juuti, T., Merikanto, J., Kajos, M. K., Nieminen, T., D'Andrea, S. D., Asmi, A.,
1144 Pierce, J. R., Kulmala, M., and Riipinen, I.: Semi-empirical parameterization of size-dependent atmospheric nanoparticle
1145 growth in continental environments, Atmos. Chem. Phys., 13, 7665–7682, https://doi.org/10.5194/acp-13-7665-2013, 2013.

1146

1147 Hakola, H., Arey, J., Aschmann, S. M., and Atkinson, R.: Product formation from the gas phase reactions of OH radicals and
1148 O3 with a series of monoterpenes, J. Atmos. Chem., 18, 75-102, https://doi.org/10.1007/BF00694375, 1994.

1149

1150 Hari, P., Kulmala, M., Pohja, T., Lahti, T., Siivola, R., Palva, L., Aalto, P., Hämeri, K., Vesala, T., Luoma, S., and Pulliainen,
1151 E.: Air pollution in eastern Lapland: challenge for an environmental measurement station, Silva Fenn., 28, 29-39,
1152 https://doi.org/10.14214/sf.a9160, 1994.

1153

1154 Harrington, R., Clark, S. J., Welham, S. J., Verrier, P. J., Denholm, C. H., Hullé, M., Maurice, D., Rounsevell, M. D., and
1155 Cocu, N.: Environmental change and the phenology of European aphids, Glob. Chang. Biol., 13, 1550-1564, 10.1111/j.1365-
1156 2486.2007.01394.x, 2007.

1157

Haukioja, E., Neuvonen, S., Hanhimäki, S., and Niemelä, P.: The autumnal moth in Fennoscandia. In: Dynamics of forest insect populations, Springer, pp. 163-178, 1988.

Heinritzi, M., Dada, L., Simon, M., Stolzenburg, D., Wagner, A. C., Fischer, L., Ahonen, L. R., Amanatidis, S., Baalbaki, R., Baccarini, A., Bauer, P. S., Baumgartner, B., Bianchi, F., Brilke, S., Chen, D., Chiu, R., Dias, A., Dommen, J., Duplissy, J., Finkenzeller, H., Frege, C., Fuchs, C., Garmash, O., Gordon, H., Granzin, M., El Haddad, I., He, X., Helm, J., Hofbauer, V., Hoyle, C. R., Kangasluoma, J., Keber, T., Kim, C., Kürten, A., Lamkaddam, H., Laurila, T. M., Lampilahti, J., Lee, C. P., Lehtipalo, K., Leiminger, M., Mai, H., Makhmutov, V., Manninen, H. E., Marten, R., Mathot, S., Mauldin, R. L., Mentler, B., Molteni, U., Müller, T., Nie, W., Nieminen, T., Onnela, A., Partoll, E., Passananti, M., Petäjä, T., Pfeifer, J., Pospisilova, V., Quéléver, L. L. J., Rissanen, M. P., Rose, C., Schobesberger, S., Scholz, W., Scholze, K., Sipilä, M., Steiner, G., Stozhkov, Y., Tauber, C., Tham, Y. J., Vazquez-Pufleau, M., Virtanen, A., Vogel, A. L., Volkamer, R., Wagner, R., Wang, M., Weitz, L., Wimmer, D., Xiao, M., Yan, C., Ye, P., Zha, Q., Zhou, X., Amorim, A., Baltensperger, U., Hansel, A., Kulmala, M., Tomé, A., Winkler, P. M., Worsnop, D. R., Donahue, N. M., Kirkby, J., and Curtius, J.: Molecular understanding of the suppression of new-particle formation by isoprene, Atmos. Chem. Phys., 20, 11809–11821, https://doi.org/10.5194/acp-20-11809-2020, 2020.

Heiskanen, J.: Estimating aboveground tree biomass and leaf area index in a mountain birch forest using ASTER satellite data, Int. J. Remote Sens., 6, 1135-1158, https://doi.org/10.1080/01431160500353858, 2006.

Hirsikko, A., Laakso, L., Hõrrak, U., Aalto, P. P., Kerminen, V.-M., and Kulmala, M.: Annual and size dependent variation of growth rates and ion concentrations in boreal forest, Boreal Environ. Res., 10, 357-369, 2005.

Holopainen, J. K. and Gershenzon, J.: Multiple stress factors and the emission of plant VOCs, Trends Plant Sci. Special Issue: Induc. Biog. Volatile Org. Compd. Plant, 15, 176-184, 10.1016/j.tplants.2010.01.006, 2010.

Hunter, M. D., Kozlov, M. V., Itämies, J., Pulliainen, E., Bäck, J., Kyrö, E. M., and Niemelä, P.: Current temporal trends in moth abundance are counter to predicted effects of climate change in an assemblage of subarctic forest moths, Glob. Change Biol., 20, 1723-1737, doi: 10.1111/gcb.12529, 2014.

Hyvönen, S., Junninen, H., Laakso, L., Dal Maso, M., Grönholm, T., Bonn, B., Keronen, P., Aalto, P., Hiltunen, V., Pohja, T., Launiainen, S., Hari, P., Mannila, H., and Kulmala, M.: A look at aerosol formation using data mining techniques, Atmos. Chem. Phys., 5, 3345–3356, https://doi.org/10.5194/acp-5-3345-2005, 2005.

ICP Forests - Forest Condition in Europe: The 2020 Assessment, ICP Forests Technical Report under the UNECE Convention on Long-range Transboundary Air Pollution (Air Convention), https://www.icp-forests.org/pdf/ICPForests_TR2020.pdf

IPCC (2013). "Climate Change 2013: the physical science basis," in Contribution of Working Group I to the Fifth Assessment Report of the Intergovernmental Panel on Climate Change, eds F. T. Stocker et al. (Cambridge: Cambridge University Press), 1535.

Jenkin, M. E. and Clemitshaw, K. C.: Ozone and other secondary photochemical pollutants: chemical processes governing their formation in the planetary boundary layer, Atmos. Environ., 34, 2499-2527, 2000.

1201 Jenkin, M. E., Young, J. C., and Rickard, A. R.: The MCM v3.3.1 degradation scheme for isoprene, Atmos. Chem. Phys., 15,
1202 11433–11459, https://doi.org/10.5194/acp-15-11433-2015, 2015.

1203

1204 Jiang, Y., Ye, J., Veromann, L.-L., and Niinemets, Ü.: Scaling of photosynthesis and constitutive and induced volatile
1205 emissions with severity of leaf infection by rust fungus (Melampsora larici-populina) in Populus balsamifera var. suaveolens,
1206 Tree Physiol., 36, 856-872, doi: 10.1093/treephys/tpw035, 2016.

1207

1208 Jimenez, J. L., Canagaratna, M. R., Donahue, N. M., Prevot, A. S., Zhang, Q., Kroll, J. H., DeCarlo, P. F., Allan, J. D., Coe,
1209 H., Ng, N. L., Aiken, A. C., Docherty, K. S., Ulbrich, I. M., Grieshop, A. P., Robinson, A. L., Duplissy, J., Smith, J. D., Wilson,
1210 K. R., Lanz, V. A., Hueglin, C., Sun, Y. L., Tian, J., Laaksonen, A., Raatikainen, T., Rautiainen, J., Vaattovaara, P., Ehn, M.,
1211 Kulmala, M., Tomlinson, J. M., Collins, D. R., Cubison, M. J., Dunlea, E. J., Huffman, J. A., Onasch, T. B., Alfarra, M. R.,
1212 Williams, P. I., Bower, K., Kondo, Y., Schneider, J., Drewnick, F., Borrmann, S., Weimer, S., Demerjian, K., Salcedo, D.,
1213 Cottrell, L., Griffin, R., Takami, A., Miyoshi, T., Hatakeyama, S., Shimono, A., Sun, J. Y., Zhang, Y. M., Dzepina, K., Kimmel,
1214 J. R., Sueper, D., Jayne, J. T., Herndon, S. C., Trimborn, A. M., Williams, L. R., Wood, E. C., Middlebrook, A. M., Kolb, C.
1215 E., Baltensperger, U., Worsnop, D. R.: Evolution of organic aerosols in the atmosphere, Science, 326, 1525-1529, doi:
1216 10.1126/science.1180353, 2009.

1217

1218 Johnson, D. M., Liebhold, A. M., and Bjørnstad, O. N.: Geographical variation in the periodicity of gypsy moth outbreaks,
1219 Ecogeg., 29, 367-374, doi: 10.1111/j.2006.0906-7590.04448.x,2006.

1220

1221 Johansson, L. K.-H. and Alström, S.: Field resistance to willow leaf rust Melampsora epitea in inter- and intraspecific hybrids
1222 of Salix viminalis and S. dasyclados, Eur. J. Plant Pathol., 106, 763-769, https://doi.org/10.1023/A:1026573219481, 2000.

1223

1224 Jokinen, T., Berndt, T., Makkonen, R., Kerminen, V.-M., Junninen, H., Paasonen, P., Stratmann, F., Herrmann, H., Guenther,
1225 A. B., Worsnop, D. R., Kulmala, M., Ehn, M., and Sipilä, M.: Production of extremely low volatile organic compounds from
1226 biogenic emissions: Measured yields and atmospheric implications, Proc. Natl. Acad. Sci. U. S. A., 112, 7123-7128,
1227 https://doi.org/10.1073/pnas.1423977112, 2015.

1228

1229 Joutsensaari, J., Yli-Pirilä, P., Korhonen, H., Arola, A., Blande, J. D., Heijari, J., Kivimäenpää, M., Mikkonen, S., Hao, L.,
1230 Miettinen, P., Lyytikäinen-Saarenmaa, P., Faiola, C. L., Laaksonen, A., and Holopainen, J. K.: Biotic stress accelerates
1231 formation of climate-relevant aerosols in boreal forests, Atmos. Chem. Phys., 15, 12139–12157, https://doi.org/10.5194/acp-
1232 15-12139-2015, 2015.

1233

1234 Kaitaniemi, P., Ruohomäki, K., and Haukioja, E.: Consequences of defoliation on phenological interaction between Epirrita
1235 autumnata and its host plant, mountain birch, Funct. Ecol., 11, 199-208, https://doi.org/10.1046/j.1365-2435.1997.00063.x,
1236 1997.

1237

1238 Kaitaniemi, P., Ruohomäki, K., Ossipov, V., Haukioja, E., and Pihlaja, K.: Delayed induced changes in the biochemical
1239 composition of host plant leaves during an insect outbreak, Oecologia, 116, 182-190, https://doi.org/10.1007/s004420050578,
1240 1998.

1241

1242 Kaitaniemi, P. and Ruohomäki, K.: Effects of autumn temperature and oviposition date on timing of larval development and
1243 risk of parasitism in a spring folivore, Oikos, 84, 435-442, doi: 10.2307/3546422, 1999.

1244

Kanakidou, M., Seinfeld, J. H., Pandis, S. N., Barnes, I., Dentener, F. J., Facchini, M. C., Van Dingenen, R., Ervens, B., Nenes, A., Nielsen, C. J., Swietlicki, E., Putaud, J. P., Balkanski, Y., Fuzzi, S., Horth, J., Moortgat, G. K., Winterhalter, R., Myhre, C. E. L., Tsigaridis, K., Vignati, E., Stephanou, E. G., and Wilson, J.: Organic aerosol and global climate modelling: a review, Atmos. Chem. Phys., 5, 1053–1123, https://doi.org/10.5194/acp-5-1053-2005, 2005.

Kanawade, V. P., Jobson, B. T., Guenther, A. B., Erupe, M. E., Pressley, S. N., Tripathi, S. N., and Lee, S.-H.: Isoprene suppression of new particle formation in a mixed deciduous forest, Atmos. Chem. Phys., 11, 6013–6027, https://doi.org/10.5194/acp-11-6013-2011, 2011.

Karel, T. H. and Man, G.:Major Forest Insect and Disease Conditions in the United States: 2015 (No. FS-1093), U. S. Department of Agriculture, 2017.

Kari, E., Faiola, C. L., Isokääntä, S., Miettinen, P., Yli-Pirilä, P., Buchholz, A., Kivimäenpää, M., Mikkonen, S., Holopainen, J. K., and Virtanen, A.: Time-resolved characterization of biotic stress emissions from Scots pines being fed upon by pine weevil by means of PTR-ToF-MS, Boreal Environ. Res., 24, 25-49, 2019.

Kerminen, V.-M. and Kulmala, M.: Analytical formulae connecting the "real" and the "apparent" nucleation rate and the nuclei number concentration for atmospheric nucleation events, J. Aerosol Sci., 33, 609-622, doi: 10.1016/S0021-8502(01)00194-X, 2002.

Kerminen, V.-M., Lihavainen, H., Komppula, M., Viisanen, Y., and Kulmala, M.: Direct observational evidence linking atmospheric aerosol formation and cloud droplet activation, Geophys. Res. Lett., 32, 10.1029/2005GL023130, 2005.

Kerminen, V.-M., Paramonov, M., Anttila, T., Riipinen, I., Fountoukis, C., Korhonen, H., Asmi, E., Laakso, L., Lihavainen, H., Swietlicki, E., Svenningsson, B., Asmi, A., Pandis, S. N., Kulmala, M., and Petäjä, T.: Cloud condensation nuclei production associated with atmospheric nucleation: a synthesis based on existing literature and new results, Atmos. Chem. Phys., 12, 12037– 12059, https://doi.org/10.5194/acp-12-12037-2012, 2012.

Kiendler-Scharr, A., Wildt, J., Dal Maso, M., Hohaus, T., Kleist, E., Mentel, T. F., Tillmann, R., Uerlings, R., Schurr, U., and Wahner, A.: New particle formation in forests inhibited by isoprene emissions, Nature, 461, 381-384, DOI: 10.1038/nature08292, 2009.

Kiendler-Scharr, A., Andres, S., Bachner, M., Behnke, K., Broch, S., Hofzumahaus, A., Holland, F., Kleist, E., Mentel, T. F., Rubach, F., Springer, M., Steitz, B., Tillmann, R., Wahner, A., Schnitzler, J.-P., and Wildt, J.: Isoprene in poplar emissions: effects on new particle formation and OH concentrations, Atmos. Chem. Phys., 12, 1021–1030, https://doi.org/10.5194/acp-12-1021-2012, 2012.

Kirkby, J., Duplissy, J., Sengupta, K., Frege, C., Gordon, H., Williamson, C., Heinritzi, M., Simon, M., Yan, C., Almeida, J., Tröstl, J., Nieminen, T., Ortega, I. K., Wagner, R., Adamov, A., Amorim, A., Bernhammer, A.-K., Bianchi, F., Breitenlechner, M., Brilke, S., Chen, X., Craven, J., Dias, A., Ehrhart, S., Flagan, R. C., Franchin, A., Fuchs, C., Guida, R., Hakal, J., Hoyle, C. R., Jokinen, T., Junninen, H., Kangasluoma, J., Him, J., Krapf, M., Kürten, A., Laaksonen, A., Lehtipalo, K., Makhmutov, V., Mathot, S., Molteni, U., Onnela, A., Peräkylä, O., Piel, F., Petäjä, T., Praplan, A. P., Pringle, K., Rap, A., Richards, N. A. D., Riipinen, I., Rissanen, M. P., Rondo, L., Sarnela, N., Schobesberger, S., Scott, C. E., Seinfeld, J. H., Sipilä, M., Steiner, G., Stozhkov, Y., Stratmann, F., Tomé, A., Virtanen, A., Vogel, A. L., Wagner, A. C., Wagner, P. E., Weingartner, E.,

Wimmer, D., Winkler, P. M., Ye, P., Zhang, X., Hansel, A., Dommen, J., Donahue, N. M., Worsnop, D. R., Baltensperger, U., Kulmala, M., Carslaw, K. S., and Curtius, J.: Ion-induced nucleation of pure biogenic particles, Nature, 533, 521–526, https://doi.org/10.1038/nature17953, 2016.

Kivimäenpää, M., Ghimire, R. P., Sutinen, S., Häikiö, E., Kasurinen, A., Holopainen, T., and Holopainen, J. K.: Increases in volatile organic compound emissions of Scots pine in response to elevated ozone and warming are modified by herbivory and soil nitrogen availability, Eur. J. For. Res., 135, 343-360, 10.1007/s10342-016-0939-x, 2016.

Klemola, T., Ruohomäki, K., Andersson, T., and Neuvonen, S.: Reduction in size and fecundity of the autumnal moth, Epirrita autumnata, in the increase phase of a population cycle, Oecologia, 141, 47-56, https://doi.org/10.1007/s00442-004-1642-z, 2004.

Komppula, M., Sihto, S.-L., Korhonen, H., Lihavainen, H., Kerminen, V.-M., Kulmala, M., and Viisanen, Y.: New particle formation in air mass transported between two measurement sites in Northern Finland, Atmos. Chem. Phys., 6, 2811–2824, https://doi.org/10.5194/acp-6-2811-2006, 2006.

Kula, E., Pešlová, A., Martinek, P., and Mazal, P.: The development of caterpillars of gypsy moth (Lymantria dispar L.) feeding on food affected by nitrogen, Sumar. List, 137, 51-60, 2013.

Kulmala, M., Petäjä, T., Nieminen, T., Sipilä, M., Manninen, H. E., Lehtipalo, K., Dal Maso, M., Aalto, P. P., Junninen, H., Paasonen, P., Riipinen, I., Lehtinen, K. E. J., Laaksonen, A., and Kerminen, V.-M.: Measurement of the nucleation of atmospheric aerosol particles, Nat. Protoc., 7, 1651–1667, https://doi.org/10.1038/nprot.2012.091, 2012.

Kulmala, M., Kontkanen, J., Junninen, H., Lehtipalo, K., Manninen, H. E., Nieminen, T., Petäjä, T., Sipilä, M., Schobesberger, S., Rantala, P., Franchin, A., Jokinen, T., Järvinen, E., Äijälä, M., Kangasluoma, J., Hakala, J., Aalto, P. P., Paasonen, P., Mikkilä, J., Vanhanen, J., Aalto, J., Hakola, H., Makkonen, U., Ruuskanen, T., Mauldin, R. L. III, Duplissy, J., Vehkamäki, H., Bäck, J., Kortelainen, A., Riipinen, I., Kurtén, T., Johnston, M. V., Smith, J. N., Ehn, M., Mente,l T. F., Lehtinen, K. E. J., Laaksonen, A., Kerminen, V.-M., and Worsnop, D. R.: Direct observations of atmospheric aerosol nucleation, Science, 339, 943-946, DOI: 10.1126/science.1227385, 2013.

Kulmala, M., Petäjä, T., Ehn, M., Thornton, J., Sipilä, M., Worsnop, D. R., Kerminen, V.-M.: Chemistry of atmospheric nucleation: on the recent advances on precursor characterization and atmospheric cluster composition in connection with atmospheric new particle formation, Annu. Rev. Phys. Chem., 65, 21-37, https://doi.org/10.1146/annurev-physchem-040412-110014, 2014.

Kyrö, E.-M., Väänänen, R., Kerminen, V.-M., Virkkula, A., Petäjä, T., Asmi, A., Dal Maso, M., Nieminen, T., Juhola, S., Shcherbinin, A., Riipinen, I., Lehtipalo, K., Keronen, P., Aalto, P. P., Hari, P., and Kulmala, M.: Trends in new particle formation in eastern Lapland, Finland: effect of decreasing sulfur emissions from Kola Peninsula, Atmos. Chem. Phys., 14, 4383–4396, https://doi.org/10.5194/acp-14-4383-2014, 2014.

Lee, S.-H., Uin, J., Guenther, A. B., de Gouw, J. A., Yu, F., Nadykto, A. B., Herb, J., Ng, N. L., Koss, A., Brune, W. B., Baumann, K., Kanawade, V. P., Keutsch, F. N., Nenes, A., Olsen, K., Goldstein, A., and Ouyang, Q.: Isoprene suppression of new particle formation: Potential mechanisms and implications, J. Geophys. Res., 121, 14621-14635, https://doi.org/10.1002/2016JD024844, 2016.

1333

1334 Lehtinen, K. E. J., Dal Maso, M., Kulmala, M., and Kerminen, V. M.: Estimating nucleation rates from apparent particle

1335 formation rates and vice versa: Revised formulation of the Kerminen-Kulmala equation, J. Aerosol Sci., 38, 988-994,

1336 https://doi.org/10.1016/j.jaerosci.2007.06.009, 2007.

1337

1338 Lelieveld, J., Butler, T. M., Crowley, J. N., Dillon, T. J., Fischer, H., Ganzeveld, L., Harder, H., Lawrence, M. G., Martinez,

1339 M., Taraborrelli, D., and Williams, J.: Atmospheric oxidation capacity sustained by a tropical forest, Nature, 452, 737–740,

1340 https://doi.org/10.1038/nature06870, 2008.

1341

1342 Lempa, K., Agrawal, A. A., Salminen, J.P., Turunen, T., Ossipov, V., Ossipova, S., Haukioja, E., and Pihlaja, K.: Rapid

1343 herbivore-induced changes in mountain birch phenolics and nutritive compounds and their effects on performance of the major

1344 defoliator, Epirrita autumnata, J. Chem. Ecol., 30, 303-321, https://doi.org/10.1023/B:JOEC.0000017979.94420.78, 2004.

1345

1346 Li, T., Holst, T., Michelsen, A., and Rinnan, R.: Amplification of plant volatile defence against insect herbivory in a warming

1347 Arctic tundra, Nat. Plants, 5, 568-574, doi:10.1038/s41477-019-0439-3, 2019.

1348

1349 Lin, Y. H., Zhang, H., Pye, H. O. T., Zhang, Z., Marth, W. J., Park, S., Arashiro, M., Cui, T., Budisulistiorini, S. H., Sexton,

1350 K. G., Vizuete, W., Xie, Y., Luecken, D. J., Piletic, I. R., Edney, E. O., Bartolotti, L. J., Gold, A., and Surratt, J. D.: Epoxide

1351 as a precursor to secondary organic aerosol formation from isoprene photooxidation in the presence of nitrogen oxides, Proc.

1352 Natl. Acad. Sci. U.S.A., 110, 6718–6723, https://doi.org/10.1073/pnas.1221150110, 2013.

1353

1354 Major, I. T., Nicole, M.-C., Duplessis, S., and Seguin, A.: Photosynthetic and respiratory changes in leaves of poplar elicited

1355 by rust infection, Photosynth. Res., 104, 41-48, doi: 10.1007/s11120-009-9507-2, 2010.

1356

1357 Makkonen, R., Asmi, A., Korhonen, H., Kokkola, H., Järvenoja, S., Räisänen, P., Lehtinen, K. E. J., Laaksonen, A., Kerminen,

1358 V.-M., Järvinen, H., Lohmann, U., Bennartz, R., Feichter, J., Kulmala, M.: Sensitivity of aerosol concentrations and cloud

1359 properties to nucleation and secondary organic distribution in ECHAM5-HAM global circulation model, Atmos. Chem. Phys.,

1360 9, 1747-1766, 10.5194/acp-9-1747-2009, 2009.

1361

1362 Marçais, B. and Desprez-Loustau, M.-L.: European oak powdery mildew: impact on trees, effects of environmental factors,

1363 and potential effects of climate change, Ann. For. Sci., 71, 633-642, https://doi.org/10.1007/s13595-012-0252-x, 2014.

1364

1365 Marçais, B., Kavkova, M., and Desprez-Loustau, M.-L.: Phenotypic variation in the phenology of ascospore production

1366 between European populations of oak powdery mildew, Ann. For. Sci., 66, 814-822, https://doi.org/10.1051/forest/2009077,

1367 2009.

1368

1369 McFiggans, G., Mentel, T. F., Wildt, J., Pullinen, I., Kang, S., Kleist, E., Schmitt, S., Springer, M., Tillmann, R., Wu, C., Zhao,

1370 D., Hallquist, M., Faxon, C., Le Breton, M., Hallquist, Å. M., Simpson, D., Bergström, R., Jenkin, M. E., Ehn, M., Thornton,

1371 J. A., Alfarra, M. R., Bannan, T. J., Percival, C. J., Priestley, M., Topping, D., and Kiendler-Scharr, A.: Secondary organic

1372 aerosol reduced by mixture of atmospheric vapours, Nature, 565, 587-593, 10.1038/s41586-018-0871- y, 2019.

1373

1374 McManus, M., Schneeberger, N., Reardon, R., and Mason, G.: Forest insect and disease (No 162): Gypsy Moth, Washington,

1375 D.C.: United States Department of Agriculture Forest Service, 1989.

1376

Mentel, Th. F., Kleist, E., Andres, S., Dal Maso, M., Hohaus, T., Kiendler-Scharr, A., Rudich, Y., Springer, M., Tillmann, R., Uerlings, R., Wahner, A., and Wildt, J.: Secondary aerosol formation from stress-induced biogenic emissions and possible climate feedbacks, Atmos. Chem. Phys., 13, 8755-8770, https://doi.org/10.5194/acp-13-8755-2013, 2013.

Merikanto, J., Spracklen, D. V., Mann, G. W., Pickering, S. J., and Carslaw, K. S.: Impact of nucleation on global CCN, Atmos. Chem. Phys., 9, 8601-8616, 10.5194/acp-9-8601-2009, 2009.

Miller, J. C., Hanson, P. E., and Kimberling, D. N.: Development of the gypsy moth (Lepidoptera: Lymantriidae) on garry oak and red alder in Western North America, Environ. Entomol., 20, 1097-1101, https://doi.org/10.1093/ee/20.4.1097, 1991.

Mogensen, D., Smolander, S., Sogachev, A., Zhou, L., Sinha, V., Guenther, A., Williams, J., Nieminen, T., Kajos, M. K., Rinne, J., Kulmala, M., and Boy, M.: Modelling atmospheric OH-reactivity in a boreal forest ecosystem, Atmos. Chem. Phys., 11, 9709–9719, https://doi.org/10.5194/acp-11-9709-2011, 2011.

Mogensen, D., Gierens, R., Crowley, J. N., Keronen, P., Smolander, S., Sogachev, A., Nölscher, A. C., Zhou, L., Kulmala, M., Tang, M. J., Williams, J., and Boy, M.: Simulations of atmospheric OH, O_3 and NO_3 reactivities within and above the boreal forest, Atmos. Chem. Phys., 15, 3909–3932, https://doi.org/10.5194/acp-15-3909-2015, 2015.

Monson, R. K., Harley, P. C., Litvak, M. E., Wildermuth, M., Guenther, A. B., Zimmerman, P. R., and Fall, R.: Environmental and developmental controls over the seasonal pattern of isoprene emission from aspen leaves, Oecologia, 99, 260–270, https://doi.org/10.1007/BF00627738, 1994.

Mutzel, A., Poulain, L., Berndt, T., Iinuma, Y., Rodigast, M., Böge, O., Richters, S., Spindler, G., Sipilä, M., Jokinen, T., Kulmala, M., and Herrmann, H.: Highly oxidized multifunctional organic compounds observed in tropospheric particles: a field and laboratory study, Environ. Sci. Technol., 49, 7754-7761, https://doi.org/10.1021/acs.est.5b00885, 2015.

Naja, M., Akimoto, H., and Staehelin, J.: Ozone in background and photochemically aged air over central Europe: analysis of long-term ozonesonde data from Hohenpeissenberg and Payerne, J. Geophys. Res., 108, 4063, doi:10.1029/2002JD002477 2003.

Nieminen, T., Lehtinen, K. E. J., and Kulmala, M.: Sub-10 nm particle growth by vapor condensation – effects of vapor molecule size and particle thermal speed, Atmos. Chem. Phys., 10, 9773–9779, https://doi.org/10.5194/acp-10-9773-2010, 2010.

Nieminen, T., Asmi, A., Dal Maso, M., Aalto, P. P., Keronen, P., Petäjä, T., Kulmala, M., and Kerminen, V.-M.: Trends in atmospheric new-particle formation: 16 years of observations in a boreal-forest environment, Boreal Environ. Res., 19, suppl. B, 191–214, 2014.

Nieminen, T., Yli-Juuti, T., Manninen, H., Petäjä, T., Kerminen, V.-M., and Kulmala, M.: Technical note: New particle formation event forecasts during PEGASOS–Zeppelin Northern mission 2013 in Hyytiälä, Finland, Atmos. Chem. Phys., 15, 12385– 12396, doi:10.5194/acp-15-12385-2015, 2015.

Niinemets, Ü.: Mild versus severe stress and BVOCs: thresholds, priming and consequences, Trends Plant Sci., 15, 145-153, https://doi.org/10.1016/j.tplants.2009.11.008, 2010.

1421

Niinemets, Ü., Reichstein, M., Staudt, M., Seufert, G., and Tenhunen, J. D.: Stomatal constraints may affect emission of oxygenated monoterpenoids from the foliage of Pinus pinea, Plant Physiol., 130, 1371-1385, https://doi.org/10.1104/pp.009670, 2002.

Niinemets Ü., Kännaste, A., and Copolovici, L.: Quantitative patterns between plant volatile emissions induced by biotic stresses and the degree of damage, Front. Plant Sci., 4, 262, https://doi.org/10.3389/fpls.2013.00262, 2013.

Nikula, A.: Animals as Forest Pests in Finnish Lapland, 22-29, 1993.

Nölscher, A. C., Williams, J., Sinha, V., Custer, T., Song, W., Johnson, A. M., Axinte, R., Bozem, H., Fischer, H., Pouvesle, N., Phillips, G., Crowley, J. N., Rantala, P., Rinne, J., Kulmala, M., Gonzales, D., Valverde-Canossa, J., Vogel, A., Hoffmann, T., Ouwersloot, H. G., Vilà-Guerau de Arellano, J., and Lelieveld, J.: Summertime total OH reactivity measurements from boreal forest during HUMPPA-COPEC 2010, Atmos. Chem. Phys., 12, 8257–8270, https://doi.org/10.5194/acp-12-8257-2012, 2012.

Nölscher, A. C., Yañez-Serrano, A. M., Wolff, S., Carioca de Araujo, A., Lavrič, J. V., Kesselmeier, J., and Williams, J.: Unexpected seasonality in quantity and composition of Amazon rainforest air reactivity, Nat. Commun., 7, 10383, https://doi.org/10.1038/ncomms10383, 2016.

Oláh, V., Szőllősi, E., Lakatos, Á., Kanalas, P., Nyitrai, B., and Mészáros, I.: Springtime leaf development of mature sessile oak trees as based on multi-seasonal monitoring data, Acta Silv. Lign. Hung., 8, 21-30, https://doi.org/10.2478/v10303-012-0002-7, 2012.

Paasonen, P., Nieminen, T., Asmi, E., Manninen, H. E., Petäjä, T., Plass-Dülmer, C., Flentje, H., Birmili, W., Wiedensohler, A., Hõrrak, U., Metzger, A., Hamed, A., Laaksonen, A., Facchini, M. C., Kerminen, V.-M., and Kulmala, M.: On the roles of sulphuric acid and low-volatility organic vapours in the initial steps of atmospheric new particle formation, Atmos. Chem. Phys., 10, 11223–11242, https://doi.org/10.5194/acp-10-11223-2010, 2010.

Paasonen, P., Asmi, A., Petäjä, T., Kajos, M. K., Äijälä, M., Junninen, H., Holst, T., Abbatt, J. P. D., Arneth, A., Birmili, W., van der Gon, H. D., Hamed, A., Hoffer, A., Laakso, L., Laaksonen, A., Leaitch, W. R., Plass-Dülmer, C., Pryor, S. C., Räisänen, P., Swietlicki, E., Wiedensohler, A., Worsnop, D. R., Kerminen, V.-M., and Kulmala, M.: Warming-induced increase in aerosol number concentration likely to moderate climate change, Nat. Geosci., 6, 438-442, https://doi.org/10.1038/ngeo1800, 2013.

Pacifico, F., Folberth, G. A., Sitch, S., Haywood, J. M., Rizzo, L. V., Malavelle, F. F., and Artaxo, P.: Biomass burning related ozone damage on vegetation over the Amazon forest: a model sensitivity study, Atmos. Chem. Phys., 15, 2791–2804, https://doi.org/10.5194/acp-15-2791-2015, 2015.

Pautasso, M., Döring, T. F., Garbelotto, M., Pellis, L., and Jeger, M. J.: Impacts of climate change on plant diseases - opinions and trends, Eur. J. Plant Pathol., 133, 295-313, https://doi.org/10.1007/s10658-012-9936-1, 2012.

Perez-Rial, D., Penuelas, J., Lopez-Mahia, P., and Llusia, J.: Terpenoid emissions from Quercus robur. A case study of Galicia (NW Spain), J. Environ. Monitor., 11, 1268-1275, doi: 10.1039/b819960d, 2009.

1465

Petäjä, T., Mauldin, III, R. L., Kosciuch, E., McGrath, J., Nieminen, T., Paasonen, P., Boy, M., Adamov, A., Kotiaho, T., and Kulmala, M.: Sulfuric acid and OH concentrations in a boreal forest site, Atmos. Chem. Phys., 9, 7435–7448, https://doi.org/10.5194/acp-9-7435-2009, 2009.

Petron, G., Harley, P., Greenberg, J., and Guenther, A.: Seasonal temperature variations influence isoprene emission, Geophys. Res. Lett., 28 (9), 1707–1710, https://doi.org/10.1029/2000GL011583, 2001.

Pinon, J., Frey, P., and Husson, C.: Wettability of poplar leaves influences dew formation and infection by Melampsora laricipopulina, Plant Dis., 90, 177-184, doi: 10.1094/PD-90-0177, 2006.

Pöhlker, C., Wiedemann, K. T., Sinha, B., Shiraiwa, M., Gunthe, S. S., Smith, M., Su, H., Artaxo, P., Chen, Q., Cheng, Y., Elbert, W., Gilles, M. K., Kilcoyne, A. L. D., Moffet, R. C., Weigand, M., Martin, S. T., Pöschl, U., and Andreae, M. O.: Biogenic potassium salt particles as seeds for secondary organic aerosol in the Amazon, Science, 337, 1075-1078, DOI: 10.1126/science.1223264, 2012.

Pöschl, U., Martin, S. T., Sinha, B., Chen, Q., Gunthe, S. S., ¨Huffman, J. A., Borrmann, S., Farmer, D. K., Garland, R. M., Helas, G., Jimenez, J. L., King, S. M., Manzi, A., Mikhailov, E., Pauliquevis, T., Petters, M. D., Prenni, A. J., Roldin, P., Rose, D., Schneider, J., Su, H., Zorn, S. R., Artaxo, P., and O., A. M.: Rainforest aerosols as biogenic nuclei of clouds and precipitation in the Amazon, Science, 329, 1513–1516, DOI: 10.1126/science.1191056, 2010.

Praplan, A. P., Tykkä, T., Chen, D., Boy, M., Taipale, D., Vakkari, V., Zhou, P., Petäjä, T., and Hellén, H.: Long-term total OH reactivity measurements in a boreal forest, Atmos. Chem. Phys., 19, 14431–14453, https://doi.org/10.5194/acp-19-14431-2019, 2019.

Pullinen, I., Schmitt, S., Kang, S., Sarrafzadeh, M., Schlag, P., Andres, S., Kleist, E., Mentel, T. F., Rohrer, F., Springer, M., Tillmann, R., Wildt, J., Wu, C., Zhao, D., Wahner, A., and Kiendler-Scharr, A.: Impact of NOx on secondary organic aerosol (SOA) formation from α-pinene and β-pinene photooxidation: the role of highly oxygenated organic nitrates, Atmos. Chem. Phys., 20, 10125–10147, https://doi.org/10.5194/acp-20-10125-2020, 2020.

Quéléver, L. L. J., Kristensen, K., Normann Jensen, L., Rosati, B., Teiwes, R., Daellenbach, K. R., Peräkylä, O., Roldin, P., Bossi, R., Pedersen, H. B., Glasius, M., Bilde, M., and Ehn, M.: Effect of temperature on the formation of highly oxygenated organic molecules (HOMs) from alpha-pinene ozonolysis, Atmos. Chem. Phys., 19, 7609–7625, https://doi.org/10.5194/acp-19-7609-2019, 2019.

Radhakrishnan, K. and Hindmarsh, A. C.: Description and use of LSODE, the Livermore Solver for Ordinary Differential Equations, LLNL report UCRL-ID-113855, December 1993.

Riccobono, F., Schobesberger, S., Scott, C. E., Dommen, J., Ortega, I. K., Rondo, L., Almeida, J., Amorim, A., Bianchi, F., Breitenlechner, M., David, A., Downard, A., Dunne, E. M., Duplissy, J., Ehrhart, S., Flagan, R. C., Franchin, A., Hansel, A., Junninen, H., Kajos, M., Keskinen, H., Kupc, A., Kürten, A., Kvashin, A. N., Laaksonen, A., Lehtipalo, K., Makhmutov, V., Mathot, S., Nieminen, T., Onnela, A., Petäjä, T., Praplan, A. P., Santos, F. D., Schallhart, S., Seinfeld, J. H., Sipilä, M., Spracklen, D. V., Stozhkov, Y., Stratmann, F., Tomé, A., Tsagkogeorgas, G., Vaattovaara, P., Viisanen, Y., Vrtala, A., Wagner, P. E., Weingartner, E., Wex, H., Wimmer, D., Carslaw, K. S., Curtius, J., Donahue, N. M., Kirkby, J., Kulmala, M., Worsnop,

D. R., and Baltensperger, U.: Oxidation products of biogenic emissions contribute to nucleation of atmospheric particles, Science, 344, 717-721, DOI: 10.1126/science.1243527, 2014.

Rieksta, J., Li, T., Junker, R. R., Jepsen, J. U., Ryde, I., and Rinnan, R.: Insect herbivory strongly modifies mountain birch volatile emissions, Front. Plant Sci., 11: 558979, https://doi.org/10.3389/fpls.2020.558979, 2020.

Riipi, M., Lempa, K., Haukioja, E., Ossipov, V., and Pihlaja, K.: Effects of simulated winter browsing on mountain birch foliar chemistry and on the performance of insect herbivores, Oikos, 111, 221-234, https://doi.org/10.1111/j.0030-1299.2005.13781.x, 2005.

Riipinen, I., Yli-Juuti, T., Pierce, J. R., Petäjä, T., Worsnop, D. R., Kulmala, M., and Donahue, N. M.: The contribution of organics to atmospheric nanoparticle growth, Nat. Geosci., 5, 453-458, https://doi.org/10.1038/ngeo1499, 2012.

Rohrer, F. and Berresheim, H.: Strong correlation between levels of tropospheric hydroxyl radicals and solar ultraviolet radiation, Nature, 442, 184-187, https://doi.org/10.1038/nature04924, 2006.

Rosenfeld, D., Andreae, M. O., Asmi, A., Chin, M., de Leeuw, G., Donovan, D. P., Kahn, R., Kinne, S., Kivekäs, N., Kulmala, M., Lau, W., Schmidt, S., Suni, T., Wagner, T., Wildt, M., and Quass, J.: Global observations of aerosol-cloud-precipitation-climate interactions, Rev. Geophys., 52, 750–808, https://doi.org/10.1002/2013RG000441, 2014.

Ruohomäki, K., Tanhuanpää, M., Ayres, M. P., Kaitaniemi, P., Tammaru, T., and Haukioja, E.: Causes of cyclicity of Epirrita autumnata (Lepidoptera, Geometridae): grandiose theory and tedious practice, Popul. Ecol., 42, 211-223, https://doi.org/10.1007/PL00012000, 2000.

Ruuhola, T., Salminen, J.-P., Haviola, S., Yang, S., and Rantala, M. J.: Immunological memory of mountain birches: effects of phenolics on performance of the autumnal moth depend on herbivory history of trees, J. Chem. Ecol., 33, 1160-1176, doi: 10.1007/s10886-007-9308-z, 2007.

Ruuskanen, T. M., Reissell, A., Keronen, P., Aalto, P. P., Laakso, L., Grönholm, T., Hari, P., and Kulmala, M.: Atmospheric trace gas and aerosol particle concentration measurements in Eastern Lapland, Finland 1992-2001, Boreal Environ. Res., 8, 335-349, 2003.

Schaub, A., Blande, J. D., Graus, M., Oksanen, E., Holopainen, J. K., and Hansel, A.: Real-time monitoring of herbivore induced volatile emissions in the field, Physiol. Plant., 138, 123-133, 10.1111/j.1399-3054.2009.01322.x, 2010.

Schnitzler, J.-P., Lehning, A., and Steinbrecher, R.: Seasonal pattern of isoprene synthase activity in Quercus robur leaves and its significance for modeling isoprene emission rates, Bot. Acta, 110, 240–243, https://doi.org/10.1111/j.1438-8677.1997.tb00635.x, 1997.

Schobesberger, S., Junninen, H., Bianchi, F., Lönn, G., Ehn, M., Lehtipalo, K., Dommen, J., Ehrhart, S., Ortega, I. K., Franchin, A., Nieminen, T., Riccobono, F., Hutterli, M., Duplissy, J., Almeida, J., Amorim, A., Breitenlechner, M., Downard, A. J., Dunne, E. M., Flagan, R. C., Kajos, M., Keskinen, H., Kirkby, J., Kupc, A., Kürten, A., Kurtén, T., Laaksonen, A., Mathot, S., Onnela, A., Praplan, A. P., Rondo, L., Santos, F. D., Schallhart, S., Schnitzhofer, R., Sipilä, M., Tomé, A., Tsagkogeorgas, G., Vehkamäki, H., Wimmer, D., Baltensperger, U., Carslaw, K. S., Curtius, J., Hansel, A., Petäjä, T., Kulmala, M., Donahue,

N. M., and Worsnop, D. R.: Molecular understanding of atmospheric particle formation from sulfuric acid and large oxidized organic molecules, PNAS 110, 17223-17228, https://doi.org/10.1073/pnas.1306973110, 2013.

Seidel, D. J., Zhang, Y., Beljaars, A., Golaz, J.-C., Jacobson, A. R., and Medeiros, B.: Climatology of the planetary boundary layer over the continental United States and Europe, J. Geophys. Res. A, 117, D17106, doi:10.1029/2012JD018143, 2012.

Shifflett, S. D., Hazel, D. W., and Guthrie Nichols, E.: Sub-soiling and genotype selection improves Populus productivity grown on a North Carolina sandy soil, Forests, 7, 74-84, doi: 10.3390/f7040074, 2016.

Simon, M., Dada, L., Heinritzi, M., Scholz, W., Stolzenburg, D., Fischer, L., Wagner, A. C., Kürten, A., Rörup, B., He, X.-C., Almeida, J., Baalbaki, R., Baccarini, A., Bauer, P. S., Beck, L., Bergen, A., Bianchi, F., Bräkling, S., Brilke, S., Caudillo, L., Chen, D., Chu, B., Dias, A., Draper, D. C., Duplissy, J., El-Haddad, I., Finkenzeller, H., Frege, C., Gonzalez-Carracedo, L., Gordon, H., Granzin, M., Hakala, J., Hofbauer, V., Hoyle, C. R., Kim, C., Kong, W., Lamkaddam, H., Lee, C. P., Lehtipalo, K., Leiminger, M., Mai, H., Manninen, H. E., Marie, G., Marten, R., Mentler, B., Molteni, U., Nichman, L., Nie, W., Ojdanic, A., Onnela, A., Partoll, E., Petäjä, T., Pfeifer, J., Philippov, M., Quéléver, L. L. J., Ranjithkumar, A., Rissanen, M. P., Schallhart, S., Schobesberger, S., Schuchmann, S., Shen, J., Sipilä, M., Steiner, G., Stozhkov, Y., Tauber, C., Tham, Y. J., Tomé, A. R., Vazquez-Pufleau, M., Vogel, A. L., Wagner, R., Wang, M., Wang, D. S., Wang, Y., Weber, S. K., Wu, Y., Xiao, M., Yan, C., Ye, P., Ye, Q., Zauner-Wieczorek, M., Zhou, X., Baltensperger, U., Dommen, J., Flagan, R. C., Hansel, A., Kulmala, M., Volkamer, R., Winkler, P. M., Worsnop, D. R., Donahue, N. M., Kirkby, J., and Curtius, J.: Molecular understanding of new-particle formation from α-pinene between −50 and +25 °C, Atmos. Chem. Phys., 20, 9183–9207, https://doi.org/10.5194/acp-20-9183-2020, 2020.

Simpson, D. Winiwarter, W., Börjesson, G., Cinderby, S., Ferreiro, A., Guenther, A., Hewitt, C. N., Janson, R., Aslam K. Khalil, M., Owen, S., Pierce, T. E., Puxbaum, H., Shearer, M., Skiba, U., Steinbrecher, R., Tarrasón, L., and Öquist, M. G.: Inventorying emissions from Nature in Europe, J. Geophys. Res. A, 104, 8113-8152, https://doi.org/10.1029/98JD02747, 1999.

Simpson, D., Benedictow, A., Berge, H., Bergström, R., Emberson, L. D., Fagerli, H., Flechard, C. R., Hayman, G. D., Gauss, M., Jonson, J. E., Jenkin, M. E., Nyíri, A., Richter, C., Semeena, V. S., Tsyro, S., Tuovinen, J.-P., Valdebenito, Á., and Wind, P.: The EMEP MSC-W chemical transport model – technical description, Atmos. Chem. Phys., 12, 7825–7865, https://doi.org/10.5194/acp-12-7825-2012, 2012.

Sinha, V., Williams, J., Lelieveld, J., Ruuskanen, T. M., Kajos, M. K., Patokoski, J., Hellén, H., Hakola, H., Mogensen, D., Boy, M., Rinne, J., and Kulmala, M.: OH reactivity measurements within a boreal forest: evidence for unknown reactive emissions, Environ. Sci. Technol., 44, 6614–6620, 2010.

Smiatek, G. and Steinbrecher, R.: Temporal and spatial variation of forest VOC emissions inGermany in the decade 1994– 2003, Atmos. Environ., 40, S166, 166-177, https://doi.org/10.1016/j.atmosenv.2005.11.071, 2006.

Spear, R. J. The Great Gypsy Moth War: A history of the first campaign in Massachusetts to eradicate the gypsy moth, 1890-1901, University of Massachusetts Press, 2005.

Spracklen, D. V., Carslaw, K. S., Kulmala, M., Kerminen, V.-M., Sihto, S.-L., Riipinen, I., Merikanto, J., Mann, G. W., Chipperfield, M. P., Wiedensohler, A., Birmili, W., and Lihavainen, H.: Contribution of particle formation to global cloud condensation nuclei concentrations, Geophys. Res. Lett., 35, doi: 10.1029/2007GL033038, 2008.

Stolzenburg, D., Fischer, L., Vogel, A. L., Heinritzi, M., Schervish, M., Simon, M., Wagner, A. C., Dada, L., Ahonen, L. R., Amorim, A., Baccarini, A., Bauer, P. S., Baumgartner, B., Bergen, A., Bianchi, F., Breitenlechner, M., Brilke, S., Mazon, S. B., Chen, D., Dias, A., Draper, D. C., Duplissy, J., El Haddad, I., Finkenzeller, H., Frege, C., Fuchs, C., Garmash, O., Gordon, H., He, X., Helm, J., Hofbauer, V., Hoyle, C. R., Kim, C., Kirkby, J., Kontkanen, J., Kürten, A., Lampilahti, J., Lawler, M., Lehtipalo, K., Leiminger, M., Mai, H., Mathot, S., Mentler, B., Molteni, U., Nie, W., Nieminen, T., Nowak, J. B., Ojdanic, A., Onnela, A., Passananti, M., Petäjä, T., Quéléver, L. L. J., Rissanen, M. P., Sarnela, N., Schallhart, S., Tauber, C., Tomé, A., Wagner, R., Wang, M., Weitz, L., Wimmer, D., Xiao, M., Yan, C., Ye, P., Zha, Q., Baltensperger, U., Curtius, J., Dommen, J., Flagan, R. C., Kulmala, M., Smith, J. N., Worsnop, D. R., Hansel, A., Donahue, N. M., and Winkler, P. M.: Rapid growth of organic aerosol nanoparticles over a wide tropospheric temperature range, P. Natl. Acad. Sci. USA, 115, 9122-9127, https://doi.org/10.1073/pnas.1807604115, 2018.

Stoyenoff, J. L., Witter, J. A., and Montgomery, M. E.: Nutritional indices in the gypsy moth (Lymantria dispar (L.)) under field conditions and host switching situations, Oecologia, 97, 158-170, https://doi.org/10.1007/BF00323145, 1994.

Sun, Z., Copolovici, L., and Niinemets, Ü.: Can the capacity for isoprene emission acclimate to environmental modifications during autumn senescence in temperate deciduous tree species Populus tremula?, J. Plant Res., 125, 263–274, https://doi.org/10.1007/s10265-011-0429-7, 2012.

Surratt, J. D., Chan, A. W. H., Eddingsaas, N. C., Chan, M., Loza, C. L., Kwan, A. J., Hersey, S. P., Flagan, R. C., Wennberg, P. O., and Seinfeld, J. H.: Reactive intermediates revealed in secondary organic aerosol formation from isoprene, Proc. Natl. Acad. Sci. U. S. A., 107, 6640-6645, https://doi.org/10.1073/pnas.0911114107, 2010.

Tammaru, T., Kaitaniemi, P., and Ruohomäki, K.: Realized fecundity in Epirrita autumnata (Lepidoptera: Geometridae): relation to body size and consequences to population dynamics, Oikos, 77, 407-16, doi: 10.2307/3545931, 1996.

Taipale, D., Aalto, J., Schiestl-Aalto, P., Kulmala, M., and Bäck, J.: The importance of accounting for enhanced emissions of monoterpenes from new Scots pine foliage in models - A Finnish case study, Atmos. Environ. X., 8, 100097, https://doi.org/10.1016/j.aeaoa.2020.100097, 2020.

Taipale, D.: Impact of biotic and environmental stress and perturbations of Scots pines on formation and growth of atmospheric aerosol particles - a modelling study with quantitative estimates, in prep.

Taraborrelli, D., Lawrence, M., G., Crowley, J. N., Dillon, T. J., Gromov, S., Groß, C. B. M., Vereecken, L., and Lelieveld, J.: Hydroxyl radical buffered by isoprene oxidation over tropical forests, Nat. Geosci., 5, 190-193, https://doi.org/10.1038/ngeo1405, 2012.

Tenow, O.: Topographical dependence of an outbreak of oporinia autumnata Bkh. (lep., geometridae) in a mountain birch forest in northern Sweden, Zoon, 3, 85-110, 1975.

Tripathi, A. M., Fischer, M., Orság, M., Marek, M. V., Žalud, Z., and Trnka, M.: Evaluation of indirect measurement method of seasonal patterns of leaf area index in a high-density short rotation coppice culture of poplar, Acta Univ. Agric. Silvic. Mendelianae Brun., 64, 549-556, https://doi.org/10.11118/actaun201664020549, 2016.

Tröstl, J., Chuang, W. K., Gordon, H., Heinritzi, M., Yan, C., Molteni, U., Ahlm, L., Frege, C., Bianchi, F., Wagner, R., Simon, M., Lehtipalo, K., Williamson, C., Craven, J. S., Duplissy, J., Adamov, A., Almeida, J., Bernhammer, A.-K., Breitenlechner, M., Brilke, S., Dias, A., Ehrhart, S., Flagan, R. C., Franchin, A., Fuchs, C., Guida, R., Gysel, M., Hansel, A., Hoyle, C. R., Jokinen, T., Junninen, H., Kangasluoma, J., Keskinen, H., Kim, J., Krapf, M., Kürten, A., Laaksonen, A., Lawler, M., Leiminger, M., Mathot, S., Möhler, O., Nieminen, T., Onnela, A., Petäjä, T., Piel, F. M., Miettinen, P., Rissanen, M. P., Rondo, L., Sarnela, N., Schobesberger, S., Sengupta, K., Sipilä, M., Smith, J. N., Steiner, G., Tomè, A., Virtanen, A., Wagner, A. C., Weingartner, E., Wimmer, D., Winkler, P. M., Ye, P., Carslaw, K. S., Curtius, J., Dommen, J., Kirkby, J., Kulmala, M., Riipinen, I., Worsnop, D. R., Donahue, N. M., and Baltensperger, U.: The role of low-volatility organic compounds in initial particle growth in the atmosphere, Nature, 533, 527–531, https://doi.org/10.1038/nature18271, 2016.

Twomey, S.: The influence of pollution on the shortwave albedo of clouds, J., Atmos. Sci., 34, 1149–1152, https://doi.org/10.1175/1520-0469(1977)034<1149:TIOPOT>2.0.CO;2, 1977.

Vana, M., Komsaare, K., Hõrrak, U., Mirme, S., Nieminen, T., Kontkanen, J., Manninen, H. E., Petäjä, T., Noe, S. M., and Kulmala, M.: Characteristics of new-particle formation at three SMEAR stations, Boreal Environ. Res., 21, 345-362, 2016.

van Meeningen, Y., Schurgers, G., Rinnan, R., and Holst, T.: BVOC emissions from English oak (Quercus robur) and European beech (Fagus sylvatica) along a latitudinal gradient, Biogeosciences, 13, 6067–6080, https://doi.org/10.5194/bg-13-6067-2016, 2016.

Vapaavuori, E., Holopainen, J. K., Holopainen, T., Julkunen-Tiitto, R., Kaakinen, S., Kasurinen, A., Kontunen-Soppela, S., Kostiainen, K., Oksanen, E., Peltonen, P., Riikonen, J., and Tulva, I.: Rising atmospheric CO2 concentration partially masks the negative effects of elevated O3 in silver birch (Betula pendula roth), Ambio, 38, 418-424, 10.1579/0044-7447-38.8.418, 2009.

Verlinden, M. S., Broeckx, L. S., Van den Bulcke, J., Van Acker, J., and Ceulemans, R.: Comparative study of biomass determinants of 12 poplar (Populus) genotypes in a high-density short-rotation culture, Forest Ecol. Manag., 307, 101-111, https://doi.org/10.1016/j.foreco.2013.06.062, 2013.

Vialle, A., Frey, P., Hambleton, S., Bernier, L., and Hamelin, R. C.: Poplar rust systematics and refinement of Melampsora species delineation, Fungal Divers., 50, 227-248, https://doi.org/10.1007/s13225-011-0129-6, 2011.

Voegele, R. T. and Mendgen, K.: Rust haustoria: nutrient uptake and beyond, New Phytol., 159, 93-100, https://doi.org/10.1046/j.1469-8137.2003.00761.x, 2003.

Waring, P. and Townsend, M.: Field Guide to the Moths of Great Britain and Ireland, British Wildlife Publishing, 2009.

Wells, K. C., Millet, D. B., Payne, V. H., Deventer, M. J., Bates, K. H., de Gouw, J., Graus, M., Warneke, C., Wisthaler, A., and Fuentes, J. D.: Satellite isoprene retrievals constrain emissions and atmospheric oxidation, Nature, 585, 225-233, https://doi.org/10.1038/s41586-020-2664-3, 2020.

1682

1683 Williamson, C. J., Kupc, A., Axisa, D., Bilsback, K. R., Bui, T., Campuzano-Jost, P., Dollner, M., Froyd, K. D., Hodshire, A.

1684 L., Jimenez, J. L., Kodros, J. K., Luo, G., Murphy, D. M., Nault, B. A., Ray, E. A., Weinzierl, B., Wilson, J. C., Yu, F., Yu,

1685 P., Pierce, J. R., and Brock, C. A.: A large source of cloud condensation nuclei from new particle formation in the tropics,

1686 Nature, 574, 399-403, https://doi.org/10.1038/s41586-019-1638-9, 2019.

1687

1688 Winterhalter, R., Herrmann, F., Kanawati, B., Nguyen, T. L., Peeters, J., Vereecken, L., and Moortgat, G. K.: The gas-phase

1689 ozonolysis of β-caryophyllene ($C_{15}H_{24}$), Part I: an experimental study, Phys. Chem. Chem. Phys., 11, 4152-4172,

1690 https://doi.org/10.1039/B817824K, 2009.

1691

1692 Yan, C., Nie, W., Vogel, A. L., Dada, L., Lehtipalo, K., Stolzenburg, D., Wagner, R., Rissanen, M. P., Xiao, M., Ahonen, L.,

1693 Fischer, L., Rose, C., Bianchi, F., Gordon, H., Simon, M., Heinritzi, M., Garmash, O., Roldin, P., Dias, A., Ye, P., Hofbauer,

1694 V., Amorim, A., Bauer, P. S., Bergen, A., Bernhammer, A.-K., Breitenlechner, M., Brilke, S., Buchholz, A., Buenrostro

1695 Mazon, S., Canagaratna, M. R., Chen, X., Ding, A., Dommen, J., Draper, D. C., Duplissy, J., Frege, C., Heyn, C., Guida, R.,

1696 Hakala, J., Heikkinen, L., Hoyle, C. R., Jokinen, T., Kangasluoma, J., Kirkby, J., Kontkanen, J., Kürten, A., Lawler, M. J.,

1697 Mai, H., Mathot, S., Maulding III, R. L., Molteni, U., Nichman, L., Nieminen, T., Nowak, J., Ojdanic, A., Onnela, A., Pajunoja,

1698 A., Petäjä, T., Piel, F., Quéléver, L. L. J., Sarnela, N., Schallhart, S., Sengupta, K., Sipilä, M., Tomé, A., Tröstl, J., Väisänen,

1699 O., Wagner, A. C., Ylisirniö, A., Zha, Q., Baltensperger, U., Carslaw, K. S., Curtius, J., Flagan, R. C., Hansel, A., Riipinen,

1700 I., Smith, J. N., Virtanen, A., Winkler, P. M., Donahue, N. M., Kerminen, V.-M., Kulmala, M., Ehn, M., and Worsnop, D. R.:

1701 Size-dependent influence of NOx on the growth rates of organic aerosol particles, Sci. Adv., 6, eaay4945, doi:

1702 10.1126/sciadv.aay4945, 2020.

1703

1704 Ye, J., Jiang, Y., Veromann-Jürgenson, L.-L., Niinemets, Ü.: Petiole gall aphid (Pemphigus spyrothecae) infestation of Populus

1705 × petrovskiana leaves alters foliage photosynthetic characteristics and leads to enhanced emissions of both constitutive and

1706 stress-induced volatiles, Trees, 33, 37–51, 10.1007/s00468-018-1756-2, 2019.

1707

1708 Yli-Juuti, T., Riipinen, I., Aalto, P. P., Nieminen, T., Maenhaut, W., Janssens, I. A., Claeys, M., Salma, I., Ocskay, R., Hoffer,

1709 A., Imre, K., and Kulmala, M.: Characteristics of new particle formation events and cluster ions at K-puszta, Hungary, Boreal

1710 Environ. Res., 14, 683-698, 2009.

1711

1712 Yli-Juuti, T., Nieminen, T., Hirsikko, A., Aalto, P. P., Asmi, E., Hõrrak, U., Manninen, H. E., Patokoski, J., Dal Maso, M.,

1713 Petäjä, T., Rinne, J., Kulmala, M., and Riipinen, I.: Growth rates of nucleation mode particles in Hyytiälä during 2003−2009:

1714 variation with particle size, season, data analysis method and ambient conditions, Atmos. Chem. Phys., 11, 12865–12886,

1715 https://doi.org/10.5194/acp-11-12865-2011, 2011.

1716

1717 Yli-Pirilä, P., Copolovici, L., Kännaste, A., Noe, S., Blande, J. D., Mikkonen, S., Klemola, T., Pulkkinen, J., Virtanen, A.,

1718 Laaksonen, A., Joutsensaari, J., Niinemets, Ü., Holopainen, J. K.: Herbivory by an outbreaking moth increases emissions of

1719 biogenic volatiles and leads to enhanced secondary organic aerosol formation capacity, Environ. Sci. Technol, 50, 11501-

1720 11510, doi: 10.1021/acs.est.6b02800, 2016.

1721

1722 Ylisirniö, A., Buchholz, A., Mohr, C., Li, Z., Barreira, L., Lambe, A., Faiola, C., Kari, E., Yli-Juuti, T., Nizkorodov, S. A.,

1723 Worsnop, D. R., Virtanen, A., and Schobesberger, S.: Composition and volatility of secondary organic aerosol (SOA) formed

1724 from oxidation of real tree emissions compared to simplified volatile organic compound (VOC) systems, Atmos. Chem. Phys.,

1725 20, 5629–5644, https://doi.org/10.5194/acp-20-5629-2020, 2020.

1726

Ylivinkka, I., Itämies, J., Klemola, T., Ruohomäki, K., Kulmala, M., and Taipale, D.: Investigating evidence of enhanced aerosol formation and growth due to autumnal moth larvae feeding on mountain birch at SMEAR I in northern Finland, Boreal Environ. Res., 25, 121-143, 2020.

Yu, H., Ortega, J., Smith, J. N., Guenther, A. B., Kanawade, V. P., You, Yi., Liu, Y., Hosman, K., Karl, T., Seco, R., Geron, C., Pallardy, S. G., Gu, L., Mikkilä, J., and Lee, S.-H.: New particle formation and growth in an isoprene-dominated Ozark forest: from sub-5 nm to CCN-active sizes, Aerosol Sci. Technol., 48, 1285-1298, DOI: 10.1080/02786826.2014.984801, 2014.

Zannoni, N., Gros, V., Lanza, M., Sarda, R., Bonsang, B., Kalogridis, C., Preunkert, S., Legrand, M., Jambert, C., Boissard, C., and Lathiere, J.: OH reactivity and concentrations of biogenic volatile organic compounds in a Mediterranean forest of downy oak trees, Atmos. Chem. Phys., 16, 1619–1636, https://doi.org/10.5194/acp-16-1619-2016, 2016.

Zhao, D., Pullinen, I., Fuchs, H., Schrade, S., Wu, R., Acir, I.-H., Tillmann, R., Rohrer, F., Wildt, J., Guo, Y., Kiendler-Scharr, A., Wahner, A., Kang, S., Vereecken, L., and Mentel, T. F.: Highly oxygenated organic molecules (HOM) formation in the isoprene oxidation by NO3 radical, Atmos. Chem. Phys. Discuss., https://doi.org/10.5194/acp-2020-1178, in review, 2020.

Zúbrik, M., Novotný, J., and Kozánek, M.: The effect of gamma radiation on the host preferences of the gypsy moth larvae (Lymantria dispar L., Lep.: Lymantriidae), Lesn. Čas. For. J., 53, 15-23, 2007.

Appendix A: Emission factors at a few different degrees of stress

The emission factors utilised in our simulations depend on the degree of stress. The equations to calculate the emission factors, as a function of the degree of stress, are presented in Table 1 in the main paper. In this appendix, the emission factors at a few different degrees of stress are shown (Table A1). 25 ºC and 1000 μmol m^{-2} s^{-1} are here considered standard conditions (see Sec. 2.4).

Table A1. Emission factors ($\varepsilon_{i,Æ}$, in unit nmol m^{-2} one-sided LAI s^{-1}) at a few different degrees of stress ($Æ$). ISO = isoprene, MT = monoterpenes, MeSa = methyl salicylate, LOX = lipoxygenase pathway volatile compounds, DMNT = 4,8-dimethyl-1,3,7-nonatriene, MeOH = methanol, SQT = sesquiterpenes, α-Eud = α-Eudesmol.

Infestation of pedunculate oak (*Quercus robur*) by European gypsy moth (*Lymantria dispar*) based on Copolovici et al. (2017).					
$Æ$ (%)	0	10	30	60	80
ε_{iso} (nmol m^{-2} s^{-1})	30.3	19.6	8.21	0.161	0.0804
ε_{MT} (nmol m^{-2} s^{-1})	0.0400	2.16	4.40	5.96	6.54
ε_{MeSa} (nmol m^{-2} s^{-1})	0.0	0.0347	0.104	0.208	0.277
ε_{LOX} (nmol m^{-2} s^{-1})	0.0	0.577	2.37	6.63	10.5

ε_{DNMT} (nmol m^{-2} s^{-1})	0.0	0.0138	0.0475	0.113	0.167

Infection of pedunculate oak (*Quercus robur*) by oak powdery mildew (*Erysiphe alphitoides*) based on Copolovici et al. (2014)

$Æ$ (%)	0	10	30	60	80
ε_{iso} (nmol m^{-2} s^{-1})	10.6	8.50	6.04	4.79	4.17
ε_{MT} (nmol m^{-2} s^{-1})	0.0400	0.120	0.247	0.386	0.471
ε_{MeSa} (nmol m^{-2} s^{-1})	0.0	0.136	0.279	0.437	0.533
ε_{LOX} (nmol m^{-2} s^{-1})	0.00213	0.0645	0.189	0.377	0.501

Infection of balsam poplar (*Populus balsamifera* var. *suaveolens*) by poplar rust (*Melampsora larici-populina*) based on Jiang et al. (2016)

$Æ$ (%)	0	10	30	60	80
ε_{iso} (nmol m^{-2} s^{-1})	86.0	36.8	22.8	17.9	16.6
ε_{MT} (nmol m^{-2} s^{-1})	0.0625	0.145	0.302	0.762	1.22
ε_{MeSa} (nmol m^{-2} s^{-1})	0.0	0.0552	0.128	0.194	0.249
ε_{LOX} (nmol m^{-2} s^{-1})	0.481	1.96	3.96	11.8	19.8
ε_{DNMT} (nmol m^{-2} s^{-1})	0.0	0.0199	0.0460	0.0698	0.0898
ε_{MeOH} (nmol m^{-2} s^{-1})	16.9	14.9	19.0	45.6	76.9
ε_{SQT} (nmol m^{-2} s^{-1})	0.0	0.133	0.308	0.468	0.602
$\varepsilon_{\alpha\text{-Eud}}$ (nmol m^{-2} s^{-1})	0.0	0.0219	0.0507	0.0768	0.0989

Infestation of mountain birch (*Betula pubescens* var. *pumila*) by autumnal moth (*Epirrita autumnata*) based on Yli-Pirilä et al. (2016)

$Æ$ (%)	0	10	30	60	80
ε_{MT} (nmol m^{-2} s^{-1})	0.131	0.278	0.423	0.475	0.485
ε_{LOX} (nmol m^{-2} s^{-1})	0.0868	0.200	0.425	0.764	0.989
ε_{DNMT} (nmol m^{-2} s^{-1})	0.00122	0.00662	0.0125	0.0148	0.0153
ε_{SQT} (nmol m^{-2} s^{-1})	0.0437	0.0926	0.141	0.158	0.161

1756

Appendix B: Leaf age effect

Simulations of pedunculate oak infested with European gypsy moth larvae

1759 It seems likely that Copolovici et al. (2017) conducted their measurements on leaves that emit isoprene at peak rate, since their
1760 reported emission rate of isoprene from non-infested leaves is comparable to the rates reported from mature leaves in previous
1761 studies (e.g. Smiatek and Steinbrecher, 2006; Perez-Rial et al., 2009; van Meeningen et al., 2016). The impact of leaf age was
1762 tested during the period with stress utilising the moderations shown in Table B1. The first period covers the number of days
1763 between budbreak and the induction of isoprene emission, while the second period ends when initiation of peak isoprene
1764 emission rates has been reached. The duration of these two periods were calculated using Eq. 18a and Eq. 19 in Guenther et
1765 al. (2006) and our assumptions about the ambient temperature conditions (Fig. 4b). Since isoprene does not show an induced
1766 response in emission upon gypsy moth herbivory, the emission rate of isoprene was reduced in simulations of both non-infested
1767 and infested oak forest. The applied factors used for reductions are from Guenther et al. (2012). The emission rate of
1768 monoterpenes was increased in the beginning of the growing season for simulations of a non-infested oak stand utilising the
1769 coefficients from Guenther et al. (2012). Stress-induced emissions were not altered, since we do not know the effect of leaf
1770 age on these types of emissions and Guenther et al. (2012) e.g. also assumed the same. The results are shown in Fig. B1-2.

1771

1772 **Table B1.** Moderations made in order to consider the effect of leaf age. $\varepsilon_{isoprene}$ and $\varepsilon_{monoterpenes}$ are the emission factors
1773 of isoprene and monoterpenes, respectively, used in the simulations when the leaf age effect has been considered, while
1774 $\varepsilon_{iso,mature}$ and $\varepsilon_{mono,mature}$ are the emission factors of isoprene and monoterpenes, respectively, used in the default
1775 simulations (i.e. resulting in Fig. 5-6). The moderations have been applied to the simulations of either only non-infested oak
1776 or also stressed oak as indicated under "simulations".

| Period (day/month)	$\varepsilon_{isoprene}$	Simulations	$\varepsilon_{monoterpenes}$	Simulations
15-26/5	$0.05 \times \varepsilon_{iso,mature}$	Non-infested, moderate stress, severe stress	$2 \times \varepsilon_{mono,mature}$	Non-infested
27/5-11/6	$0.6 \times \varepsilon_{iso,mature}$	Non-infested, moderate stress, severe stress	$1.8 \times \varepsilon_{mono,mature}$	Non-infested
12/6-	$\varepsilon_{iso,mature}$	Non-infested, moderate stress, severe stress	$\varepsilon_{mono,mature}$	Non-infested, moderate stress, severe stress

1777
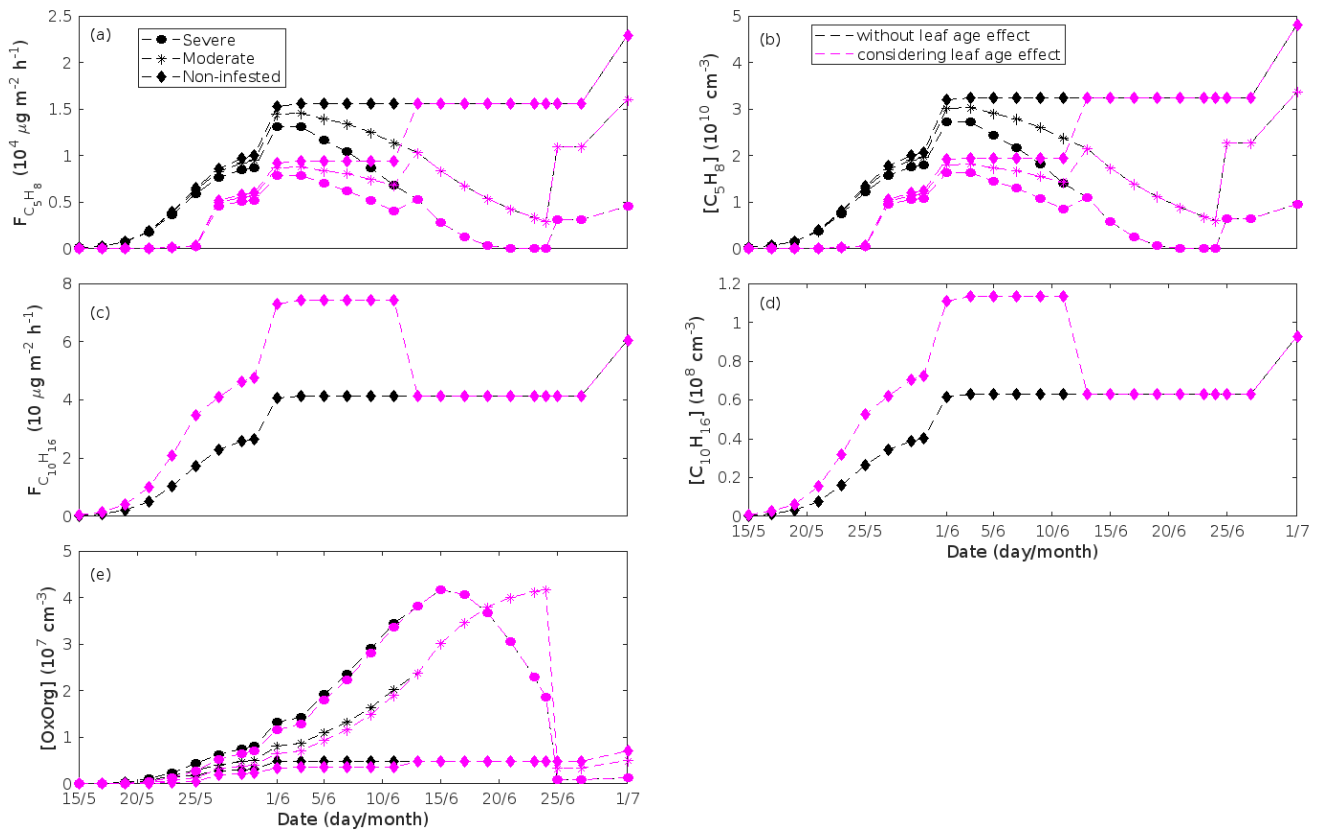
Figure B1. An oak stand infested with European gypsy moth larvae in comparison to a non-infested oak stand simulated with and without considering the impact of leaf age on the rates of emissions. Canopy emissions of **(a)** isoprene and **(c)** monoterpenes, atmospheric concentrations of **(b)** isoprene, **(d)** monoterpenes and **(e)** OxOrg. "Moderately" and "severely" refer to 30 % and 80 %, respectively, of the leaf area that has been consumed by the end of the feeding period. Black makers are for simulations where the effect of leaf age was not considered, while magenta markers are for simulations where the effect of leaf age was considered. Simulation results (independently of whether the effect of leaf age was considered or not) for "severe" is always indicated by circles, for "moderate" by asterisks, and for "non-infested" by diamonds.
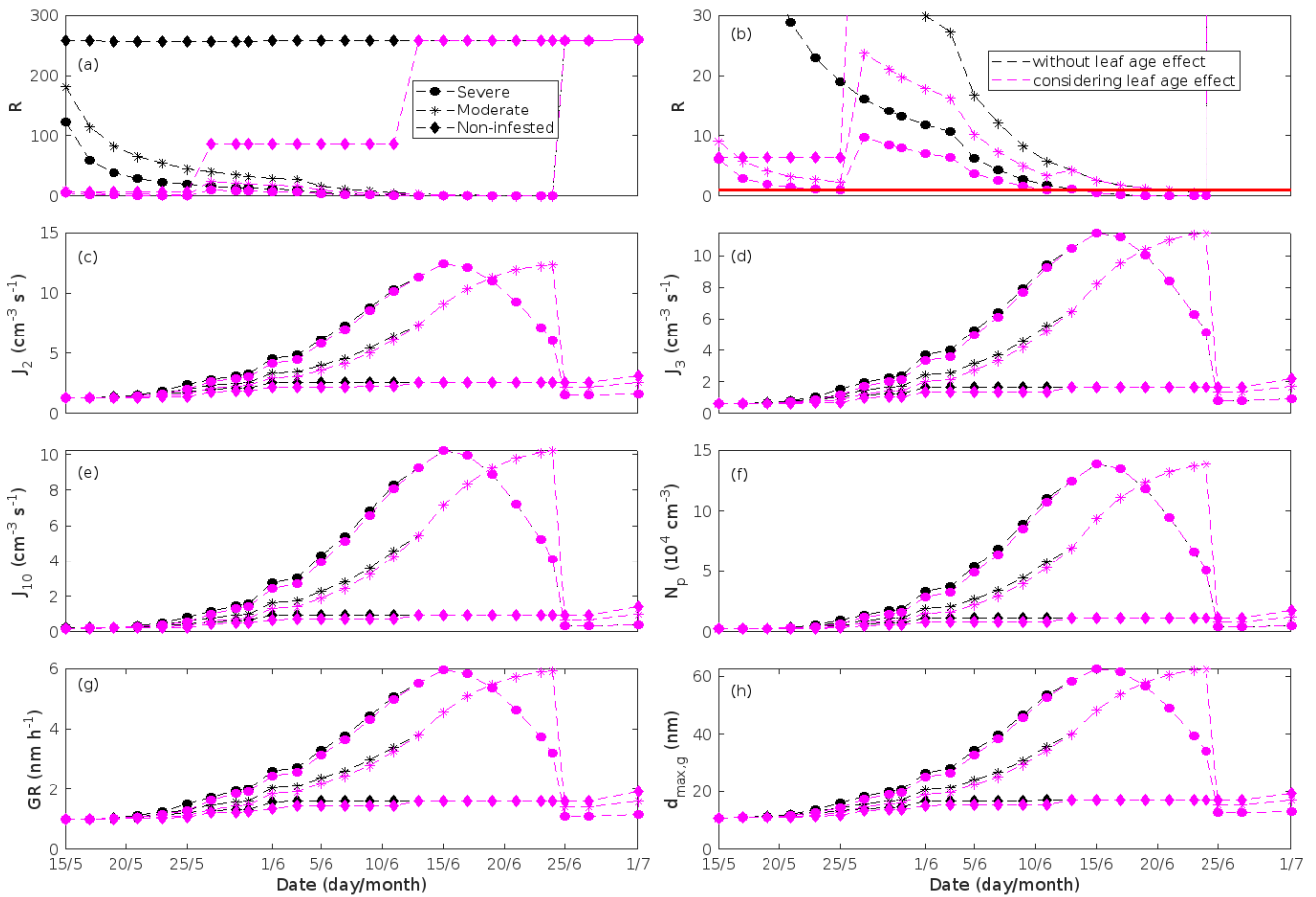
Figure B2. An oak stand infested with European gypsy moth larvae in comparison to a non-infested oak stand simulated with and without considering the impact of leaf age on the rates of emissions. (a) the ratios of isoprene-to-monoterpene carbon concentrations provided as a zoom in (b), where the red line indicates R = 1. Formation rates of (c) 2, (d) 3 and (e) 10 nm particles. (f) number concentrations of formed particles, (g) growth rates of newly formed particles, and (h) the daily maxima diameter of the growing particle mode. Symbols mean the same as in Fig. B1.

Simulations of pedunculate oak infected by oak powdery mildew and balsam poplar infected by rust fungi

The emission rates used for simulations of oak and poplar, with and without pathogenic infection, were measured in the middle and beginning of September, respectively, in Estonia (Copolovici et al., 2014; Jiang et al. 2016). Representative photographs of control leaves indicate that the measured leaves were mature and without any visible signs of senescence (Copolovici et al., 2014; Jiang et al. 2016).

When leaves grow old, they eventually lose their ability to photosynthesise and produce isoprene (Monson et al., 1994; Schnitzler et al., 1997; Sun et al., 2012) and Guenther et al. (2012) e.g. assumed a reduction of 10 % in the emissions of isoprene from senescing leaves (compared to that of mature leaves). However, a reduction on such a scale (i.e. 10 %) is not sufficient to decrease the ratio of isoprene to monoterpene carbon concentration to less than one in our simulations of oak and poplar infected by fungi. The impact of leaf age was therefore tested during the period with stress by decreasing the emission rate of isoprene to such a degree that R was either just under 22.5 or just under 1. Since isoprene does not show an induced response in emission upon oak powdery mildew or rust infection, the emission rate of isoprene was reduced in simulations of both non-infected and stressed oak and poplar forest. The results are shown in Fig. B3-4.
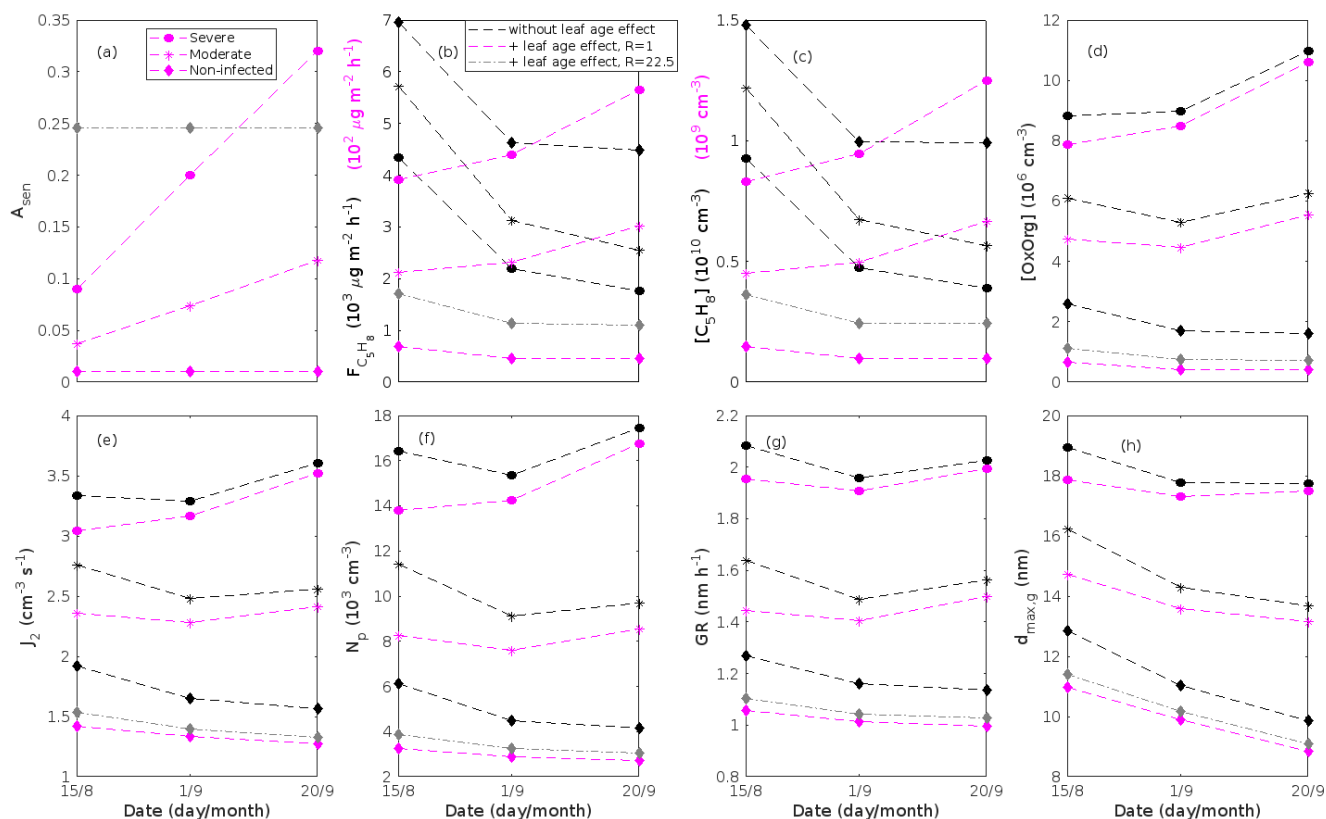
Figure B3. An oak stand infected by oak powdery mildew in comparison to a non-infected oak stand simulated with and without considering the impact of leaf age on the rates of isoprene emissions. **(a)** the fraction of isoprene emitted in comparison to simulations where the leaf age effect was not considered. For example, in order to reach R = 1 in simulations of a non-infected stand (magenta diamonds), the leaves are assumed to only emit 1 % of isoprene compared to our default simulations of a non-infected stand (black diamonds in Fig. 7a). The syntax is equivalent to that of Guenther et al. (2012, p. 1476). **(b)** canopy emissions of isoprene and atmospheric concentrations of **(c)** isoprene and **(d)** OxOrg. The units provided in black in **(b-c)** are connected to black and grey data points, while the units in magenta in **(b-c)** are connected to magenta data points. **(e)** formation rate of 2 nm particles, **(f)** number concentrations of formed particles, **(g)** growth rates of newly formed particles, and **(h)** the daily maxima diameter of the growing particle mode. The values of other parameters during these simulations are the same as in Fig. 7. "Moderately" and "severely" refer to 30 % and 80 %, respectively, of the leaf area being infected by fungi by the 20th of September. Black makers are for simulations where the effect of leaf age was not considered (see Fig. 7 for what R is then), while magenta markers are for simulations where the emission of isoprene was reduced sufficiently for R to be just under 1. Grey diamonds are used to illustrate simulation results of a non-infected oak stand, where the emission of isoprene has been reduced sufficiently for R to be just under 22.5. Simulation results (independently of whether the effect of leaf age was considered or not) for "severe" are always indicated by circles, for "moderate" by asterisks, and for "non-infected" by diamonds.
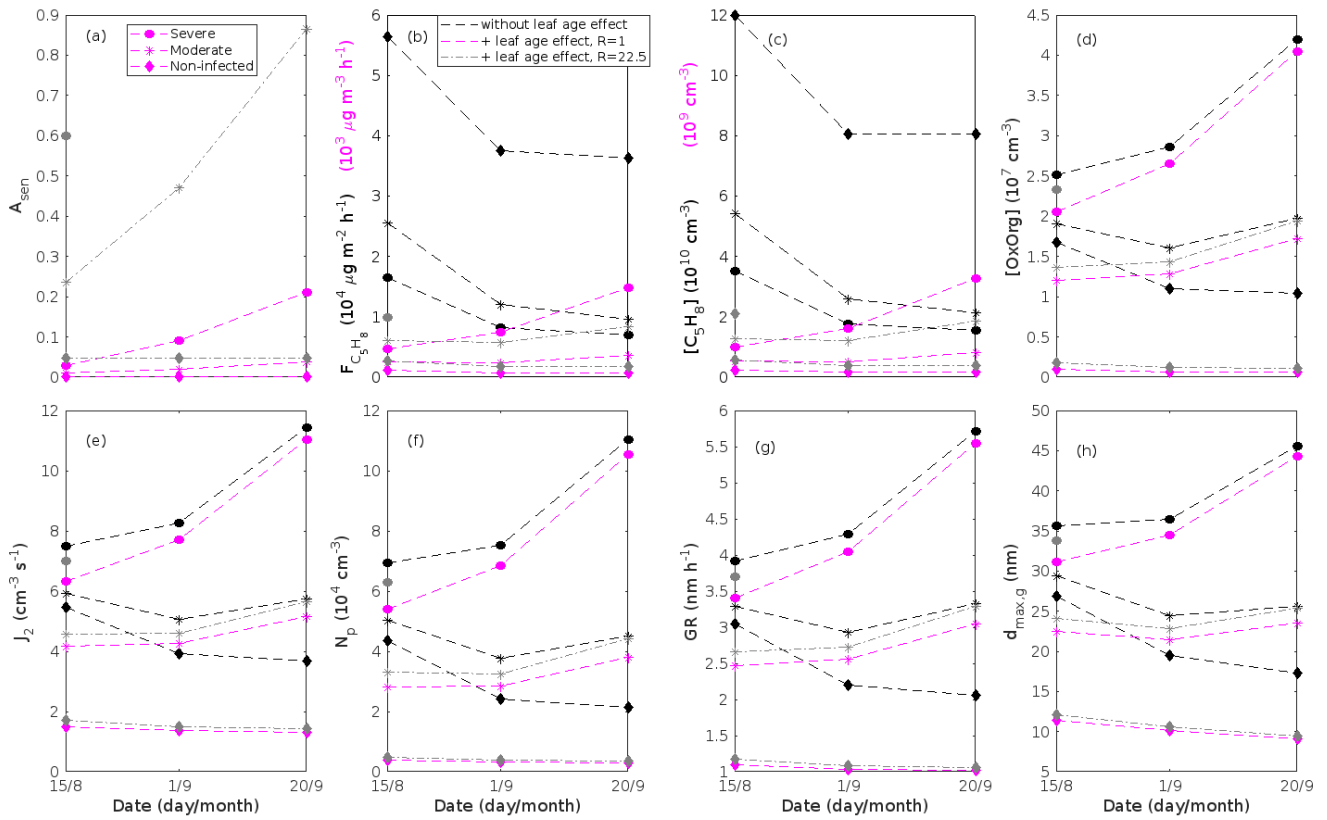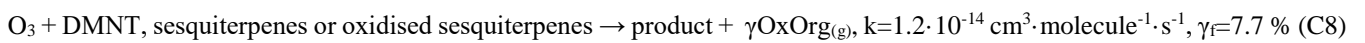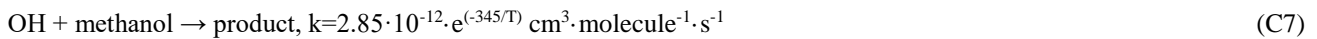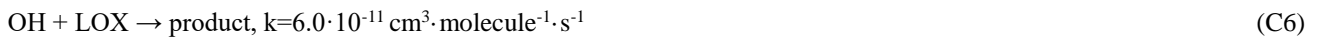
Figure B4. A poplar stand infected by rust in comparison to a non-infected poplar stand simulated with and without considering the impact of leaf age on the rates of isoprene emissions. **(a)** the fraction of isoprene emitted in comparison to simulations where the leaf age effect was not considered. **(b)** canopy emissions of isoprene and atmospheric concentrations of **(c)** isoprene and **(d)** OxOrg. The units provided in black in **(b-c)** are connected to black and grey data points, while the units in magenta in **(b-c)** are connected to magenta data points. **(e)** formation rate of 2 nm particles, **(f)** number concentrations of formed particles, **(g)** growth rates of newly formed particles, and **(h)** the daily maxima diameter of the growing particle mode. The values of other parameters during these simulations are the same as in Fig. 8. Grey markers are for simulations where the emission of isoprene was reduced sufficiently for R to be just under 22.5. Symbols are the same as in Fig. B3.
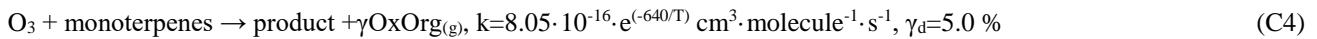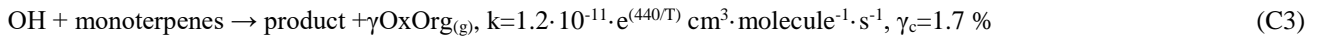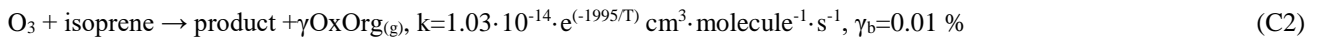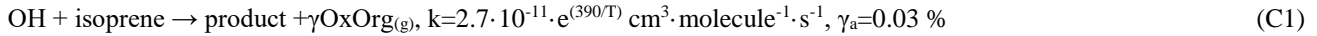
Appendix C: Chemical reactions in the model

We considered the following chemical reactions in our model:

$OH + isoprene \rightarrow product + \gamma OxOrg_{(g)}$, $k=2.7 \cdot 10^{-11} \cdot e^{(390/T)}$ cm$^3 \cdot$ molecule$^{-1} \cdot$ s^{-1}, $\gamma_a = 0.03$ % (C1)

$O_3 + isoprene \rightarrow product + \gamma OxOrg_{(g)}$, $k=1.03 \cdot 10^{-14} \cdot e^{(-1995/T)}$ cm$^3 \cdot$ molecule$^{-1} \cdot$ s^{-1}, $\gamma_b = 0.01$ % (C2)

$OH + monoterpenes \rightarrow product + \gamma OxOrg_{(g)}$, $k=1.2 \cdot 10^{-11} \cdot e^{(440/T)}$ cm$^3 \cdot$ molecule$^{-1} \cdot$ s^{-1}, $\gamma_c = 1.7$ % (C3)

$O_3 + monoterpenes \rightarrow product + \gamma OxOrg_{(g)}$, $k=8.05 \cdot 10^{-16} \cdot e^{(-640/T)}$ cm$^3 \cdot$ molecule$^{-1} \cdot$ s^{-1}, $\gamma_d = 5.0$ % (C4)

$OH + methyl\ salicylate \rightarrow product + \gamma OxOrg_{(g)}$, $k=4.0 \cdot 10^{-12}$ cm$^3 \cdot$ molecule$^{-1} \cdot$ s^{-1}, $\gamma_e = 10.0$ % (C5)

$OH + LOX \rightarrow product$, $k=6.0 \cdot 10^{-11}$ cm$^3 \cdot$ molecule$^{-1} \cdot$ s^{-1} (C6)

$OH + methanol \rightarrow product$, $k=2.85 \cdot 10^{-12} \cdot e^{(-345/T)}$ cm$^3 \cdot$ molecule$^{-1} \cdot$ s^{-1} (C7)

$O_3 + DMNT$, sesquiterpenes or oxidised sesquiterpenes $\rightarrow product + \gamma OxOrg_{(g)}$, $k=1.2 \cdot 10^{-14}$ cm$^3 \cdot$ molecule$^{-1} \cdot$ s^{-1}, $\gamma_f = 7.7$ % (C8)

$OxOrg_{(g)} \rightarrow OxOrg_{(p)}$, $k=CS \cdot 0.5$ (C9)

$OH + SO_2 \rightarrow H_2SO_{4(g)}$, $k=1.5 \cdot 10^{-12}$ cm$^3 \cdot$ molecule$^{-1} \cdot$ s^{-1} (C10)

$H_2SO_{4(g)} \rightarrow H_2SO_{4(p)}$, $k=CS$ (C11)

1849   T is temperature (K), p indicates "particle phase", CS is the condensation sink, while γ_i are the fractions of organic products

1850   which can partition to the particle phase (OxOrg). In practice, γ_i are either reported HOM yields, as defined in Ehn et al. (2014),

1851   or reported SOA yields / 2.2. SOA yields are decreased by a factor of 2.2 in order to account for the fact that SOA yields

1852   represent mass yields, and not molar yields as it is the case of HOM yields. We utilised HOM yields based on Jokinen et al.

1853   (2015) (γ_a, γ_b, γ_c, γ_d), Berndt et al. (2016) (γ_c), and Ehn et al. (2014) (γ_d). We used SOA yields from Mentel et al. (2013) (γ_e

1854   ,γ_f).

Appendix D: Sensitivity tests

1855

1856   **Table D1.** Constrained parameters for sensitivity tests and their range of values. Nine different sensitivity tests (ST1-9) were

1857   conducted for all plant species and infections, where only one parameter was changed at a time. BHL is the planetary boundary

1858   layer height, $PPFD_{max}$ is the daily maximum photosynthetic photon flux density, T_{max} is the maximum daily temperature, LAI

1859   is the leaf area index of non-infested leaves, CS is the condensation sink, and γ_{OxOrg} is the yield of OxOrg. "HPB" and "SMEAR

1860   I" refer to simulations conducted in Hohenpeissenberg (i.e. oak and poplar) and SMEAR I (i.e. birch) conditions, respectively.

| Sensitivity test no.	Parameter that changes	HPB	SMEAR I	Notes and references
ST1	BLH (m)	200 - 2500		Classical textbook example.
ST2	$PPFD_{max}$ ($\mu mol\ m^{-2}\ s^{-1}$)	200 – 2000	200 - 1600	The lower limit is based on observations at the SMEAR I station, the upper on the theoretical clear sky maxima.
ST3	T_{max} (ºC)	10 - 40	5 - 35	Based on observations and the IPCC 2014 predictions of the regional temperature increase.
ST4	LAI ($m^2\ m^{-2}$)	1 - 9	0.5 – 4	The upper limit is based on Tripathi et al. (2016).
ST5	$[O_3]$ (ppb)	35 - 100	20 - 70	Naja et al. (2003), Ruuskanen et al. (2003). The upper end for HPB simulations is similar to the highest values which are observed in the Amazon where concentrations of isoprene can be very high (e.g. Pacifico et al., 2015)
ST6	$[OH]_{max}$ (molec cm^{-3})	$0.1\text{-}10\cdot10^6$	$1\text{-}25\cdot10^5$	Petäjä et al. (2009), Berresheim et al. (2000), Rohrer and Berresheim (2006). The lower limit has not been observed in HPB, but is included in order to test the impact of potential OH depletion on our results.
ST7	$[H_2SO_4]_{max}$ (molec cm^{-3})	$5\text{-}25\cdot10^6$	$1\text{-}6.5\cdot10^6$	Birmili et al. (2003), Kyrö et al. (2014).
ST8	CS (s^{-1})	$2\text{-}8\cdot10^{-3}$	$0.2\text{-}3.5\cdot10^{-3}$	Birmili et al. (2003), Vana et al. (2016), Kyrö et al. (2014).
ST9	γ_{OxOrg}	$0.1\text{ - }2\cdot\gamma_{OxOrg,default}$		Ehn et al. (2014), Jokinen et al. (2015), Bianchi et al. (2019), McFiggans et al. (2019).

1861

1862
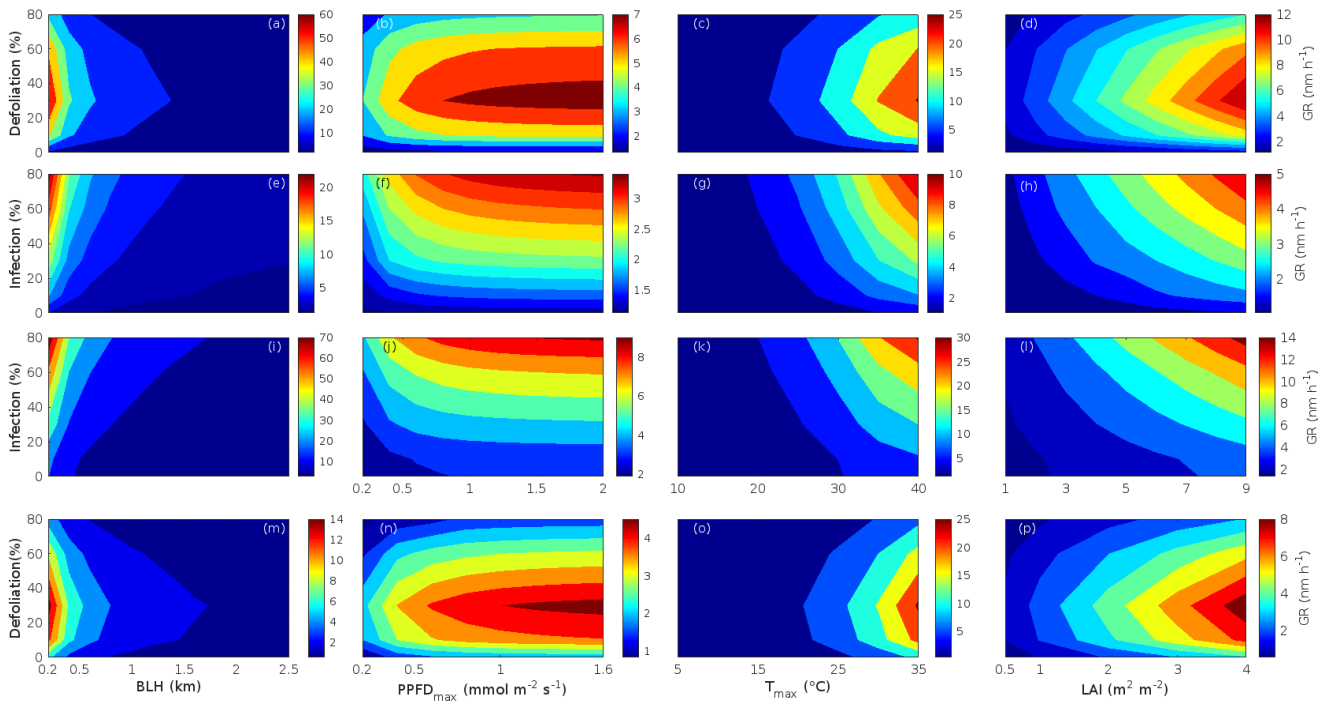
Figure D1. Impact of changed boundary conditions on the growth rate of small particles in non-infected and biotically stressed forest stands. The subplots correspond to those in Fig. 10, except the subplots here display growth rate, and not number of particles. Thus we refer to Fig. 10 for further explanations.
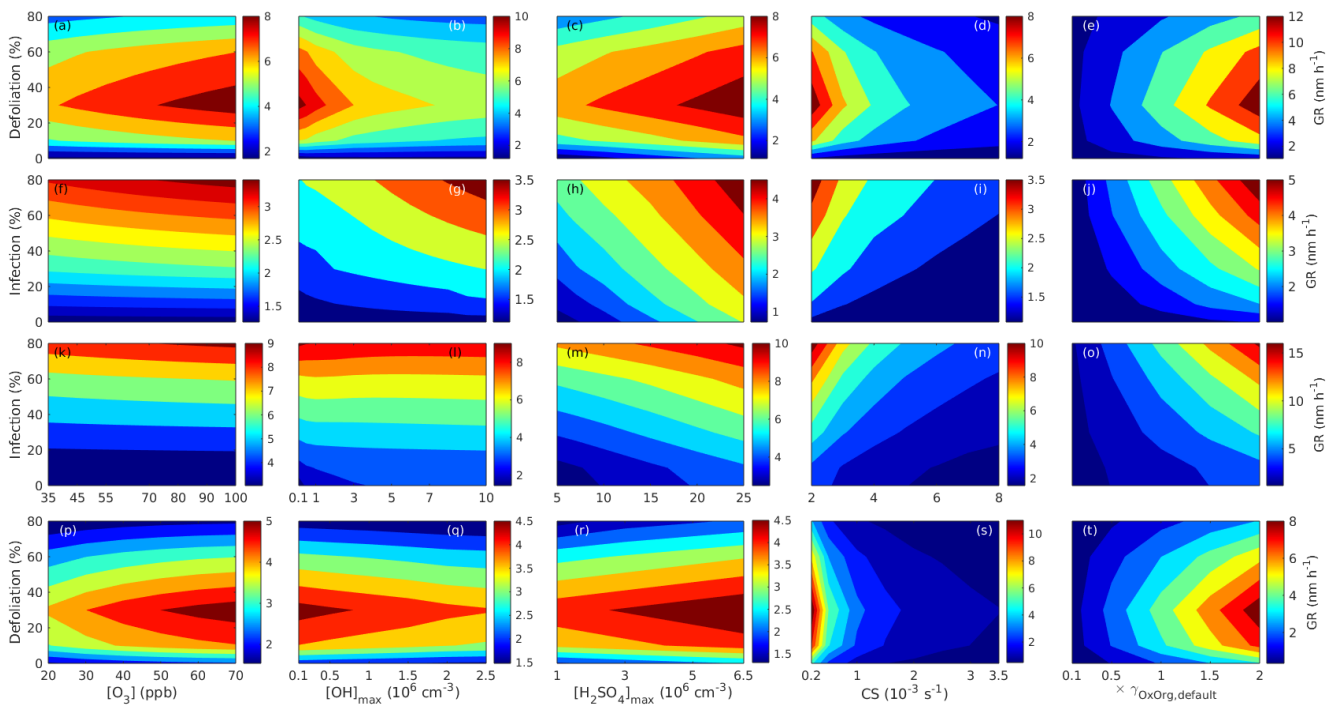

1867

Figure D2. Impact of changed boundary conditions on the growth rate of small particles in non-infected and biotically stressed forest stands. The subplots correspond to those in Fig. 11, except the subplots here display growth rate, and not number of particles. Thus we refer to Fig. 11 for further explanations.